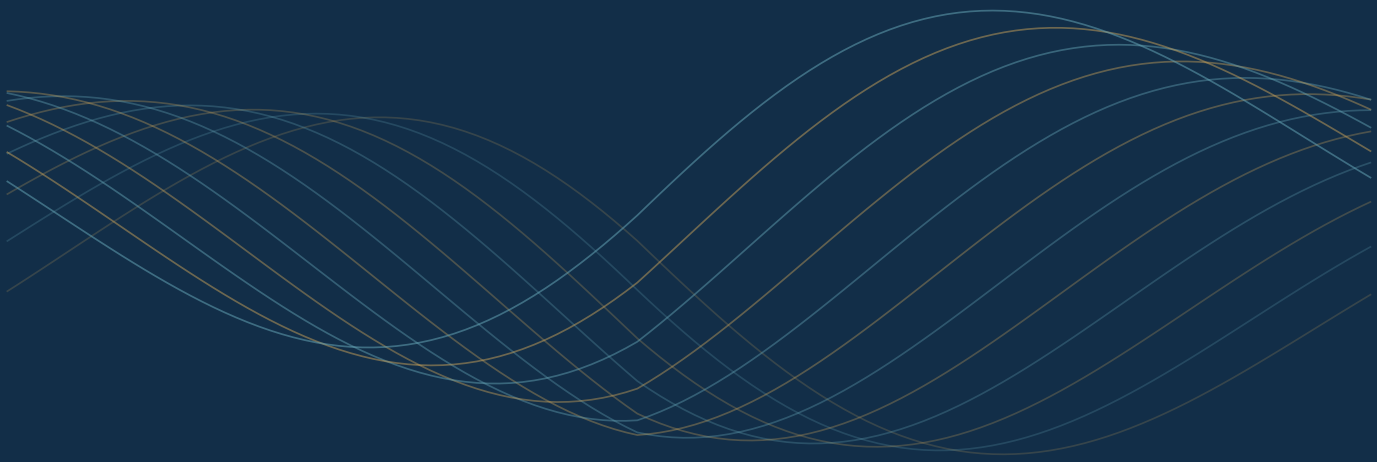
JAMSCS • VOLUME 1 • ISSUE 1

JOURNAL OF APPLIED MATHEMATICS, STATISTICS, AND COMPUTATIONAL SCIENCES



MATHEMATICAL STRUCTURES, ALGORITHMS & DYNAMIC SYSTEMS

INAUGURAL ISSUE • THREE RESEARCH ARTICLES

21 OCTOBER 2026

OPEN ACCESS

EDITOR-IN-CHIEF Dr. Bal Kumar Khadka

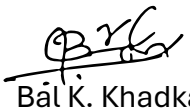
MANAGING EDITOR Dr. Dipesh Baral

Editor's Message

It is my great pleasure to present the inaugural volume of the *STAR Journal of Applied Mathematics, Statistics, and Computational Science*. This milestone reflects our commitment to advancing scientific knowledge, promoting interdisciplinary collaboration, and providing a platform for innovative research in mathematics, statistics, and computational science.

As a peer-reviewed journal, we are dedicated to upholding academic excellence, research integrity, methodological rigor, and a fair and transparent publication process. We aim to foster the exchange of ideas among researchers, academicians, and practitioners worldwide and to encourage research that addresses both theoretical developments and practical challenges.

I extend my sincere gratitude to our authors, reviewers, and editorial team for their invaluable contributions to this inaugural publication. I look forward to building a journal that supports scholarly innovation, collaboration, and lasting contributions to the international research community.



Bal K. Khadka, Ph.D.

Editor-in-Chief

STAR Journal of Applied Mathematics, Statistics, and Computational Science

About This Issue

The inaugural issue of the Journal of Applied Mathematics, Statistics, and Computational Sciences brings together three contributions spanning computational lattice algorithms, nonlinear economic dynamics, and complex analysis. The articles illustrate the connections between mathematical theory, computational methods, and applications.

In “Techniques in Lattice Basis Reduction,” Bal K. Khadka and Spyros S. Magliveras investigate approaches to lattice basis reduction, including computational strategies for identifying shorter vectors.

“Predator–Prey Dynamics from Growth Cycles to Financial Instability: Deterministic Structure and Stochastic Fragility,” by Deepak Bastola, Pitambar Acharya, Dipak Dulal, and Pawan Kumar BK, examines predator–prey models as a framework for understanding economic cycles and financial instability.

In “Nevanlinna–Pick Interpolation in Selected Subalgebras of H∞(D),” Debendra P. Banjade and Jeremiah Dunivin study interpolation in selected subalgebras of bounded analytic functions.

Together, these articles reflect the journal’s interest in rigorous mathematics and computational science across theoretical and applied settings.

Editorial Leadership

Editor-in-Chief

Dr. Bal Kumar Khadka

Managing Editor

Dr. Dipesh Baral

Contents

Editor’s Message i

About This Issue ii

Contents iii

RESEARCH ARTICLES

1. Techniques in Lattice Basis Reduction 1–12

2. Predator–Prey Dynamics from Growth Cycles to Financial Instability 13–35

3. Nevanlinna–Pick Interpolation in Selected Subalgebras of H∞(D) 36–44

Journal of Applied Mathematics, Statistics, and Computational Sciences
JAMSCS ISSN

OA
OPEN ACCESS

Copyright © Authors, 2026

Research Article

Techniques in Lattice Basis Reduction

Bal K. Khadka[1] and Spyros S. Magliveras[2]

Received: 2026-07-14
Revised: 2026-09-21
Accepted: 2026-10-01
Published: 2026-10-21

Article: 001
DOI:

Open access under the Creative Commons Attribution (CC BY 4.0) license.

[1]Department of Mathematics, Georgia Military College, Martinez, GA 30907, USA; bkhadka@gmc.edu
[2]Department of Mathematical Sciences, Florida Atlantic University, Boca Raton, FL 33431; spyros@fau.edu

Abstract

The shortest vector (SVP) and closest vector (CVP) problems, presently considered intractable, are algorithmic tasks that lie at the core of many theoretical and applied problems. We consider the LLL algorithm as a *black box* lattice basis reduction component, and the degree to which the shortest vector of the output basis compares with the Minkowski or weaker bounds as a measure of the *potency* of a basis reduction step. We make the assumption that a single LLL operation costs little, and that the payback of a very short vector is high, particularly if the vector satisfies the Minkowski bound. In this paper, we explore the effect of permuting the input basis B on the potency of a subsequent LLL reduction, and establish experimentally the sensitivity of LLL to permutations of B. In particular, we observe that permutations of large Hamming distance from the identity are more efficient in increasing the reduction potency. Regarding these factors, we investigate the efficacy of new optimization techniques to be used along with the LLL algorithm. The techniques we propose are: (i) *hill climbing (HC)* and (ii) *lattice diffusion-sublattice fusion (LDSF)*. The first technique relies on the sensitivity of LLL to permutations of the input basis B, and optimization ideas over the symmetric group Σ_m viewed as a metric space. The second technique relies on partitioning the lattice into sublattices, performing basis reduction on the sublattice blocks, fusing the sublattices, and repeating. Our approach provides better results for finding shortest vectors than LLL and other traditional methods.

Keywords: Lattice bases; unimodular matrices; right permutations; LLL algorithm; BKZ algorithm

1 Introduction: Historical Background

The development of lattice basis reduction began in 1773 by L. Lagrange [24], C. F. Gauss [9], C. Hermite [17] (1850), A. Korkin and Y. R. Zolotarev [21] (1873), H. Minkowski [26] (1896), and B. L. van der Waerden [35] (1956). The Hermite, Korkin, Zolotarev (HKZ [14]) lattice basis reduction method is assumed to be the strongest but impractical reduction approach. In 1982, Arjen Lenstra, Hendrik Lenstra and László Lovász [25], introduced a polynomial time basis reduction algorithm, presently known as LLL, to factor a rational polynomial. LLL approximates the *shortest vector* within a factor of $2^{n/2}$, where n is the rank of the lattice. Thus, LLL is fast but weak due to the large approximation factor. In 1986, L. Babai [3], proposed an algorithm that approximates the *closest vector* to a lattice point by a factor of $\left(\frac{3}{\sqrt{2}}\right)^n$. In 1987, C. P. Schnorr [30] proposed a further refinement of the LLL algorithm that improved the shortest vector approximation factor to $(1+\varepsilon)^n$. The *Block Korkin Zolotarev* (BKZ) algorithm was introduced and studied [3, 31] by Babai and Schnorr respectively. In 1993, M. Seysen [28] showed that each full rank n lattice $\mathscr{L}$ has a basis B and an associated basis B^* of the reciprocal lattice $\mathscr{L}^*$, with $S(B) \leq \exp(c_2 \cdot (\ln n)^2)$, where $S(B) = \max_{1\leq i\leq n}(\|b_i\| \cdot \|b_i^*\|)$ and c_2 independent of n. This was an improvement on the relation $S(B) \leq \exp(c_1 \cdot n^{1/3})$ established by J. Hastard and J. C. Lagarias [16]. In 1994, Schnorr and Euchner [32] introduced improved algorithms for BKZ and *deep insertion*, but the runtime of these algorithms is not polynomial. In 2001, M. Ajtai et al., [2] introduced a *Sieve* algorithm for the shortest lattice vector problem. In *Eurocrypt* 2008, *N. Gama and P. Nguyen* [13] observed experimentally that BKZ's practical runtime seems to grow exponentially with lattice dimension. In 2010, O. Dagdelen and M. Schneider, [8] presented a parallel version of the *lattice enumeration algorithm* using a multi-core CPU system. The shortest vector (SVP) and closest vector (CVP) problems, presently considered intractable, are algorithmic tasks that lie at the core of many number theoretic problems, integer programming, finding irreducible factors of polynomials, minimal polynomials of algebraic numbers, and simultaneous Diophantine approximation.

Lattice basis reduction has deep and extensive connections with modern cryptography, and cryptanalysis particularly in the

post-quantum era. At present, lattice based cryptosystems do not appear to be vulnerable to quantum attacks. Also, an implementation of a lattice based cryptosystem is faster than RSA or an ECC based system, at an equivalent security level, as proposed by T. Güneysu et al. in 2012, [15] and by J. Howe in 2015, [19].

In 1982, A. Shamir [33] proposed a polynomial-time algorithm for breaking the basic Merkle-Hellman cryptosystem. In 1985, J. C. Lagarias and A. M. Odlyzko, [22] solved low density knapsack problems. In 1996, Hoffstein et al., [18] proposed NTRU, a ring theory based public key cryptosystem. In 1997, D. Coppersmith [6] published a paper on small solutions to polynomial equations, exploiting low exponent RSA vulnerabilities. In this paper, Coppersmith showed how to find small integer solutions to a modular polynomial equation in a single variable and extended the method to the multivariate case. In 1997, M. Ajtai and C. Dwork [1] designed a probabilistic public key cryptosystem whose security relies on the hardness of lattice problems. Their cryptosystem is quite impractical because of the massive data expansion, as it encrypts data bit-by-bit. Inspired by the Ajtai-Dwork cryptosystem, O. Goldreich et al., [12] proposed a public key cryptosystem based on the closest vector problem in a lattice, and J.-Y. Cai and T. W. Cusick, [5] introduced similar work on a lattice based public key cryptosystem in 1999. In 2001, C. Gentry, [10] published a paper on Key Recovery and Message Attacks on NTRU-Composite, where he recovers information about the private key used in NTRU. In 2001, D. Coppersmith and A. Shamir, [7] proposed a new lattice basis reduction technique to cryptanalyze the NTRU scheme. In 2009, Craig Gentry, [11], in his Ph.D. thesis, described a fully homomorphic encryption scheme based on ideal lattices. Currently, there are many mathematicians vigorously contributing to lattice basis reduction theory, and improving best lattice bounds.

2 Preliminaries

Let $B = \{b_1, b_2, ..., b_m\}$ be a set of m linearly independent row vectors in $\mathbb{R}^n$, where $m \leq n$. The *lattice* $\mathscr{L} \subset \mathbb{R}^n$, generated by B, is the set of all integral linear combinations of the vectors of B, that is:

$$\mathscr{L} = \{a_1 b_1 + a_2 b_2 + \cdots + a_m b_m : a_i \in \mathbb{Z}\}.$$

B is called a *basis* for $\mathscr{L}$, and m the *rank* or *dimension* of $\mathscr{L}$. If $m = n$, then $\mathscr{L}$ is called a *full-rank* lattice. Therefore, an arbitrary lattice vector $v = (v_1, \ldots, v_n) \in \mathscr{L}$ is given by $(v_1, \ldots, v_n) = (a_1, \ldots, a_m)B$, where $a_i \in \mathbb{Z}$. If $B = \{b_1, b_2, ..., b_m\}$ is a set of m linearly independent vectors on $\mathbb{R}^n$, as above, we denote the *span* of B over $\mathbb{R}$ by:

$$\langle B \rangle_{\mathbb{R}} = \Big\{ \sum_{i=1}^{m} x_i b_i : \ x_i \in \mathbb{R} \Big\}.$$

Similarly, we denote the span of B over $\mathbb{Z}$ by:

$$\langle B \rangle_{\mathbb{Z}} = \Big\{ \sum_{i=1}^{m} x_i b_i : \ x_i \in \mathbb{Z} \Big\} = \mathscr{L} \ .$$

The *weight of lattice basis* $B = \{b_1, b_2, \ldots, b_m\}$ is defined as the product of the lengths of all the basis vectors. That is, $\mathrm{wt}(B) = \prod_{i=1}^{m} \|b_i\|$.

The *determinant of the lattice* $\mathscr{L}$ is defined by

$$\det(\mathscr{L}) = \sqrt{\det(BB^t)}.$$

Lattices are invariant under unimodular transformations. That is, for any two bases B and C of the lattice $\mathscr{L}$ of rank m, there is an $m \times m$ unimodular matrix U such that $B = UC$. A square integer matrix U is said to be unimodular if $\det(U) = \pm 1$. There exist infinitely many unimodular matrices of size $m \times m$ for $m \geq 2$. Therefore, a lattice of rank $m \geq 2$ is generated by infinitely many lattice bases.

2.1 Geometry of numbers

Let $\mathscr{L}$ be a rank-m lattice in n-dimensional Euclidean space $\mathbb{R}^n$. The *first minimum* of the lattice, denoted $\lambda_1(\mathscr{L})$, is the length of a shortest nonzero vector $v_1 \in \mathscr{L}$. It is well known that for any full rank lattice, $\lambda_1(\mathscr{L})$ satisfies the Minkowski bound, i.e., $\lambda_1(\mathscr{L}) \leq \sqrt{n}(\det(\mathscr{L}))^{1/n}$. The *second minimum* of the lattice, denoted by $\lambda_2(\mathscr{L})$, is the smallest real number r such that there exist two $\mathbb{R}$-linearly independent lattice vectors v_1 and v_2 such that $\|v_1\|, \|v_2\| \leq r$. In general, for $i = 1, 2, \ldots, m$, the i^{th} *successive minimum* of the lattice, denoted $\lambda_i(\mathscr{L})$, is the smallest real number r such that there exist "i" $\mathbb{R}$-linearly independent vectors $v_1, v_2, \ldots, v_i \in \mathscr{L}$ such that $\|v_1\|, \|v_2\|, \ldots, \|v_i\| \leq r$. If we can find lattice vectors $v_1, v_2, \ldots, v_m \in \mathscr{L}$ which form a basis for $\mathscr{L}$, such that $\|v_i\| = \lambda_i(\mathscr{L})$ for $i = 1, 2, \ldots, m$, then, this basis is almost orthogonal and a "best possible" basis for the lattice. However, such a basis is very difficult to find.

2.2 Permutations and groups

The symmetric group on $X = \{1, 2, \ldots, n\}$ is the collection of all $n!$ permutations of the symbols of X, denoted by Σ_n. Σ_n forms a group under the usual composition of functions. If $\pi \in \Sigma_n$, one of several ways of representing π is as a two-row matrix of the form $\pi = \left(\begin{smallmatrix} 1 & 2 & \cdots & n \\ \pi(1) & \pi(2) & \cdots & \pi(n) \end{smallmatrix}\right)$, exhibiting the bijection. The *Cartesian form* of π is simply the vector of images $[\pi(1), \pi(2), \ldots, \pi(n)]$.

For example $[4,5,3,2,1]$ is the Cartesian form of permutation $\begin{pmatrix}1&2&3&4&5\\4&5&3&2&1\end{pmatrix}$. The symmetric group Σ_n can be made into a metric space by defining the distance between two permutations $x,y\in\Sigma_n$ as the number of places the Cartesian forms of x and y differ. For example, the distance between the permutations $x=[4,5,3,2,1]$ and $y=[4,1,3,2,5]$ is 2. We denote the distance between x and y by $d(x,y)$. Note that this metric is the well known *Hamming distance* on Σ_n.
Given a permutation $\pi\in\Sigma_n$, we associate with π an $n\times n$ matrix $A=(a_{i,j})^T$, where $a_{i,j}=1$ if $\pi(i)=j$ and $a_{i,j}=0$ otherwise. Such a matrix A is called a permutation matrix. This is a matrix obtained from the identity matrix I_n by permuting its rows by π. The $n\times n$ matrix associated with $[4,5,3,2,1]$ is

$$\pi=\begin{pmatrix}0&0&0&0&1\\0&0&0&1&0\\0&0&1&0&0\\1&0&0&0&0\\0&1&0&0&0\end{pmatrix}$$

Obviously, there are $n!$ $n\times n$ permutation matrices. If some of the 1's in A are replaced by -1, the resulting matrix is called a *signed* permutation matrix. Clearly, there are $2^n n!$ signed permutation unimodular matrices that can rearrange the given lattice basis vectors. Let $c\in\Sigma_n$, and r a non negative integer, we define the *sphere* of radius r and center c as follows:

$$S_c(r)=\{x\in\Sigma_n : d(c,x)=r\}.$$

We define the *radius* of a permutation as its *Hamming distance* from the identity permutation. A permutation π_r of radius r in the symmetric group Σ_n is said to be a *left permutation* if $r\le\frac{n}{2}$, otherwise, it is a *right permutation*.

2.3 The Gram-Schmidt Orthogonalization (GSO)

The GSO procedure is a method for getting an orthogonal basis for a given subspace $V\le\mathbb{R}^n$, when a basis B for V is given. Let $B=\{b_1,b_2,\ldots,b_m\}$ be a basis of V. The GSO of B is the basis $B^*=\{b_1^*,b_2^*,\ldots,b_m^*\}$ such that

1. $b_1{}^* = b_1$
2. $b_i{}^* = b_i - \sum_{j=1}^{i-1}\mu_{i,j}b_j^*, \quad$ for $2\le i\le m$.

where,

3. $\mu_{i,j}=\dfrac{\langle b_i,b_j^*\rangle}{\langle b_j^*,b_j^*\rangle}$ for $1\le j<i\le m$) . (1)

From this, we can write $b_i=\sum_{j=1}^{i}\mu_{i,j}b_j^*$ for any $1\le i\le m$. That is $B=MB^*$, Where $M=(\mu_{i,j})$, $\mu_{i,j}=0$ for $i<j$, and $\mu_{i,i}=1$ for $1\le i\le m$. That is,

$$\begin{bmatrix}b_1\\b_2\\\vdots\\b_m\end{bmatrix}=\begin{bmatrix}\mu_{1,1}&0&0&\ldots&0\\\mu_{2,1}&\mu_{2,2}&0&\ldots&0\\\vdots&&\ddots&&\vdots\\\mu_{m,1}&\mu_{m,2}&\mu_{m,3}&\ldots&\mu_{m,m}\end{bmatrix}\begin{bmatrix}b_1^*\\b_2^*\\\vdots\\b_m^*\end{bmatrix}$$

Here, $M=(\mu_{i,j})$ is a lower triangular matrix with $\det(M)=1$. If the vectors $b_1,b_2,\ldots,b_m$ are in $\mathbb{Q}^n$, then so are the vectors $b_1^*,b_2^*,\cdots,b_m^*$. In general, $b_1^*,b_2^*,\ldots,b_m^*$ are not integral linear combinations of the $b_1,b_2,\ldots,b_m$. So, the Gram-Schmidt basis vectors $b_1^*,b_2^*,\ldots,b_m^*$ are not necessarily in the lattice generated by $b_1,b_2,\ldots,b_m$. Here, B^* is an orthogonal basis for the vector subspace $V\le\mathbb{R}^n$, and $\|b_i^*\|\neq 0$ for $1\le i\le m$.

2.4 LLL Reduced Bases

Let $\mathscr{L}=\langle B\rangle_{\mathbb{Z}}$ with basis $B=\{b_1,b_2,...,b_n\}$ be a full rank lattice in $\mathbb{R}^n$ with GSO vectors $\{b_1^*,b_2^*,...,b_n^*\}$. For a real number $\alpha\in\left(\frac{1}{4},1\right)$, B is said to be α-*reduced* (or α-LLL-reduced) if the following conditions hold:

1. $|\mu_{i,j}|\le\frac{1}{2}$ for $1\le j<i\le n$,
2. $\|b_i^*+\mu_{i,(i-1)}b_{i-1}^*\|^2\ge\alpha\|b_{i-1}^*\|^2$, for $2\le i\le n$.

Condition (2) is called the *exchange* condition. We can rewrite (2) as

3. $\|b_i^*\|^2\ge(\alpha-\mu_{i,(i-1)}^2)\|b_{i-1}^*\|^2$, for $2\le i\le n$.

In 1982, A.K. Lenstra, H.W. Lenstra and L. Lovász [25] described an algorithm, known as the LLL algorithm, which produces an $\alpha-$reduced basis B' for the lattice $\mathscr{L}(B)$ in polynomial time. LLL also provides a relatively short lattice vector of length ℓ, and it is convenient to denote this LLL operation in the form: $(B',\ell)\leftarrow\Lambda_\alpha(B)$ or simply, $(B',\ell)\leftarrow\Lambda(B)$. Note that B could be just a

generating set of the lattice and not necessarily a basis. However, the resulting B' will always be a basis for $\mathscr{L}(B)$. We will not describe the LLL algorithm here, however, we will be using LLL as a basic *black box* operational component in the basis reduction systems that we will be discussing. For high dimensional lattices it is very hard to find a short vector satisfying the Minkowski bound, using a single LLL application. For practical purposes we consider a lattice reduction procedure satisfactory if the shortest vector $\|v\| \leq m^t(\det(\mathscr{L}))^{1/m}$ where $t \leq 1$, and extremely satisfactory if $t \leq 1/2$.

3 Sensitivity of LLL under basis permutations

We denote a single LLL operation on a permuted basis B^π by $\Lambda(B^\pi)$. In our experiments the row vectors of the basis B of a lattice $\mathscr{L}$ are permuted under the permutation π. A repeated application of LLL on the same ordered basis B yields identical output. Consider a case where a single LLL operation can not completely reduce a lattice basis B. If we apply LLL lattice basis reduction after randomly (or systematically) reordering the original basis B, it will almost always yield a different basis.

Consider a basis $B = B_{54}$, of an ideal lattice of rank 54, taken from the ideal lattice challenge [27]. The length l of the shortest vector of $\Gamma = \Lambda(B)$ turns out to be

$$l = 2745.73.$$

For each radius $r \in \{5, 10, \ldots, 50\}$, we select a random sample P_r of $N = 100$ permutations and compute $\{\Lambda(\Gamma^{\pi_i}) : \pi_i \in P_r\}$. This yields a 100 shortest vectors of lengths $L_r = \{l_1, l_2, \cdots, l_{100}\}$, see table (1) . We then record the minimum, maximum, mean (μ), the standard deviation (σ), and the range of L_r.

radius	min	max	μ	σ	range
05	1946.87	2512.98	2241.26	115.51	566.11
10	1968.17	2535.28	2256.89	102.84	567.11
15	1946.77	2532.94	2256.88	122.84	586.17
20	1946.87	2521.33	2282.65	95.86	574.46
25	1946.87	2469.95	2264.28	96.69	523.08
30	1968.17	2473.17	2263.23	101.65	505.00
35	1968.17	2558.02	2271.41	125.97	589.85
40	1946.77	2493.44	2254.79	115.24	546.67
45	1968.17	2552.18	2284.52	109.11	584.01
50	2010.59	2490.98	2260.74	100.35	480.39

Table 1. LLL reduction over permuted basis

3.1 Effectiveness of right permutation

The significant values of σ and range in table (1) provide strong evidence of the sensitivity of LLL to permuting the lattice basis. We proceed to analyze the reduction pattern when basis rows are permuted. In the experiments below, we take a basis B of an ideal lattice of rank 52 from the *Hall of Fame* website [27] and reduce it by the LLL algorithm. Let $\Gamma = \Lambda(B)$. Γ is not of high quality and requires further reduction. We proceed as follows: for each possible radius $r \in \{2, 3, \ldots, 52\}$, we select a random sample $P_r = \{\pi_{r,1}, \ldots, \pi_{r,N}\}$ of N permutations, where $N \in \{100, 500\}$. Recall that a permutation $\pi_{r,j} \in P_r$ is of distance r from the identity permutation. We compute $\Lambda(\Gamma^\pi)$ for all $\pi \in P = \bigcup_{r=2}^{52} P_r$, and observe how often a basis gets reduced for each sample. The output parameters l, L, and $\log(wt)$ are the resulting lengths of the **shortest** vector, **longest** vector, and the $\log_{10}$ of the **weight** of the reduced basis respectively.

In the graph below, we use the following notation.

$$llb \leftarrow l_{\min}, \qquad lub \leftarrow L_{\min}, \qquad \text{and} \qquad mwt \leftarrow \min(\log_{10} wt)$$

where min represents the minimum over the complete sample of size N, for each radius.

The relative frequency 0.6 corresponding to the radius r in the above graphs represents that the basis gets further reduced 60% of the time if we rearrange Γ with permutations of radius r. From the above graphs, we observe that increasing the permutation radius results in an increase of the relative frequency of the shortest vector. More precisely, the lim_{inf} and lim_{sup} of the relative frequency is monotonically increasing with radius.

Next, we compute the averages for $l, L, \log_{10}(wt)$ over the 500 permutations for each radius $r \in \{2, 3, \ldots, 52\}$ and analyze the pattern of these averages versus the radius. Further, we normalize the average values by using the transformation

$$\text{normalized value} = \frac{\text{value - minimum value}}{\text{maximum value - minimum value}}$$

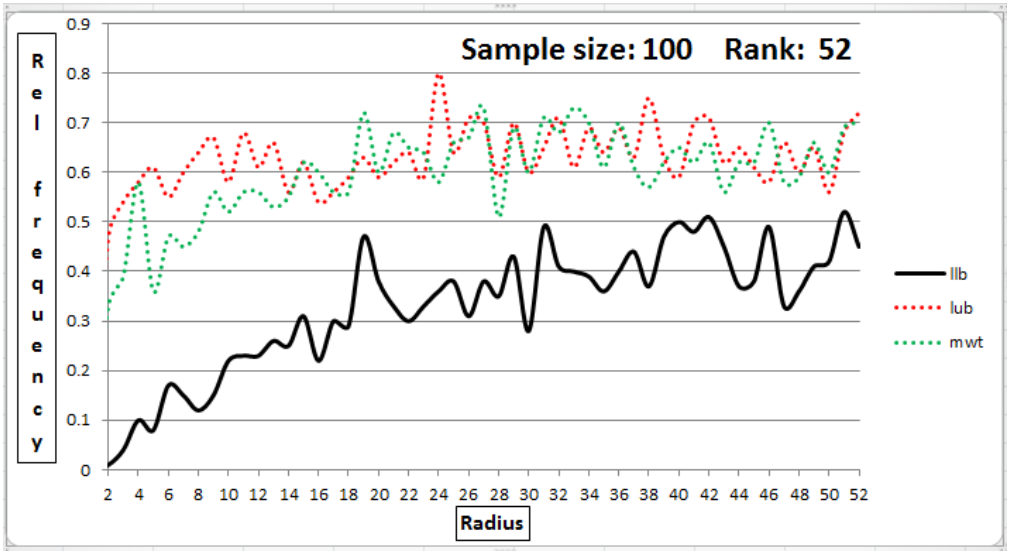


Figure 1. Relative Frequency vs radius

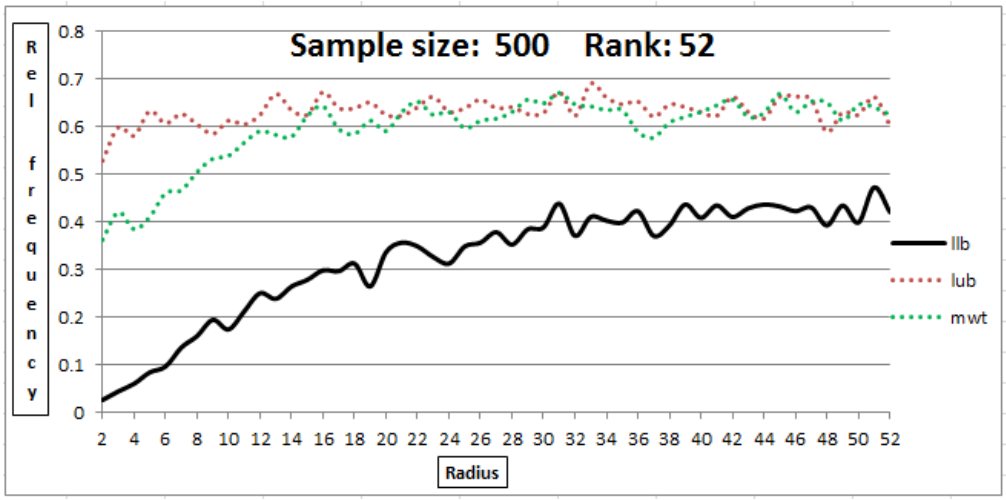


Figure 2. Relative Frequency vs radius

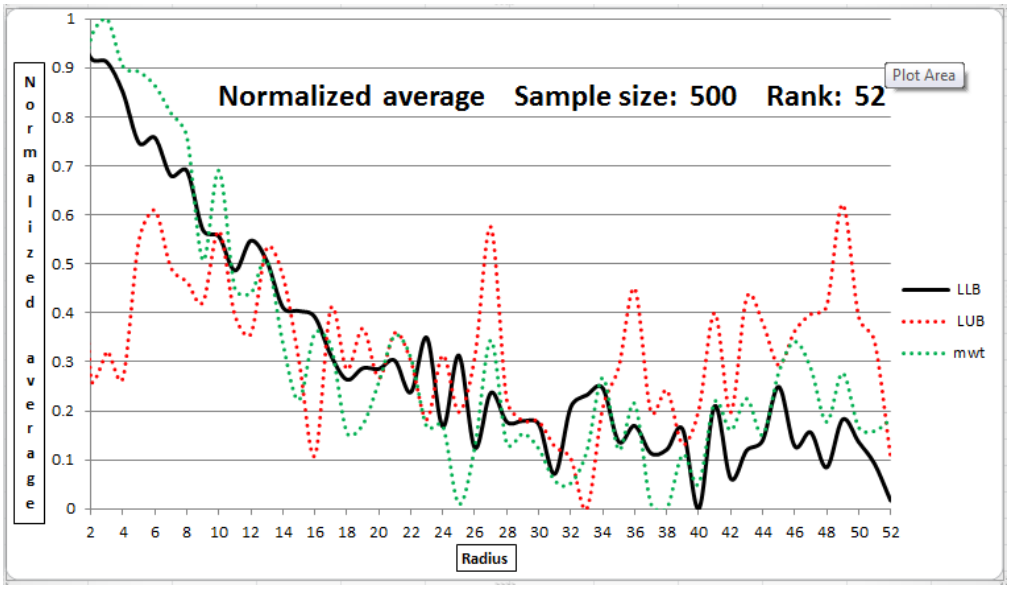


Figure 3. Normalized average vs radius

 doi:

The normalized average values 0 and 1 corresponding to the radii r_1 and r_2 represent the least and the greatest average among all experiments occurring under permutations of radii r_1 and r_2 respectively.
In the above experiments, the decreasing pattern of the curve corresponding to the shortest vector, makes clear that on average, the shortest vector length is achieved more efficiently if the radius of the permutation is larger. This means that the length of the shortest vector is effectively reduced by an application of **right** permutations. This is true for the predominant number of experiments we have performed on lattice bases of different dimensions. Based on our observations in 3.1 and 3.2, we propose the following lattice basis reduction techniques.

4 Hill Climbing Lattice Basis Reduction

Hill climbing reduction is an optimization technique that attempts to search for a better solution locally and repeats the procedure until it finds a prescribed global solution. In our research, this method takes advantage of the sensitivity of LLL to permuting the input basis. We propose two types of Hill climbing lattice basis reduction techniques:

1. Reduction with a fixed radius (spherical random walk).
2. Reduction with variable radius (spiral random walk).

The second method differs from the first in the sense that the radii of successive permutations samples are systematically increased from one step to the next step, while radii are fixed in the first method. In the methods discussed below we relax the upper bound condition from the Minkowski bound ($\lambda_1(\mathscr{L}) \leq m^{1/2} \cdot (\det \mathscr{L})^{1/m}$) to an approximation $\|v\| \leq m \cdot (\det \mathscr{L})^{1/m}$ which is much easier to achieve, but was deemed sufficient for a submission of a solution to the *Ideal Lattice Hall of Fame* [27].

4.1 Hill climbing lattice basis reduction algorithm

(Type I: *Fixed radius*)
Input: Basis $B = \{b_1, b_2, \cdots, b_{m \leq n}\}$ of $\mathscr{L} \subset \mathbb{R}^n$, and parameters: $k,\ p,\ r$.
Output: $v \in \mathscr{L}$, where $\|v\| \leq m \cdot (\det \mathscr{L})^{1/m}$.

1. $l_{min} \leftarrow nmax,\ \pi_{min} \leftarrow identity$
2. for $i \in \{1, 2, \cdots, p\}$ do:
3. for $j \in \{1, 2, \cdots, k\}$ do:
   3.1 Choose a random $\pi \in \Sigma_m$ of radius r
   3.2 $(B', l) \leftarrow \Lambda(B^{\pi})$
   3.3 if $(l \leq l_{min})$ do: $\{l_{min} \leftarrow l \ \ \& \ \ \pi_{min} \leftarrow \pi\}$
   3.4 next j
4. Update: $B \leftarrow B^{\pi_{min}}$
5. next i

(Type II: *Variable radius*)
Input: Basis $B = \{b_1, b_2, \cdots, b_{m \leq n}\}$ of $\mathscr{L} \subset \mathbb{R}^n$ and $r_0, rstep, k, p$, parameters.
Output: $v \in \mathscr{L}$, where $\|v\| \leq m \cdot (\det \mathscr{L})^{1/m}$.

1. $r \leftarrow r_0 - rstep,\ l_{min} \leftarrow nmax,\ \pi_{min} \leftarrow identity$
2. for $i \in \{1, 2, \cdots, p\}$ do:
3. $r \leftarrow r + rstep$
4. for $j \in \{1, 2, \cdots, k\}$ do:
   3.1 Choose a random $\pi \in \Sigma_m$ of radius r
   3.2 $(B', l) \leftarrow \Lambda(B^{\pi})$
   3.3 if $(l \leq l_{min})$ do: $\{l_{min} \leftarrow l \ \ \& \ \ \pi_{min} \leftarrow \pi\}$
   3.4 next j
5. Update: $B \leftarrow B^{\pi_{min}}$
6. next i

doi:

In the tables below, we compare the length of the shortest vector by using the hill climbing reduction approach on the ideal lattice of rank 68 and the ideal lattice of rank 108 taken from the ideal lattice *Hall of Fame* website [27]. The value at HC-r represents the length of the shortest vector achieved using the hill climbing algorithm of radius r. The value at $HC-PSL2$ represents the length of the shortest vector achieved using the hill climbing algorithm in the group $PSL(2,q)$ on $q+1$ points, $q \in \{67, 107\}$. For these examples the LLL-RR (arbitrary precision floating point) version of LLL algorithm from the NTL library [34] is used to reduce the lattice basis. The sample size taken in each step is $k = 100$.

Initially, the length of the shortest vector obtained for the lattice of rank 68 after an application of the LLL-RR algorithm with reduction parameter $\alpha = 0.9$ was 4664. The shortest vector in the experiment in the table below corresponds to the reduction parameter $\alpha = 0.9999$. We have compared the hill climbing reduction with different radii using the same parameter $\alpha = 0.9999$. The length of the shortest vector was 2222 that corresponds to BKZ-10. Here, BKZ-10 represents the Block Korkin Zolotarev [31] lattice basis reduction for block size 10. The tables below contain values from random hill steps.

Step	LLL	BKZ-10	HC-30	HC-42	HC-48	HC-54	HC-66	HC-PSL2
1	2890	2222	2172	2218	2172	2189	2154	2255
5	–	–	2152	2172	2172	2172	**2141**	2182

Table 2. Comparison for an ideal lattice of rank 68

Next, the length of the shortest vector obtained for the lattice of rank 108 after the application of the LLL-RR algorithm with reduction parameter $\alpha = 0.9$ was 12,308. Since the shortest vector corresponds to the LLL parameter $\alpha = 0.99999$, we compare the hill climbing reduction with different radii with the same parameter $\alpha = 0.99999$.

Step	LLL	BKZ-35	HC-50	HC-60	HC-70	HC-80	HC-100	HC-PSL2
1	6275	4616	4258	4129	4309	**3835**	4202	4513
4	–	–	4015	3938	4010	3835	4104	4337
7	–	–	4015	3880	4010	3835	4006	4064

Table 3. Comparison for an ideal lattice of rank 108

From the above tables, we observe that the hill climbing algorithm with any radius in the experiments produces smaller l values than the LLL or BKZ algorithms. Among all values, HC-66 in table (2) and HC-80 in table (3) have better approximations for the shortest lattice vectors. In the next section we observe the hill climbing lattice basis reduction results versus the radius of permutations. We observed a number of experimental results of lattice basis reduction using our hill climbing approach on bases each of which are already reduced by a single LLL operation. In this section, we observe convergence patterns as follows:

(i) for the length of the *shortest lattice vector at each hillstep* versus *radius*.

(ii) *average length and the shortest vectors at all hill steps* versus *radius*.

(iii) *average length* and *shortest length of all radii* versus *each hill step*.

For each step and each possible radius, we have taken a basis sample of 100 permutations. Based on our computations, we conclude that the run-time to get the shortest lattice vector using hill climbing with variable radii is **less** than the approach with fixed radius. Scatterplot with a smooth fitted lines of our experiments are given below.

5 Hill climbing reduction using a cluster

This method reduces the lattice bases using parallel computation. We perform the hill climbing lattice basis reduction algorithm sending the basis B_i to all available computer nodes, along with a single permutation $\pi_{i,j}$ from the random sample S to each node. Clearly this process reduces the computing time from T to process all k LLL operations on a single node, to T/k for each step, where k is the size of the sample of permutation which is also the number of nodes.
Sending a permuted lattice basis to parallel nodes is not a good idea for a lattice basis that requires long runtime. Instead, we "*diffuse*" the given input basis into smaller blocks (not necessarily disjoint), say $\{B_1, B_2, \cdots B_s\}$ with $B = \bigcup_{j=1}^{s} B_j$. Subsequently, we send the B_j to the server nodes with proper instructions to obtain reduced bases B'_j of $\mathscr{L}(B_j)$. The server nodes then send the B'_j to the master node where they are fused to make a new basis B' of the lattice. This method not only reduces the runtime but also reduces the value of the largest entries in the basis. As we get the output back from the server machines to the master client machine, we combine them and rearrange the basis vectors using a **right** permutation. Then, we again diffuse the basis gradually increasing the block size. The process continues until a desired bound is obtained. Using this approach, we have successfully achieved the lattice vectors whose estimated euclidean norm were less than the given bound on the **Lattice hall of fame** [27].

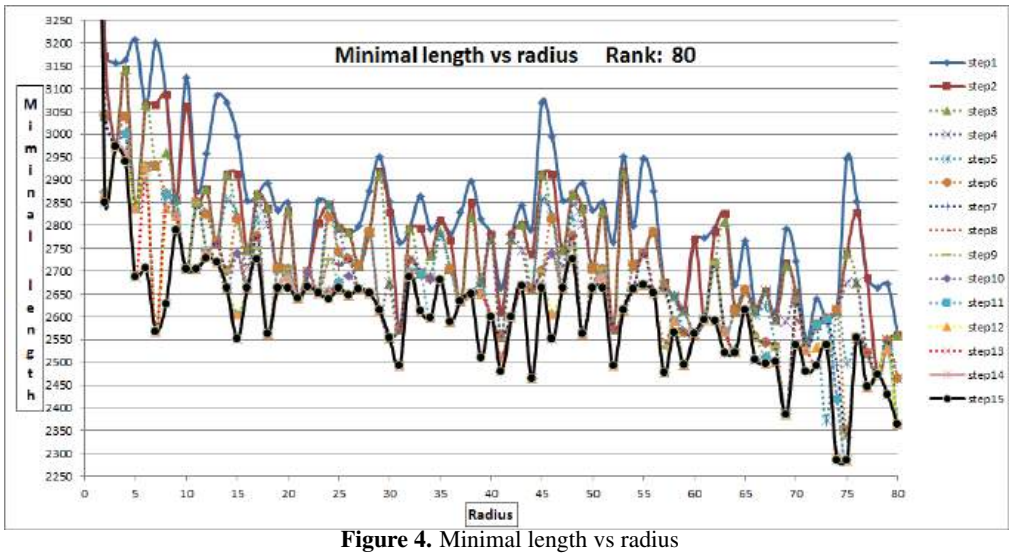


Figure 4. Minimal length vs radius

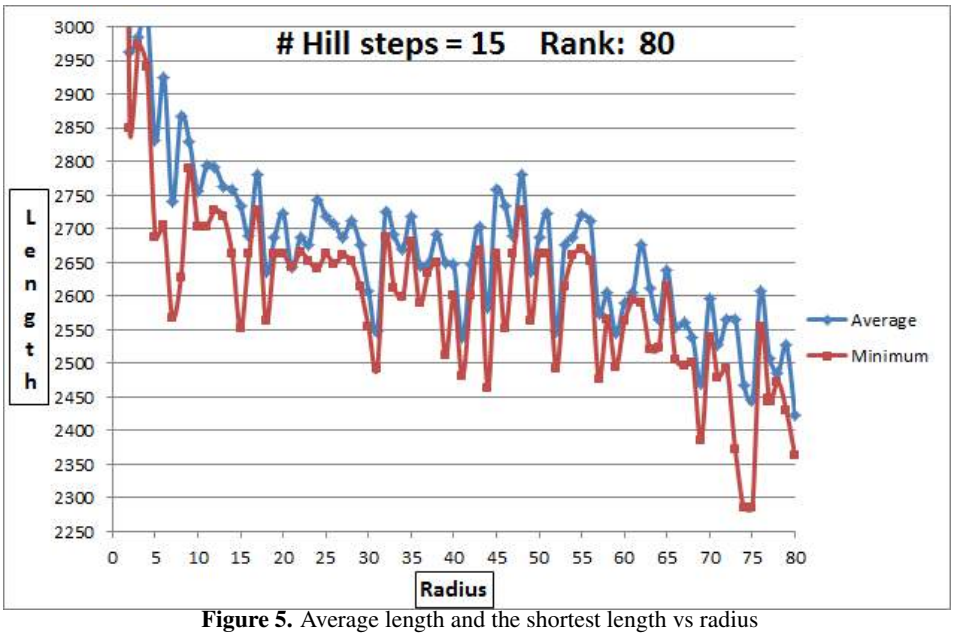


Figure 5. Average length and the shortest length vs radius

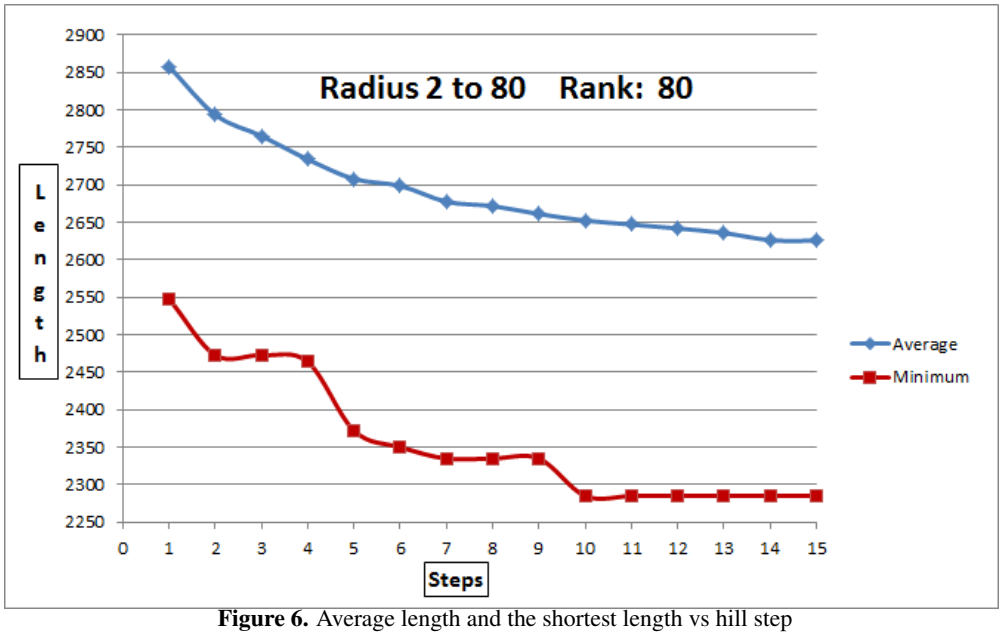


Figure 6. Average length and the shortest length vs hill step

 doi:

5.1 Lattice Diffusion and Sublattice Fusion (LDSF) Algorithm

Input: Basis B of $\mathscr{L} \subset \mathbb{R}^n$, β : Block Size, and b, N, M : parameters.

Output: A lattice vector of "minimal" length close to b.

1. $m \leftarrow$ number of rows in B $\diamond$ $l \leftarrow 1$.
2. $i \leftarrow 1$.
3. For $j = 1$ to k; k is the number of servers.
4. $B_j \leftarrow$ a block matrix of β rows taken randomly from $B \subset \bigcup_{j=1}^{k} B_j$.
5. Send B_j to server j $\diamond$ $B'_j \leftarrow$ result from server j.
6. $(B, \ell) \leftarrow (\Lambda(\cup B'_j))^{\pi}$ $\diamond$ go to step 3 if $M \geq i \leftarrow i+1$.
7. End if $\ell \leq b$.
8. Go to the step 2 if $(N \geq l \leftarrow l+1) \wedge (1 \leq k \leftarrow k-1)$.

The subroutines of lattice diffusion and sublattice fusion (LDSF) algorithms are explained by the figures below. Here LDSF(t, B) represents the algorithm that diffuses the basis B into t blocks sends those blocks into m servers and applies LLL reduction. Finally, the algorithm combines all reduced blocks to get a basis for the lattice.

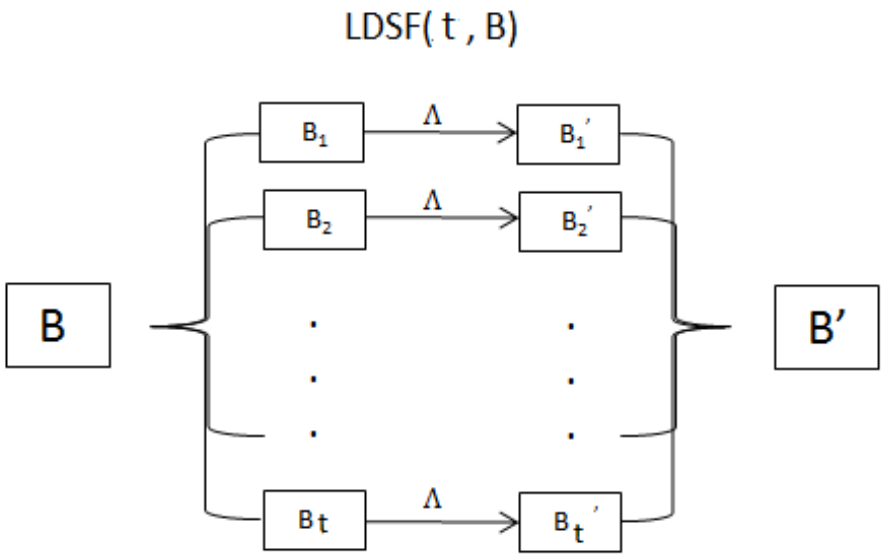


Figure 7. LDSF subroutine algorithm

We presently consider a second operator which we denote by $C = \Sigma(t,k,B)$ which consists of (i) applying a sample of k permutations $\pi_1, \pi_2, \ldots, \pi_k$ to the input base B, (ii) computing $C_i = LDSF(t, B^{\pi_i})$, for $1 \leq i \leq k$, and (iii) letting C be the best basis among the resulting C_i. We say that a basis B of a lattice is better than a basis C of the lattice if the length of the shortest vector in B is less than the length of the shortest vector in C.
If the time required to reduce a basis is very large, we use our multistage lattice diffusion and sublattice fusion technique until we get significant changes of the basis entries. In fact, a combination of the lattice diffusion and the sublattice fusion algorithms with the hill climbing algorithm improves a lattice basis. An explanation of multistage lattice diffusion and sublattice fusion plus a hill climbing algorithm is given below:

5.2 A 4-stage hybrid LDSF-HC process

In the first stage, given an initial basis B_0, which is not satisfactorily reduced by LLL, we compute $LDSF(t, B_0)$ by breaking B_0 into m blocks of sub-bases $B_{0,1}, B_{0,2}, \ldots, B_{0,t}$, and applying the LLL-RR algorithm to each $B_{0,i}$, to obtain $\Lambda(B_{0,1}), \ldots, \Lambda(B_{0,t})$. We then combine the $\Lambda(B_{0,i})$ to obtain basis B_1 of $\mathscr{L}$. This step helps to reduce the absolute value of the lattice basis entries. In the second stage, we obtain a random sample of k right permutations $\pi_1, \ldots, \pi_k$ and compute bases $C_j = LDSF(t, B_1^{\pi_j})$, for $1 \leq j \leq k$. Next, we select the best basis among the $\{C_j\}_{j=1}^{k}$ and call it B_2. The operations performed in stage 2 can be succinctly denoted by $B_2 = \Sigma(t,k,B_1)$. Stage 3 is simply $B_3 = \Sigma(l,k,B_2)$ where $l < t$. Finally there is a termination stage computing the basis $B_4 = \Lambda(B_3)$. Schematically,

 doi:

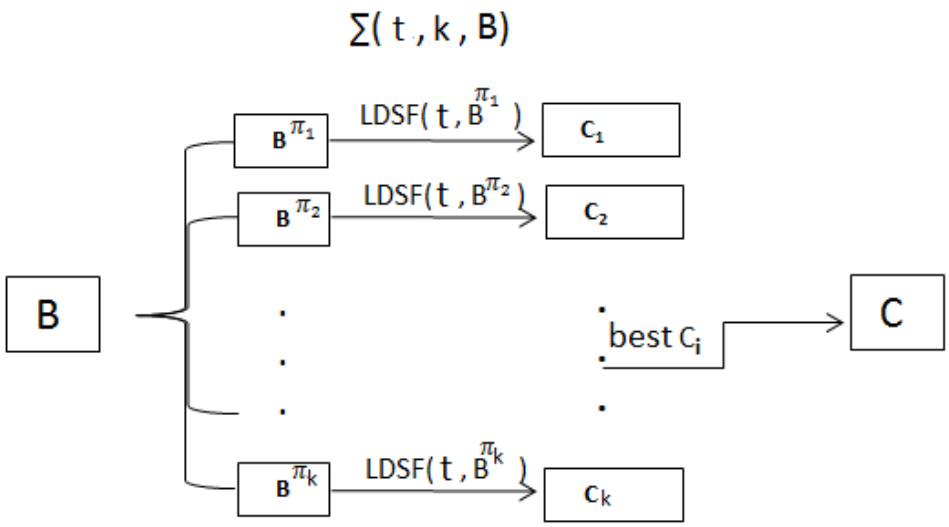


Figure 8. Operator $\Sigma(t,k,B)$

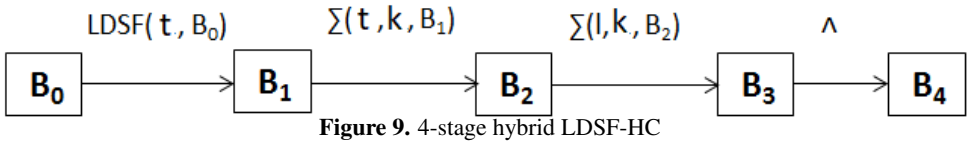


Figure 9. 4-stage hybrid LDSF-HC

If the lattice basis is not sufficiently reduced to use LLL in the 3rd stage, we add additional stages like stage 3 hoping for a better reduction. For example, a 5-stage hybrid LDSF-HC model experiment is given below.
In the experiments below, we compare our lattice diffusion and sublattice fusion algorithm with the fastest floating point version of LLL lattice reduction algorithm (LLL-FP) available in the NTL library [34] with the parameter $\alpha = 0.9$.

5.3 Experiment

The initial information is an ideal lattice of rank 300 obtained from [27].
i) The length of each basis vector is $\approx 10^{900}$.
ii) The initial time to reduce the lattice basis with our device of 24 GB/3GHz i7 processor using the NTL version of LLL-RR, with reduction parameter $\alpha = 0.9$, is approximately a week.
The total runtime by using 5-stage hybrid LDSF-HC is tabulated below.

Stage	# Sample	#*Blocks*	*llb*	*lub*	Runtime
1	1	3	19324936602	8659772341291	1hr 1 m
2	10	6	4509832663	62270235928	3 m 29 sec
3	5	3	2799147462	81977150923	33 m 51 sec
4	5	2	397155	1249483	53 m 40 sec
5	5	2	140973	236873	1 hr 6 m

Table 4. Reduction on an ideal lattice basis of order 300

In the above experiment, the length of a shortest vector reduced from $\approx 10^{900}$ to 140973 in approximately 3.5 hours. Thus the time using this model reduced from 7 days to 3.5 hours.

6 Conclusions

The LLL algorithm is an idempotent operator. If an application of LLL does not reduce satisfactorily an input basis, then a repeated application of LLL on the basis does not change the basis entries, i.e., $\Lambda^2(B) = \Lambda(B)$. However, a permutation of the basis followed by an LLL application will normally generate a different result, i.e., if $\pi \in \Sigma_m$, then almost always $\Lambda(B^\pi) \neq \Lambda(B)$. Thus, LLL is sensitive to permutations of the input basis. Exploiting this sensitivity is at the core of our research. During the experiments discussed above, we observed that the application of right permutations (2.2) on the input basis B has significantly higher probability of getting B further reduced than the application of left permutations (2.2).

Our *hill climbing* (4) algorithm outperforms traditional basis reduction techniques for a basis that is not sufficiently reduced by LLL or BKZ. M. Braun, A. Kohnert, P. Östergard, and A. Wasserman [4], constructed the world's first large set of geometric 2-designs, namely an LS[3][2,3,2^8], invariant under a Singer subgroup in $GL_8(2)$. We have constructed an additional 9 distinct, in fact pairwise non-isomorphic, large sets LS[3][2,3,2^8] [20], with the help of our hill climbing lattice basis-reduction algorithm. Further, using the hill climbing method, we are able to reduce many ideal lattices and publish vectors of several challenge problems in the lattice hall of fame [27].

When the dimension and basis entries increases, hill climbing takes much longer time to reduce the lattice basis. Therefore, a more advanced approach is required. Reducing the basis of a sublattice of smaller rank has a significantly shorter runtime and the resulting sublattice basis has much smaller entries. This property motivates our *lattice diffusion - sublattice fusion* (LDSF) method (5.1). A significant advantage of LDSF method is that it speeds up the process by reducing the magnitudes of the basis entries in the sublattices. In addition to that, each subbase gets reduced faster, and a shortest vector in the sublattice also lies in the lattice. Dividing the lattice basis in k blocks, also called subbases, reduces the LLL reduction algorithm time by an overall factor of approximately k^4. By combining hill climbing and LDSF, we construct a complex hybrid system (5.2) achieving extremely good reduction. This method performed better than currently available algorithms for lattices that had taken longer runtime.

Author Declarations

Author Contributions: Conceptualization, B.K.K.; methodology, B.K.K.; software, B.K.K.; investigation, B.K.K. and S.S.M.; formal analysis, B.K.K.; writing—original draft preparation, B.K.K.; writing—review and editing, B.K.K. and S.S.M. All authors have read and approved the final version of the manuscript.

Funding: This research received no external funding.

Data Availability Statement: All data supporting the findings of this study will be shared upon reasonable request.

Code Availability Statement: All scripts used in this study will be shared upon reasonable request.

Conflicts of Interest: The authors declare no conflicts of interest.

Institutional Review Board Statement: Not applicable. This study did not involve human participants or animals.

Informed Consent Statement: Not applicable.

Generative AI Disclosure: The authors declare that generative artificial intelligence technologies were not used in the preparation of this manuscript.

References

[1] M. Ajtai, C. Dwork, *A public-Key Cryptosystem with Worst-Case/Average-Case Equivalence*, In Proc. 29th ACM STOC, pp. 284-293, 1997.

[2] M. Ajtai, R. Kumar, and D. Sivakumar, *A Sieve Algorithm for the Shortest Lattice Vector Problem*, In Proc. of STOC, 2001, pp. 601–610.

[3] L. Babai, *On Lovász lattice reduction and the nearest lattice point problem*, Combinatorica, Vol. 6 (1986), pp. 1–13.

[4] M. Braun, A. Kohnert, P. Östergard, A. Vardy, A. Wassermann, *Large Sets of t-designs over Finite Fields*, JCTA, Vol. 124 (2014) pp. 195-202.

[5] J.-Y. Cai and T. W. Cusick, *A Lattice-Based Public-Key Cryptosystem*, Information and Computation, Vol. 151, Issues 1-2, 1999, pp. 17-31.

[6] D. Coppersmith, *Small Solutions to Polynomial Equations, and Low Exponent RSA Vulnerabilities*, Journal of Cryptology, 1997, Vol. 10, pp. 233-260.

[7] D. Coppersmith, Adi Shamir, *Lattice Attacks on NTRU*, Advances in Cryptology-EUROCRYPT '97, Vol. 1233 of LNCS, PP. 52-61, Springer 2001.

[8] O. Dagdelen, M. Schneider, *Parallel enumeration of shortest lattice vectors*, In Euro-Par 2010, Vol. 6272 of LNCS, pp. 211-222, Springer, 2010.

[9] C. F. Gauss, *Disquisitiones arithmeticae*, 1801.

[10] C. Gentry, *Key Recovery and Message Attacks on NTRU-Composite*, Advances in Cryptology-EUROCRYPT 2001, Vol. 2045 of LNCS pp. 182-194.

[11] C. GENTRY, *A Fully Homomorphic Encryption Scheme*, Ph.D. thesis, Stanford University, Department of Computer Science, 2009.

[12] O. GOLDREICH, S. GOLDWASSER, S. HALEVI, *Public-Key Cryptosystem from Lattice Reduction Problems*, Advances in Cryptology-CRYPTO 1997, Vol. 1294 of LNCS pp. 112-131.

[13] N. GAMA, P. Q. NGUYEN, *Predicting lattice Reduction*, Eurocrypt 2008: Advances in Cryptology, 31-51.

[14] GUILLAUME HANROT, DAMIEN STEHLÉ* *Worst-Case Hermite-Korkin-Zolotarev Reduced Lattice Bases* Théme SYM-Systémes symboliques Projects Cacao et Arénaire, Rapport de recherche n^{o}6422-Novembre 2007-25 pages.

[15] T, GUNEYSU, V. LYUBASHEVSKY, T. POPPELMANN, *Practical Lattice-Based Cryptography: A signature Scheme for Embedded System*, CHES 2012, LNCS 7428, pp. 530-547, 2012.

[16] J. HASTAD and J. C. LAGARIAS, Math. Annalen 2287 (1990), pp. 167-174.

[17] C. HERMITE, Extraits de lettres de M. Hermite à M. Jacobi sur différents objects de la théorie des nombres, J. Reine Angew. Math., 40 (1850), pp. 279-290.

[18] J. HOFFSTEIN , J. PIPHER , AND J. H. SILVERMAN, *NTRU: A Ring Based Public Key Cryptosystem*, In Proc. of ANTS, 1998, pp.267-288.

[19] J. HOWE, T. PÖPPELMANN, M. O'NEILL, E. O'SULLIVAN, T. GÜNEYSU, *Practical Lattice-Based Digital Signature Schemes*, ACM Trans. Embeded Computing System, 2015, Vol. 14(3), Article No. 41, pp. 1-24.

[20] M. HURLEY, B. KHADKA, and S. S. MAGLIVERAS, *Some new large sets of geometric designs of type LS[3][2,3,2^8]*, Algebra Comb. Discrete Appl. 3(3) (2016), *pp*. 165 – 176

[21] A. KORKIN, and G. ZOLOTAREFF, *Sur lef formes quadratiques positives*, Mathematische Annalen Vol. 6 (1873), Issue 3, pp. 366-389.

[22] J. C. LAGARIAS and A. M. ODLYZKO, *Solving low-density subset sum problems*, J. Assoc. Comp. Mach., 32 (1985), pp. 229-246.

[23] J. C. LAGARIAS, H. W. LENSTRA, JR. and C. P. SCHNORR, *Korkin-Zolotarev bases and successive minima of a lattice and its reciprocal lattice*, Combinatorica, 10 (4) (1990), pp. 333-348.

[24] L. LAGRANGE, *Recherches d'arithmétique,*Nouv. Mém. Acad., Berlin, 1773.

[25] A. K. LENSTRA, H. W. LENSTRA JR., and L. LOVÁSZ, *Factoring Polynomials with Rational Coefficients*, Mathematische Annalen, 261 (1982), pp. 515-534.

[26] H. MINKOWSKI, *Geometrie der Zahlen*, Leipzig und Berlin, Druck und Verlag von B. G. Teubner, 1910.

[27] T. PLANTARD, F. GÖPFERT, *Ideal Lattice Challenge* http://latticechallenge.org/ideallattice-challenge/

[28] M. SEYSEN, *Simultaneous reduction of a lattice basis and its reciprocal basis*, Combinatorica, September 1993, Volume 13, Issue 3, pp 363-376.

[29] M. SCHNEIDER and J. BUCHMANN, *Extended Lattice Reduction Experiments using the BKZ algorithm*, Sicherheit 2010, LNI 170, pp. 241-252, GI, 2010.

[30] C. P. SCHNORR, *A hierarchy of polynomial time lattice basis reduction algorithms*, Theoretical Computer Science, Volume 53, Issues 2-3, (1987), pp. 201–224.

[31] C.P. SCHNORR, *Block Korkin-Zolotarev Bases and Successive Minima*, *citeseerx.ist.psu.edu/*, 1992.

[32] C. P. SCHNORR, M. EUCHNER, *Lattice basis reduction: Improved practical algorithm and solving subset sum problems*. Mathematical Programming, August 1994, vol 66, pp. 181-199.

[33] A. SHAMIR, *A polynomial time algorithm for breaking the Merkle-Hellman cryptosystem*, In Proc. of the 23rd IEEE Symposium on the Foundations of Computer Science, 1982, pp. 145-152.

[34] V. SHOUP, *Number Theory Library (NTL)*, http://www.shoup.net/ntl/

[35] B. L. VAN DER WARDEN, *Die Reduktionstheorie Der Positiven Quadratischen Formen*, Acta Mathematica, December 1956, Volume 96, Issue 1, pp. 265-309.

Publisher's Note. Statements, opinions, and data contained in publications are solely those of the individual author(s) and contributor(s). The publisher and editors disclaim responsibility for injury to people or property resulting from ideas, methods, instructions, or products referred to in the content.

Journal of Applied Mathematics, Statistics, and Computational Sciences
JAMSCS

OA
OPEN ACCESS

Copyright © Authors, 2026

Research Article

Predator–Prey Dynamics from Growth Cycles to Financial Instability: Deterministic Structure and Stochastic Fragility

Deepak Bastola[1,*], Pitambar Acharya[2], Dipak Dulal[3], and Pawan Kumar BK[4]

Received: 2026-07-04
Revised: 2026-08-12
Accepted: 2026-09-09
Published: 2026-10-21

Article:

Open access under the Creative Commons Attribution (CC BY 4.0) license.

[1]Department of Mathematics and Statistics, Florida Atlantic University, FL, USA
[2]Department of Applied Mathematics, University of Alabama at Birmingham, AL, USA
[3]Department of Mathematical Sciences, Eastern New Mexico University, NM, USA
[4]Trichandra Multiple Campus, Tribhuvan University, Kathmandu, Nepal
[*]Corresponding author: dbastola2022@fau.edu
ORCID iDs: Deepak Bastola: 0009-0006-4049-4772; Pitambar Acharya: 0009-0009-5869-2955; Dipak Dulal: 0000-0001-7300-8060

Abstract

This article develops a rigorous, self-contained framework applying predator–prey dynamics to economic and financial systems. Starting from the classical Lotka–Volterra equations with positive invariance, a conserved Hamiltonian, and center-type stability, we derive three socioeconomic models. First, the Goodwin growth-cycle model is exactly algebraically isomorphic to Lotka–Volterra, so endogenous business cycles appear as closed periodic orbits. Second, a two-species debt–capital model formalizes Minsky's Financial Instability Hypothesis: the deterministic system is a neutrally stable center for all positive parameters, while under Itô noise the conserved "energy" drifts outward at rate $\frac{1}{2}(\sigma_C^2 r_D + \sigma_D^2 r_C) > 0$; the ratio r_C/r_D sets equilibrium leverage rather than a stability threshold. Third, in a three-species super-predator extension, the unique interior equilibrium is proved unstable for all positive parameters, and a closed-form transversal exponent decides whether debt is driven to extinction on the boundary. Finally, for a finite-size stochastic buyer–seller market model with herding, we prove convergence in probability, uniformly on compact intervals, to the deterministic Lotka–Volterra ODE in the joint limit of infinitely many agents and vanishing time step.

Keywords: Lotka–Volterra equations; predator–prey dynamics; Goodwin model; Minsky hypothesis; financial instability; stochastic market models; business cycles; debt–capital dynamics; financial super-predators; Lyapunov stability; transversal stability

1 Introduction

1.1 Background and Motivation

This paper asks one organizing question: how far can the predator–prey formalism be pushed, with full mathematical rigor, as a unifying description of endogenous economic and financial fluctuations? Three new results anchor our answer: a Lyapunov-based stochastic formulation of Minsky's Financial Instability Hypothesis with a closed-form noise-induced energy-drift rate (Theorem 4.4); an instability theorem for a three-species model with financial super-predators, including a closed-form exponent that decides the fate of the debt market (Theorem 4.8); and a mean-field and continuum limit theorem connecting a finite-size stochastic market model to the deterministic Lotka–Volterra dynamics (Theorem 5.1). Sections 4–5 contain these contributions; Sections 2–3 assemble, in self-contained form, the classical apparatus they require.

The mathematical analysis of complex adaptive systems–whether ecological, economic, or financial–reveals a striking family of recurring phenomena: endogenous oscillations, abrupt regime shifts, and multi-scale feedback loops whose qualitative behavior cannot be captured by linear or static equilibrium models. Among the mathematical frameworks developed to describe such behavior, the predator–prey model of Lotka [18] and Volterra [30] occupies a distinguished

position. In its classical formulation, the system comprises two coupled nonlinear ordinary differential equations (ODEs) with four parameters; yet it generates sustained periodic oscillations, continuous dependence on initial conditions with a one-parameter family of periodic orbits, and a characteristic phase-lag between interacting populations that is robustly observed in ecological field data.

The structural analogy between ecological and economic systems is deeper than mere metaphor. In both settings, agents (organisms, firms, financial intermediaries) grow by consuming a shared resource, encounter carrying-capacity constraints, and generate nonlinear feedback operating across multiple timescales. This structural isomorphism provides a rigorous mathematical basis for transferring the predator–prey apparatus to socioeconomic modeling, a research program pursued with increasing analytical sophistication over the past five decades.

1.2 Related Work

The seminal application of predator–prey dynamics to economics is due to Goodwin [10], who embedded the Lotka–Volterra structure within a one-sector macroeconomic model of growth and income distribution. In Goodwin's formulation, the employment rate and the wage share of output evolve as predator–prey variables, generating endogenous business cycles without any exogenous shock mechanism. Empirical tests of this model for ten OECD economies were conducted by Harvie [12], who documented quantitative agreement between the model's predictions and observed counter-cyclical profit-share dynamics. Extensions incorporating nonlinear investment functions were developed by Desai et al. [6], who showed that a convex investment response breaks the conservative center of the classical system and can generate either a globally attracting limit cycle or damped oscillations, depending on the curvature of the investment function. System-dynamics applications of three-trophic-level predator–prey models to industrial supply chains were carried out by Crookes and Blignaut [5], with quantitative calibration to South African steel industry data.

In financial economics, the predator–prey framework has been applied to buyer–seller order-flow dynamics by Montero [22], who demonstrated that stochastic perturbations of the Lotka–Volterra buyer–seller system generate fat-tailed return distributions consistent with empirical equity-market data. The connection between predator–prey dynamics and Minsky's Financial Instability Hypothesis [21] was developed by Keen [15], who calibrated a debt–capital model to US data for 1945–2007 and demonstrated that the ratio of private debt to GDP follows a destabilizing trajectory in the decade preceding the 2008 financial crisis. Closely related, Asada [2] formulates a Lotka–Volterra predator–prey model of Minsky's hypothesis with private debt as predator and income as prey, including stability analysis and policy extensions. On the stochastic side, Shaikhet and Korobeinikov [28] obtain sharp sufficient conditions for stochastic extinction and persistence of a perturbed Lotka–Volterra predator–prey model via the direct Lyapunov method. The role of highly leveraged speculative intermediaries as a destabilizing third trophic level was analyzed by Goldstein [9] (a working paper), who introduced the concept of *financial super-predators* and provided qualitative stability analysis. On the computational side, agent-based models (ABMs) of financial markets developed by Lux and Marchesi [19] and Chiarella et al. [4] demonstrate that heterogeneous trend-following and fundamentalist agents generate volatility clustering, fat-tailed returns, and herd-driven price cycles without requiring exogenous news shocks.

Despite this active literature, several gaps motivate the present work. First, the global (Lyapunov) stability analysis of the debt–capital model, and a careful treatment of the noise-induced energy drift in its stochastic perturbation, have received less attention than local linearization. Second, informal claims that an inequality between the debt-side and capital-side rates (r_D versus r_C) governs Minskyan instability have not been reconciled with the fact that a genuine Lotka–Volterra predator–prey system is a neutral center for *all* positive parameters; we clarify the correct stochastic statement. Third, while the three-population Hopf-to-chaos route is established in the ecological literature [8, 31], its financial interpretation through a super-predator (third trophic) layer has not been developed. Fourth, finite-size stochastic generalizations of the buyer–seller model would benefit from an explicit mean-field convergence result, formulated with the correct density scaling and a careful separation of the large-population and small-time-step limits. Our contribution is therefore primarily one of *unification and financial interpretation* across these settings rather than wholly new dynamical-systems theory. To be fully explicit about the demarcation between new and known material: Propositions 2.1–2.5 and 3.2 are classical results (or minor reorganizations thereof) included for self-containedness, and Table 1 surveys established applications; the new analytical content of this paper is confined to Theorems 4.4, 4.8 and 5.1, the supporting Proposition 4.7, and their corollaries.

The present study systematically addresses all four identified gaps. Our specific contributions can be summarized as follows.

(C1) Rigorous Lyapunov-based formulation of the debt–capital model. Building on the predator–prey treatments of Minsky's hypothesis by Asada [2] and Keen [15], we construct an explicit first integral / Lyapunov function for the two-species debt–capital ODE and establish three results that, to our knowledge, are new in this setting: (i) the deterministic system is a neutrally stable center for *all* positive parameters (Theorem 4.4(i)–(ii)), so that—correcting the informal "$r_D > r_C$" threshold reading—no deterministic stability threshold exists; (ii) under Itô perturbations the expected energy drifts strictly outward at the closed-form rate $\frac{1}{2}(\sigma_C^2 r_D + \sigma_D^2 r_C) > 0$ (Theorem 4.4(iv)), a quantitative measure of noise-induced Minskyan fragility; and (iii) the ratio r_C/r_D governs equilibrium leverage and

the direction of noise-driven excursions rather than deterministic stability. This provides a clean Lyapunov-based statement of Minsky's Financial Instability Hypothesis.

(C2) Three-species super-predator model: equilibrium, instability, and extinction criterion. We establish the existence and uniqueness of a positive interior equilibrium under an explicit parameter condition (Proposition 4.7), prove that this equilibrium is *unstable for all positive parameter values*—so that stable interior coexistence of capital, debt, and super-predators is impossible in this model—and derive a closed-form transversal Floquet exponent λ_D, uniform across all boundary cycles, that decides whether debt is driven to extinction (Theorem 4.8). The financial interpretation of the third trophic layer and the resulting unconditional instability mechanism are the novel contributions.

(C3) Mean-field and continuum limit for the finite-size stochastic market model. We prove a two-step limit theorem (Theorem 5.1) for a finite-size stochastic buyer–seller market model with explicit density-dependent scaling: at fixed time step Δt, the size-N process converges in probability, with an explicit $O(1/N)$ mean-square bound, to the deterministic Euler map; and in the joint limit $N \to \infty$, $\Delta t \to 0$ it converges in probability, uniformly on compact time intervals, to the deterministic Lotka–Volterra ODE. This places the finite-N fluctuations responsible for fat tails and volatility clustering on a firm asymptotic footing while keeping the discrete-time and continuous-time limits carefully separated.

(C4) Unified policy framework. We translate the structural parameters of each model into explicit policy instruments—wage floors, leverage caps, transaction taxes, circuit breakers—and characterize, via the stability criteria established in (C1)–(C2), the direction and magnitude of their effects on the equilibrium stability of each system.

The remainder of the paper is organized as follows. Section 2 presents the Lotka–Volterra framework, establishes positive invariance and the Hamiltonian conservation law, and analyzes the Rosenzweig–MacArthur logistic extension, the two-species competition model, and the reaction–diffusion generalization. Section 3 develops the economic applications: the Goodwin growth-cycle model (with an isomorphism proof), the Desai–Henry–Mosley–Pemberton investment-accelerator extension, and the three-trophic sectoral model. Section 4 presents the financial applications: the buyer–seller asset-price model, the debt–capital model with Lyapunov analysis and the Minsky criterion, and the three-species super-predator system. Section 5 formulates the finite-size stochastic market model, states the mean-field and continuum limit theorem, and collects reproducibility and sensitivity information for the numerical experiments. Section 6 discusses policy implications. Section 7 summarizes the main mathematical findings and outlines directions for future research. All proofs are placed immediately after the corresponding statements.

2 The Lotka–Volterra Framework and Its Principal Extensions

2.1 The Classical Two-Species Model

Let $x(t) > 0$ denote the prey population density and $y(t) > 0$ the predator population density at time $t \geq 0$. The classical Lotka–Volterra predator–prey system is

$$\frac{dx}{dt} = rx - axy, \tag{1a}$$

$$\frac{dy}{dt} = -my + bxy, \tag{1b}$$

where all parameters satisfy r, a, m, $b > 0$. The ecological interpretations are standard:
- r: intrinsic per-capita growth rate of the prey in the absence of predation;
- a: per-capita predation rate (encounter rate multiplied by kill probability);
- m: per-capita mortality rate of the predator in the absence of prey;
- b: biomass conversion efficiency from consumed prey to new predator biomass.

The right-hand side of (1) is of class C^∞ on $\mathbb{R}^2$, and hence locally Lipschitz. By the Picard–Lindelöf theorem, for every initial condition $(x_0, y_0) \in \mathbb{R}^2_{>0}$ there exists a unique maximal solution. The following proposition establishes that this solution is, in fact, global.

Proposition 2.1 (Positive invariance and global existence)**.** *For every initial condition $(x_0, y_0) \in \mathbb{R}^2_{>0}$, the unique solution $(x(t), y(t))$ of (1) remains in $\mathbb{R}^2_{>0}$ for all $t \geq 0$ and exists for all finite time.*

Proof. On the invariant boundary ray $\{x = 0,\, y > 0\}$ one has $\dot{x} = 0$, and on $\{y = 0,\, x > 0\}$ one has $\dot{y} = 0$. Hence the coordinate axes are forward-invariant, which prevents any trajectory starting in $\mathbb{R}^2_{>0}$ from reaching the boundary in finite time. Boundedness of the maximal solution on compact time intervals follows from the first integral established in Proposition 2.2 below, which shows that every orbit lies on a compact level set of a coercive function. Global existence then follows from the standard continuation theorem for ODEs [11, Theorem II.3.1]. □

Equilibria and linearization

Setting $\dot{x} = \dot{y} = 0$ yields exactly two equilibria in $\mathbb{R}^2_{\geq 0}$:
1. *Trivial equilibrium:* $E_0 = (0, 0)$.
2. *Interior (coexistence) equilibrium:* $E^* = \big(m/b,\ r/a\big) \in \mathbb{R}^2_{>0}$.
   The Jacobian of the vector field evaluated at E^* is

$$J(E^*) = \begin{pmatrix} 0 & -am/b \\ br/a & 0 \end{pmatrix}, \tag{2}$$

with characteristic polynomial $\lambda^2 + rm = 0$ and eigenvalues $\lambda_{1,2} = \pm i\sqrt{rm}$. Since $\operatorname{tr} J(E^*) = 0$ and $\det J(E^*) = rm > 0$, the linearization classifies E^* as a *center*, which is consistent with (but does not prove) nonlinear neutral stability. Global center stability is established through the following conserved quantity.

Proposition 2.2 (First integral and global center structure)**.** *The function $H\colon \mathbb{R}^2_{>0} \to \mathbb{R}$ defined by*

$$H(x, y) \ = \ bx - m \ln x + ay - r \ln y \tag{3}$$

is a first integral of (1): $\dot{H}(x(t), y(t)) = 0$ for every solution. Moreover, H is strictly convex on $\mathbb{R}^2_{>0}$ with a unique global minimum at E^*, and H is coercive. Consequently, for every $c > H(E^*)$ the sublevel set $\{H \leq c\}$ is a compact, connected region containing E^*, whose boundary (the level set *$\{H = c\}$) is a simple closed curve in $\mathbb{R}^2_{>0}$ surrounding E^*; all orbits of (1) in $\mathbb{R}^2_{>0}$ are periodic and surround E^*.*

Proof. A direct calculation gives

$$\begin{aligned} \frac{dH}{dt} &= \Big(b - \frac{m}{x}\Big)\dot{x} + \Big(a - \frac{r}{y}\Big)\dot{y} \\ &= \Big(b - \frac{m}{x}\Big)(rx - axy) + \Big(a - \frac{r}{y}\Big)(-my + bxy) \\ &= (bx - m)(r - ay) + (ay - r)(-m + bx) \\ &= (bx - m)(r - ay) - (r - ay)(bx - m) \ = \ 0. \end{aligned}$$

Strict convexity of H on $\mathbb{R}^2_{>0}$ follows from the computation $\nabla^2 H = \operatorname{diag}\big(m/x^2,\ r/y^2\big)$, which is positive definite for all $(x, y) \in \mathbb{R}^2_{>0}$. The unique minimum of H is attained at $\nabla H = 0$, i.e., at $(x, y) = (m/b,\ r/a) = E^*$. Compactness of sublevel sets follows from the coercivity of H (i.e., $H(x, y) \to +\infty$ as $x \to 0^+$, $y \to 0^+$, $x \to +\infty$, or $y \to +\infty$). For $c > H(E^*)$ the sublevel set $\{H \leq c\}$ is thus a compact convex region, and its boundary $\{H = c\}$ is a simple closed curve. Since H is constant on every orbit, each orbit lies in a level set; being confined to a compact simple closed curve free of equilibria, every orbit in $\mathbb{R}^2_{>0} \setminus \{E^*\}$ traverses the full curve and is periodic. □

Corollary 2.3 (Period formula near E^*)**.** *The angular frequency of small-amplitude oscillations near E^* is $\omega_0 = \sqrt{rm}$, so the period satisfies*

$$T(\varepsilon) = \frac{2\pi}{\sqrt{rm}}\big(1 + O(\varepsilon^2)\big),$$

where $\varepsilon > 0$ measures the amplitude of the orbit about E^*.

Proof. The linearization (2) has eigenvalues $\pm i\sqrt{rm}$, giving the leading period $2\pi/\sqrt{rm}$. For the order of the correction, pass to the variables $(p, q) = (\ln x, \ln y)$, in which (1) becomes the canonical analytic Hamiltonian system $\dot{p} = -\partial_q \widetilde{H}$, $\dot{q} = \partial_p \widetilde{H}$ with $\widetilde{H}(p, q) = be^p - mp + ae^q - rq$, possessing a nondegenerate minimum h_0 at $(\ln(m/b), \ln(r/a))$. For a one-degree-of-freedom analytic Hamiltonian near a nondegenerate center, the period of the orbit on the energy level h is an analytic function $T(h)$ of h near h_0 (equivalently, in Birkhoff normal form the period depends only on the value of the energy; see [17, Section 8.2]). Since $\widetilde{H} - h_0$ vanishes quadratically at the minimum, an orbit whose amplitude about E^* is of order ε has $h - h_0 = O(\varepsilon^2)$, and therefore

$$T(\varepsilon) = T(h_0) + O(h - h_0) = \frac{2\pi}{\sqrt{rm}}\big(1 + O(\varepsilon^2)\big).$$

In particular the first amplitude correction to the period is of order ε^2; its explicit coefficient follows from the third-order normal form and is not needed here. □

Remark 2.4 (Saddle structure at E_0)**.** *Complementing the forward-invariance of $\mathbb{R}^2_{>0}$ in Proposition 2.1: at $E_0 = (0, 0)$ the Jacobian is* $\operatorname{diag}(r, -m)$*, with eigenvalues $r > 0$ and $-m < 0$, so E_0 is a hyperbolic saddle whose stable manifold is the*

y-axis. Consequently no trajectory originating in the open quadrant $\mathbb{R}^2_{>0}$ approaches E_0 in forward time.

Figure 1 illustrates the time series and phase portrait for the representative parameter set $(r, a, m, b) = (1.0,\ 0.1,\ 0.5,\ 0.05)$ with initial condition $(x_0, y_0) = (10,\ 5)$, giving $E^* = (10,\ 10)$ and $T = 2\pi/\sqrt{0.5} \approx 8.89$.

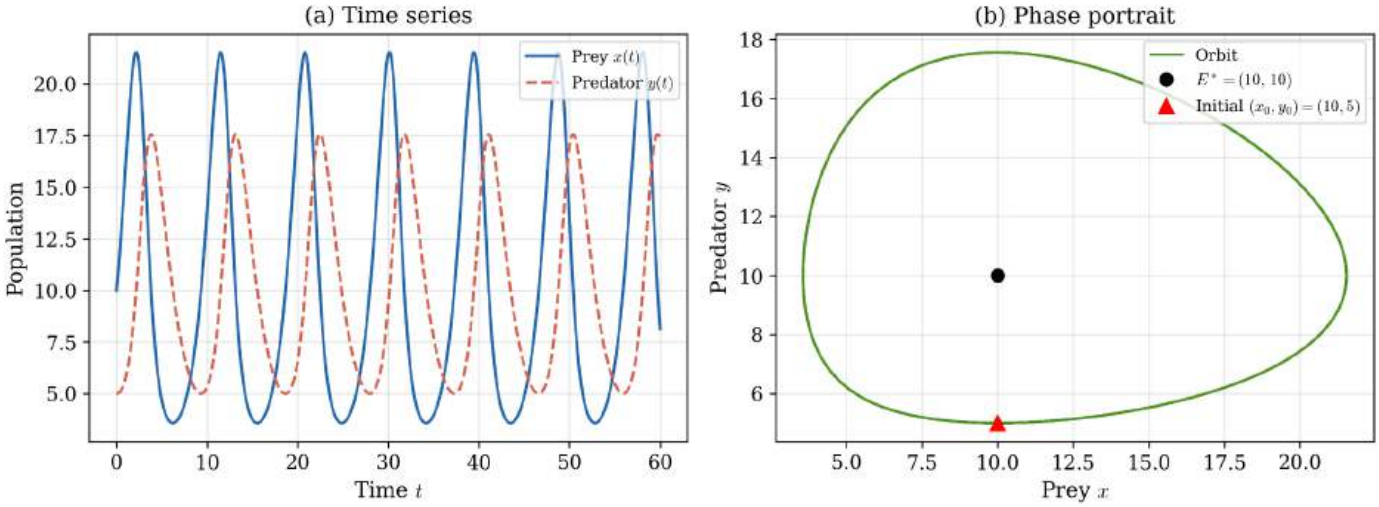


Figure 1. Numerical simulation of the Lotka–Volterra system (1) with $(r, a, m, b) = (1.0, 0.1, 0.5, 0.05)$ and $(x_0, y_0) = (10, 5)$. **(a)** Time series: prey (blue, solid) and predator (red, dashed) exhibit anti-correlated periodic oscillations with period $T = 2\pi/\sqrt{0.5} \approx 8.89$. **(b)** Phase portrait: the closed orbit surrounds the center equilibrium $E^* = (10, 10)$ (filled circle), confirming the conservative structure established in Proposition 2.2.

2.2 Extension I: Logistic Prey Growth (Rosenzweig–MacArthur Model)

The basic model (1) assumes both that the prey population grows without bound in the absence of predation and that predators consume prey at a rate linear in prey density. Both idealizations are ecologically unrealistic. Imposing a prey carrying capacity $K > 0$ *and* a saturating Holling type II functional response $g(x) = ax/(1 + ahx)$ (with handling time $h > 0$) yields the genuine *Rosenzweig–MacArthur* system:

$$\frac{dx}{dt} = rx\Big(1 - \frac{x}{K}\Big) - \frac{axy}{1 + ahx}, \tag{4a}$$

$$\frac{dy}{dt} = -my + \frac{bxy}{1 + ahx}. \tag{4b}$$

A linear functional response ($h = 0$) does not produce sustained oscillations: the interior equilibrium then has trace $-rm/(bK) < 0$ for all K and is globally attracting. The saturation $h > 0$ is precisely what destabilizes the equilibrium and generates the limit cycle below.

Proposition 2.5 (Hopf bifurcation and paradox of enrichment)**.** *Assume $b > mah$, so that the predator nullcline admits the positive root*

$$x^* = \frac{m}{b - mah},$$

and assume $K > x^*$. Then (4) has a unique interior equilibrium $E^* = (x^*, y^*) \in \mathbb{R}^2_{>0}$ with $y^* = \frac{r}{a}\big(1 - \frac{x^*}{K}\big)\big(1 + ahx^*\big)$. Let

$$x_M = \tfrac{1}{2}\big(K - \tfrac{1}{ah}\big)$$

denote the location of the maximum of the prey nullcline, and set $K_c = 2x^* + \frac{1}{ah}$ (equivalently, K_c is the value of K at which $x_M = x^*$). Then:

(i) *If $K < K_c$ (so $x^* > x_M$, the equilibrium lies on the decreasing branch of the prey nullcline), then E^* is locally asymptotically stable.*
(ii) *At $K = K_c$ ($x^* = x_M$) a Hopf bifurcation occurs.*
(iii) *If $K > K_c$ ($x^* < x_M$), then E^* is unstable and is surrounded by a stable limit cycle (the* paradox of enrichment *[27]).*

Proof. The predator nullcline $-m + bx/(1 + ahx) = 0$ gives $x^* = m/(b - mah)$, independent of K; the prey nullcline $r(1 - x/K) = ay/(1 + ahx)$ then gives y^*, positive iff $x^* < K$. Writing $g(x) = ax/(1 + ahx)$ so that $g'(x) = a/(1 + ahx)^2$,

the Jacobian at E^* is

$$J(E^*) = \begin{pmatrix} r\left(1 - \frac{2x^*}{K}\right) - y^* g'(x^*) & -g(x^*) \\ b\, y^*\, g'(x^*)/a & 0 \end{pmatrix},$$

where the $(2,2)$-entry vanishes because $-m + bx^*/(1+ahx^*) = 0$. Hence $\det J(E^*) = g(x^*)\, b\, y^* g'(x^*)/a > 0$, so E^* is nondegenerate, and $\operatorname{tr} J(E^*)$ equals the $(1,1)$-entry. Using $y^* a/(1+ahx^*) = r(1 - x^*/K)$ from the prey nullcline,

$$\operatorname{tr} J(E^*) = r\left(1 - \frac{2x^*}{K}\right) - \frac{r\,(1 - x^*/K)}{1 + ahx^*},$$

which vanishes exactly when $x^* = x_M = \frac{1}{2}(K - 1/(ah))$, i.e. at $K = K_c$; it is negative for $K < K_c$ (so E^* is stable) and positive for $K > K_c$ (so E^* is unstable). At $K = K_c$ the eigenvalues are purely imaginary, and $\partial_K[\operatorname{tr} J]_{K=K_c} \neq 0$ since x_M is strictly increasing in K while x^* is fixed, verifying the transversality condition. The sign of the first Lyapunov coefficient, which determines super- versus subcriticality of the bifurcating cycle, may be computed by the standard formula in [17, Section 8.2] and is generically negative, giving the stable limit cycle of case (iii). □

2.3 Extension II: Two-Species Lotka–Volterra Competition

For two species competing for a common resource, the Lotka–Volterra competition model takes the form

$$\frac{dx_1}{dt} = r_1 x_1 \left(1 - \frac{x_1 + \alpha_{12} x_2}{K_1}\right), \tag{5a}$$

$$\frac{dx_2}{dt} = r_2 x_2 \left(1 - \frac{x_2 + \alpha_{21} x_1}{K_2}\right), \tag{5b}$$

where $\alpha_{12} > 0$ (respectively $\alpha_{21} > 0$) is the per-capita competitive effect of species 2 (respectively species 1). The long-time behavior of (5) is determined entirely by the geometry of the two nullclines: stable coexistence occurs if and only if $\alpha_{12}\alpha_{21} < 1$ together with $K_1/\alpha_{12} > K_2$ and $K_2/\alpha_{21} > K_1$; otherwise one species excludes the other (competitive exclusion principle) [23, Chapter 3].

2.4 Extension III: Reaction – Diffusion Generalization

Incorporating random dispersal over a bounded spatial domain $\Omega \subset \mathbb{R}^n$ (with smooth boundary $\partial\Omega$) yields the reaction–diffusion system

$$\frac{\partial x}{\partial t} = rx\left(1 - \frac{x}{K}\right) - \frac{axy}{1+ahx} + D_x \nabla^2 x, \qquad (z,t) \in \Omega \times (0,\infty), \tag{6a}$$

$$\frac{\partial y}{\partial t} = -my + \frac{bxy}{1+ahx} + D_y \nabla^2 y, \tag{6b}$$

with Neumann boundary conditions $\partial_n x = \partial_n y = 0$ on $\partial\Omega$, where $D_x, D_y > 0$ are diffusion coefficients and ∇^2 denotes the Laplace–Beltrami operator on Ω. The spatially uniform equilibrium corresponding to E^* of Proposition 2.5 can become unstable with respect to spatially heterogeneous perturbations when $D_y \gg D_x$, generating stationary Turing patterns even when E^* is linearly stable in the spatially homogeneous ODE [24, Chapter 2]. In the economic context analyzed in Section 3.3, such diffusion-driven instabilities correspond to the spatial concentration and clustering of industrial productive activity.

3 Predator-Prey Models in Economics

3.1 The Goodwin Growth-Cycle Model

The model of Goodwin [10] embeds the Lotka–Volterra structure within a one-sector macroeconomic growth model under the following structural assumptions.

Assumption 3.1 (Goodwin model hypotheses)**.** (G1) *The capital–output ratio $\nu > 0$ is fixed (Leontief technology).*
(G2) *The savings rate $s \in (0,1)$ applies exclusively to profit income.*
(G3) *Labor productivity grows at the exogenous rate $\alpha > 0$, and the labor force grows at the exogenous rate $\beta > 0$.*
(G4) *The real wage adjusts according to the Phillips curve $\phi(v) = -\gamma + \rho v$ for constants $\gamma, \rho > 0$.*

Under Assumption 3.1, define the *wage share* and *employment rate*:

$$\omega(t) \;\equiv\; \frac{w(t)L(t)}{Y(t)} \in (0,1), \qquad v(t) \;\equiv\; \frac{L(t)}{N(t)} \in (0,1), \tag{7}$$

where w, L, Y, and N denote, respectively, the real wage, employment, aggregate output, and labor force. Standard

manipulations of the national-income accounting identities yield the following system (see [10, 12] for derivation):

$$\frac{d\omega}{dt} = \omega\big[\phi(v) - \alpha\big] = \omega\big[-(\gamma+\alpha) + \rho v\big], \tag{8a}$$

$$\frac{dv}{dt} = v\left[\frac{s(1-\omega)}{\nu} - (\alpha+\beta)\right], \tag{8b}$$

where $\alpha > 0$ is the rate of labor-productivity growth introduced in Assumption 3.1 (G3); we use the single symbol α for this primitive throughout.

Proposition 3.2 (Algebraic isomorphism with Lotka–Volterra)**.** *Under Assumption 3.1 and the hypothesis $s/\nu > \alpha + \beta$ (i.e., the warranted growth rate exceeds the natural growth rate), system (8) is algebraically identical to (1) under the parameter correspondence*

$$x \leftrightarrow v, \quad y \leftrightarrow \omega, \quad r \leftrightarrow \tfrac{s}{\nu} - (\alpha+\beta), \quad a \leftrightarrow \tfrac{s}{\nu}, \quad m \leftrightarrow \gamma + \alpha, \quad b \leftrightarrow \rho. \tag{9}$$

Consequently, the system (8) admits the first integral

$$H_{\mathrm{GW}}(v,\omega) = \tfrac{s}{\nu}\, v - (\gamma+\alpha)\ln v + \tfrac{s}{\nu}\,\omega - \big[\tfrac{s}{\nu} - (\alpha+\beta)\big]\ln\omega, \tag{10}$$

and every orbit in $(v,\omega) \in (0,1)^2$ is a closed curve surrounding the unique interior equilibrium

$$v^* = \frac{\gamma+\alpha}{\rho}, \qquad \omega^* = 1 - \frac{(\alpha+\beta)\nu}{s}. \tag{11}$$

Proof. Direct substitution of the correspondence (9) into (1) recovers (8) exactly. The existence, uniqueness, and positivity of the interior equilibrium (11) follow from the parameter conditions imposed. The first integral (10) is then the Hamiltonian (3) under the same substitution; its strict convexity and the periodicity of all orbits follow from Proposition 2.2. □

Economic interpretation

The Goodwin mechanism operates through the following four-phase closed feedback loop, which requires no exogenous shocks (see [6, 12]):

1. High profit share ⇒ rapid capital accumulation ⇒ rising employment rate v.
2. Rising v ⇒ tighter labor markets ⇒ rising wage share ω.
3. Rising ω ⇒ profit share compressed ⇒ investment falls ⇒ v declines.
4. Falling v ⇒ wage demands moderate ⇒ ω falls ⇒ profit share recovers.

Figure 2 presents a numerical simulation of (8) for the parameter values $\alpha = 0.03$, $\beta = 0.02$, $\rho = 1/15 \approx 0.0667$, $\gamma = 0.03$, $s = 0.8$, $\nu = 3.0$, $(v_0, \omega_0) = (0.90, 0.79)$. With these values, (11) gives the interior equilibrium $E^* = (v^*, \omega^*) = (0.900, 0.8125)$, and the small-amplitude period is $T = 2\pi/\sqrt{rm} \approx 55$ years.

3.2 Extension: Investment Accelerator and Hopf Bifurcation

Desai et al. [6] replace the linear savings function in (8) with a nonlinear investment function $I\colon (0,1) \to \mathbb{R}_{>0}$ that responds to the profit share $\pi = 1 - \omega$:

$$\frac{d\omega}{dt} = \omega\big[\phi(v) - (\alpha + \pi_0)\big], \tag{12a}$$

$$\frac{dv}{dt} = v\left[\frac{I(1-\omega)}{\nu} - (\alpha+\beta)\right]. \tag{12b}$$

A strictly convex function $I(\cdot)$ (i.e., $I'' > 0$) introduces asymmetric nonlinearity that generically destroys the conservative center structure of (8). Depending on the sign of the first Lyapunov coefficient at the Hopf bifurcation point, the system either possesses a globally attracting limit cycle (supercritical case) or exhibits a locally unstable limit cycle surrounding a stable equilibrium (subcritical case). This richer dynamical behavior is more consistent with the empirically observed amplitude variation across business cycles [6].

3.3 Three-Trophic Sectoral Model

Crookes and Blignaut [5] apply a three-trophic-level predator–prey model to the South African industrial supply chain, in which the automotive sector (top predator) depends on steel (mesopredator), which in turn depends on iron ore (primary prey). Denoting iron ore output, steel production, and automotive output by $I(t)$, $S(t)$, and $A(t)$, respectively,

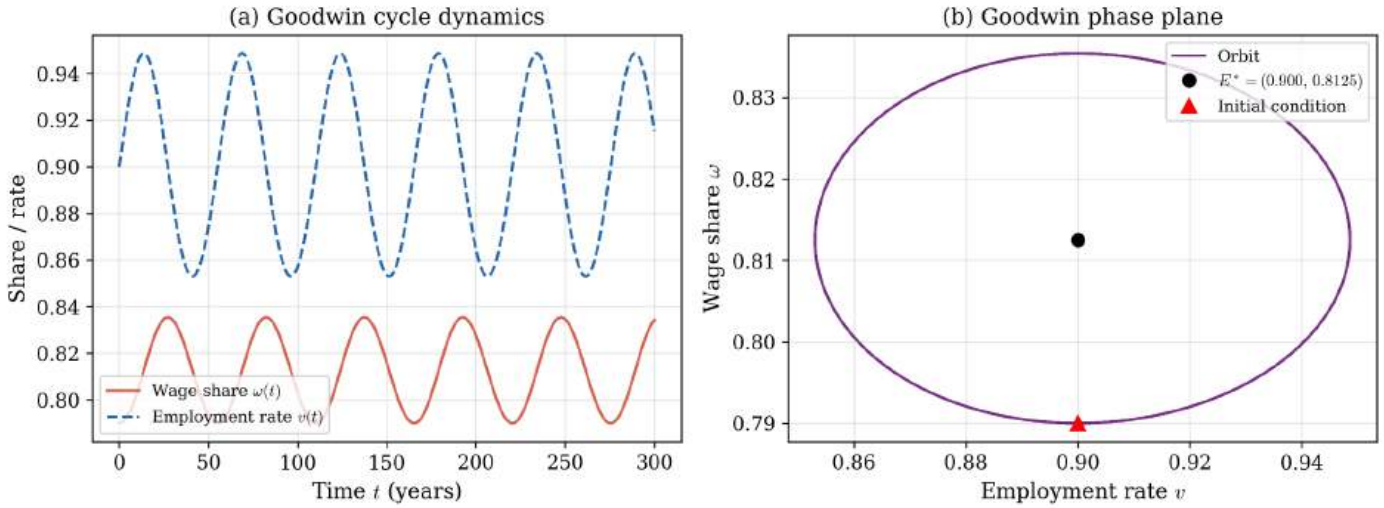


Figure 2. Numerical simulation of the Goodwin model (8) with $\alpha = 0.03$, $\beta = 0.02$, $\rho = 1/15 \approx 0.0667$, $\gamma = 0.03$, $s = 0.8$, $\nu = 3.0$, and $(v_0, \omega_0) = (0.90, 0.79)$. With these parameters, (11) yields $E^* = (v^*, \omega^*) = (0.900,\ 0.8125)$, which is the center about which the orbit closes. **(a)** Time series: the employment rate (blue, dashed) leads the wage share (red, solid) by approximately a quarter-period, reproducing the counter-cyclical profit-share dynamics documented in OECD data by Harvie [12]. **(b)** Phase portrait: the closed orbit in the (v, ω)-plane surrounds the center equilibrium (11) (filled circle), confirming the conservative Lotka–Volterra structure established in Proposition 3.2.

the system is:

$$\frac{dI}{dt} = r_I I - a_{IS} IS, \tag{13a}$$

$$\frac{dS}{dt} = -m_S S + b_{IS} IS - a_{SA} SA, \tag{13b}$$

$$\frac{dA}{dt} = -m_A A + b_{SA} SA, \tag{13c}$$

where all parameters are positive. Calibration of (13) to South African production indices for the period 1970–2010 yielded goodness-of-fit $R^2 > 0.85$ for the cyclical component [5], confirming the quantitative applicability of the trophic-cascade interpretation to industrial supply chains. We include this three-trophic model not as a new contribution but as a building block: it establishes the three-species predator–prey template that the financial super-predator system of Section 4.3 adapts to the debt–capital–intermediary setting.

Table 1. Predator–prey mappings in the economic applications of this paper. All models in rows 1–4 are derived or surveyed in Sections 3 and 4.

Model	Prey	Predator	Key analytical result
Goodwin [10]	Employment rate v	Wage share ω	Conservative center; Prop. 3.2
Desai et al. [6]	Employment v	Wage share ω	Hopf bifurcation; limit cycles
Crookes and Blignaut [5]	Iron ore / Steel	Steel / Automotive	Sectoral margin cycles; $R^2 > 0.85$
Addison et al. [1]	Buying stock B	Selling stock S	Oscillatory asset returns

4 Financial Market Applications

4.1 Buyer–Seller Dynamics and Asset Prices

We recall the buyer–seller model of Montero [22] (a preprint) not as a new result but because it is the deterministic backbone of the finite-size stochastic market model analyzed in Section 5, where our mean-field convergence theorem (Theorem 5.1) is the novel contribution. Montero [22] models a financial market as a two-species Lotka–Volterra system in

which the aggregate population of buyers $B(t) > 0$ and sellers $S(t) > 0$ interact as prey and predator, respectively:

$$\frac{dB}{dt} = r_B B - a_{BS} BS, \tag{14a}$$

$$\frac{dS}{dt} = -m_S S + b_{BS} BS. \tag{14b}$$

By the isomorphism established in Proposition 2.2 (applied with $x \leftrightarrow B$, $y \leftrightarrow S$, $r \leftrightarrow r_B$, $a \leftrightarrow a_{BS}$, $m \leftrightarrow m_S$, $b \leftrightarrow b_{BS}$), all orbits of (14) in $\mathbb{R}^2_{>0}$ are closed, with interior equilibrium

$$B^* = \frac{m_S}{b_{BS}}, \qquad S^* = \frac{r_B}{a_{BS}}.$$

The asset price $P(t)$ is coupled to the order imbalance via the standard price-impact equation:

$$\frac{dP}{dt} = \eta\big[B(t) - S(t)\big], \quad \eta > 0, \tag{15}$$

where η is the price-impact coefficient (denoted by a symbol distinct from the eigenvalue λ used elsewhere). Since $B(t) - S(t)$ oscillates periodically with angular frequency $\omega_0 = \sqrt{r_B m_S}$, the price $P(t)$ oscillates with the same fundamental frequency; the buyer and seller populations are a quarter-cycle out of phase, so the joint trajectory $(B(t), S(t), P(t))$ is a closed, non-planar periodic curve in $\mathbb{R}^3_{>0}$. (We avoid the term "Lissajous", which strictly denotes superposed sinusoids; Lotka–Volterra cycles are periodic but anharmonic.)

Remark 4.1 (Stochastic perturbations and fat-tailed returns)**.** *Multiplicative noise of intensity $\sigma > 0$ applied to (14) destroys the neutrally stable center and produces a diffusing process. Numerical evidence in [22] demonstrates that the resulting price process generates return distributions with excess kurtosis in the range $[3, 7]$, consistent with empirically documented fat tails for daily returns on major equity indices. The rigorous stochastic generalization is developed in Section 5.*

4.2 Debt–Capital Dynamics and the Minsky Hypothesis

Economic background

Minsky's Financial Instability Hypothesis [21] asserts that endogenous financial fragility accumulates during periods of sustained economic expansion: firms migrate from *hedge finance* (cash flows cover all debt obligations), through *speculative finance* (cash flows cover interest but not principal), to *Ponzi finance* (cash flows cover neither), until a *Minsky moment*—a sudden debt-deflation crisis—occurs. This narrative has a natural formalization as a predator–prey ODE, as developed below.

Model derivation from first principles

Let $C(t) > 0$ denote the aggregate stock of productive (non-financial) capital and $D(t) > 0$ the aggregate stock of outstanding debt (bonds, loans, and leveraged positions). We impose the following structural assumptions.

Assumption 4.2 (Debt–capital model)**.** (DC1) *(Autonomous capital growth). In the absence of debt, capital grows at the net rate $r_C > 0$ (gross return less depreciation).*

(DC2) *(Autonomous debt contraction). In the absence of productive capital to finance, the debt stock* contracts *at the net rate $r_D > 0$ (amortization and default dominate when there are no profitable assets to lend against).*

(DC3) *(Predatory interaction on capital). Each unit of debt–capital interaction reduces the net rate of capital accumulation by $a_{DC} > 0$, reflecting debt-service obligations that crowd out investment.*

(DC4) *(Debt feeds on capital). Each unit of debt–capital interaction* increases *the net rate of debt expansion by $b_{DC} > 0$, reflecting the tendency of profitable capital to attract new lending.*

Remark 4.3. *Under Assumption 4.2, the debt–capital interaction reduces $\dot{C}$ (via debt service crowding out investment) while it* increases *$\dot{D}$ (profitable capital attracting new lending). This is the genuine predator–prey sign structure, placing D in the role of predator and C in the role of prey, consistently with [15]. We note in passing that the alternative* competition*-type specification, in which the interaction reduces both $\dot{C}$ and $\dot{D}$, does* not *admit a Lotka–Volterra first integral and is therefore rejected on sign-structure grounds; the predator–prey form below is the appropriate model.*

Under Assumption 4.2, the debt–capital predator–prey system is

$$\dot{C} = r_C\, C - a_{DC}\, CD, \tag{16a}$$

$$\dot{D} = -r_D\, D + b_{DC}\, CD, \tag{16b}$$

with $C(t) > 0$ the stock of productive capital (prey), $D(t) > 0$ the stock of outstanding debt (predator), and parameters $r_C, r_D, a_{DC}, b_{DC} > 0$. Capital grows autonomously at rate r_C and is eroded by debt service through the interaction $a_{DC}CD$; debt *contracts* autonomously at rate r_D (amortization and default dominate in the absence of profitable capital to finance) and *expands* by feeding on capital through $b_{DC}CD$.

Theorem 4.4 (Conservative structure and noise-induced fragility of the debt–capital system)**.** *For system* (16) *with all parameters positive, the following hold.*

(i) ***(Interior equilibrium and center.)*** *The system has a unique interior equilibrium*

$$E^* = (C^*, D^*) = \left(\tfrac{r_D}{b_{DC}}, \tfrac{r_C}{a_{DC}}\right) \in \mathbb{R}^2_{>0},$$

and the Jacobian there is

$$J(E^*) = \begin{pmatrix} 0 & -a_{DC}C^* \\ b_{DC}D^* & 0 \end{pmatrix}, \qquad \operatorname{tr} J(E^*) = 0, \quad \det J(E^*) = r_C r_D > 0,$$

with eigenvalues $\lambda_{1,2} = \pm i\sqrt{r_C r_D}$. Hence E^* is a linear center.

(ii) ***(First integral and global closed-orbit structure.)*** *The function*

$$H(C, D) = b_{DC}\, C - r_D \ln C + a_{DC}\, D - r_C \ln D \tag{17}$$

is a first integral of (16)*: $\dot{H} \equiv 0$ along every solution. Moreover H is strictly convex on $\mathbb{R}^2_{>0}$, with $\nabla^2 H = \operatorname{diag}\big(r_D/C^2,\, r_C/D^2\big) \succ 0$, attains its unique global minimum at E^*, and is coercive. Consequently every orbit of* (16) *in $\mathbb{R}^2_{>0}$ is a closed curve encircling E^*; the equilibrium is Lyapunov stable but not asymptotically stable, and the small-amplitude period is $T = 2\pi/\sqrt{r_C r_D}$.*

(iii) ***(Comparative statics and leverage.)*** *The equilibrium debt level $D^* = r_C/a_{DC}$ is strictly increasing in r_C and strictly decreasing in a_{DC}; the equilibrium capital level $C^* = r_D/b_{DC}$ is strictly increasing in r_D and strictly decreasing in b_{DC}. The equilibrium leverage ratio*

$$\frac{D^*}{C^*} = \frac{b_{DC}\, r_C}{a_{DC}\, r_D}$$

is strictly increasing in r_C and strictly decreasing in r_D.

(iv) ***(Noise-induced fragility: the Minsky mechanism.)*** *Consider the Itô perturbation of* (16)*,*

$$dC = \big(r_C C - a_{DC}CD\big)\, dt + \sigma_C\, C\, dW_t^C, \qquad dD = \big(-r_D D + b_{DC}CD\big)\, dt + \sigma_D\, D\, dW_t^D, \tag{18}$$

where W^C, W^D are independent standard Brownian motions and $\sigma_C, \sigma_D > 0$. Then, for every solution,

$$\frac{d}{dt}\,\mathbb{E}\big[H(C_t, D_t)\big] = \tfrac{1}{2}\big(\sigma_C^2\, r_D + \sigma_D^2\, r_C\big) > 0. \tag{19}$$

The conserved energy of the deterministic center therefore drifts strictly outward under any *noise: the neutral cycles of part* (ii) *are destabilized into ever-larger excursions. Under symmetric noise $\sigma_C = \sigma_D = \sigma$ the drift equals $\frac{1}{2}\sigma^2(r_C + r_D)$, and the excursion is borne disproportionately by the debt coordinate precisely when $r_C > r_D$ (equivalently, when $D^*/C^* > b_{DC}/a_{DC}$), which we identify with the Minskyan high-debt regime.*

Remark 4.5. *Part* (iv) *replaces the informal claim that $r_D > r_C$ is* necessary and sufficient *for instability. A genuine Lotka–Volterra predator–prey system is a neutral center for* all *positive parameters (part* (ii)*), and the stochastic energy drift* (19) *is positive for* all *positive parameters; hence no deterministic r_D-versus-r_C stability threshold exists. The economically meaningful role of r_C relative to r_D is comparative—it governs equilibrium leverage (part* (iii)*) and the direction in which noise-driven excursions predominate (part* (iv)*)—rather than a switch between stable and unstable regimes. We also emphasize the probabilistic scope of part* (iv)*: the drift identity* (19) *concerns the* expectation *of H and does not by itself assert almost-sure outward migration of every sample path; pathwise statements would require a separate analysis of the martingale fluctuations and are not claimed here. The Monte-Carlo experiment of Figure 3(c) corroborates the mean drift.*

Proof. (i) Setting the right-hand sides of (16) to zero gives $C\,(r_C - a_{DC}D) = 0$ and $D\,(-r_D + b_{DC}C) = 0$. In $\mathbb{R}^2_{>0}$ this forces $r_C - a_{DC}D = 0$ and $-r_D + b_{DC}C = 0$, i.e. $D^* = r_C/a_{DC}$ and $C^* = r_D/b_{DC}$, which is unique. Writing

$f_1 = r_C C - a_{DC} CD$ and $f_2 = -r_D D + b_{DC} CD$, the Jacobian is

$$J = \begin{pmatrix} r_C - a_{DC} D & -a_{DC} C \\ b_{DC} D & -r_D + b_{DC} C \end{pmatrix}.$$

At E^* the diagonal entries vanish, leaving the stated antidiagonal form; then $\operatorname{tr} J(E^*) = 0$ and $\det J(E^*) = (a_{DC} C^*)(b_{DC} D^*) = r_D r_C > 0$, so $\lambda^2 + r_C r_D = 0$ and $\lambda_{1,2} = \pm i\sqrt{r_C r_D}$.

(ii) Differentiating (17) along solutions,

$$\dot{H} = \left(b_{DC} - \tfrac{r_D}{C}\right)\dot{C} + \left(a_{DC} - \tfrac{r_C}{D}\right)\dot{D}.$$

Substituting $\dot{C} = C(r_C - a_{DC} D)$ and $\dot{D} = D(b_{DC} C - r_D)$ and absorbing the factors C and D,

$$\dot{H} = (b_{DC} C - r_D)(r_C - a_{DC} D) + (a_{DC} D - r_C)(b_{DC} C - r_D).$$

Since $(a_{DC} D - r_C) = -(r_C - a_{DC} D)$, the two products are negatives of one another, so $\dot{H} \equiv 0$. The Hessian $\nabla^2 H = \operatorname{diag}(r_D/C^2,\, r_C/D^2)$ is positive definite on $\mathbb{R}^2_{>0}$, so H is strictly convex; the first-order condition $\nabla H = 0$ gives $b_{DC} = r_D/C$ and $a_{DC} = r_C/D$, i.e. $(C, D) = E^*$, the unique minimizer. Each coordinate contributes a term of the form $\kappa x - \mu \ln x \to +\infty$ as $x \to 0^+$ or $x \to \infty$, so H is coercive and every sublevel set $\{H \le c\}$ is compact. As H is constant on orbits, each level set $\{H = c\}$, $c > H(E^*)$, is invariant; being the boundary of a compact convex sublevel region of a strictly convex coercive function, it is a simple closed curve around E^*. Hence every orbit in $\mathbb{R}^2_{>0}$ is periodic and encircles E^*; H is a (non-strict) Lyapunov function, giving Lyapunov—but not asymptotic—stability since $\dot{H} = 0$. The small-amplitude period follows from the linear angular frequency $\omega_0 = \sqrt{r_C r_D}$ of part (i), so $T = 2\pi/\sqrt{r_C r_D}$.

(iii) Immediate from $D^* = r_C/a_{DC}$ and $C^* = r_D/b_{DC}$ by partial differentiation, with $D^*/C^* = (r_C/a_{DC})(b_{DC}/r_D) = b_{DC} r_C/(a_{DC} r_D)$.

(iv) Apply Itô's formula to $H(C_t, D_t)$ under (18). Because H has no mixed second derivative and the driving noises are independent,

$$dH = \underbrace{\left(H_C f_1 + H_D f_2\right)}_{=\dot{H}=0} dt + \tfrac{1}{2}\left(H_{CC}\, \sigma_C^2 C^2 + H_{DD}\, \sigma_D^2 D^2\right) dt + H_C\, \sigma_C C\, dW^C + H_D\, \sigma_D D\, dW^D.$$

The deterministic bracket vanishes by part (ii). With $H_{CC} = r_D/C^2$ and $H_{DD} = r_C/D^2$, the Itô correction is state-independent:

$$\tfrac{1}{2}\left(\tfrac{r_D}{C^2}\sigma_C^2 C^2 + \tfrac{r_C}{D^2}\sigma_D^2 D^2\right) dt = \tfrac{1}{2}\left(\sigma_C^2 r_D + \sigma_D^2 r_C\right) dt.$$

The remaining integrals

$$\int_0^t H_C \sigma_C C\, dW^C = \int_0^t (b_{DC} C_s - r_D)\sigma_C\, dW_s^C, \qquad \int_0^t H_D \sigma_D D\, dW^D = \int_0^t (a_{DC} D_s - r_C)\sigma_D\, dW_s^D$$

are martingales: under (18) the processes C_t, D_t admit finite second moments on every compact interval (Lemma 4.6 below), so the integrands lie in $L^2(\Omega \times [0,T])$ and the Itô integrals have zero expectation. Taking expectations therefore yields (19). Since $\sigma_C^2 r_D + \sigma_D^2 r_C > 0$, $\mathbb{E}[H(C_t, D_t)]$ is strictly increasing, i.e. *in expectation* the energy migrates to ever-larger values (equivalently, in mean the process occupies ever-larger sublevel sets of H). Under $\sigma_C = \sigma_D = \sigma$ the rate is $\tfrac{1}{2}\sigma^2(r_C + r_D)$; the local flatness of H in the debt direction near E^* scales as $H_{DD}^{-1/2} = \sqrt{r_C}/a_{DC}$, so the share of the excursion carried by the D-coordinate increases with r_C and dominates the capital excursion when $r_C > r_D$.

□

Lemma 4.6 (Finite second moments)**.** *Let (C_t, D_t) solve (18) from a deterministic initial condition $(C_0, D_0) \in \mathbb{R}^2_{>0}$. Then for every $T > 0$ there is a constant $M_T < \infty$ with $\sup_{0 \le t \le T} \mathbb{E}\left[C_t^2 + D_t^2\right] \le M_T$.*

Proof. For $n \in \mathbb{N}$ let $\tau_n = \inf\{t : C_t + D_t \ge n\}$. On $[0, \tau_n]$, Itô's formula gives $d(C_t^2) = \left(2r_C C_t^2 - 2a_{DC} C_t^2 D_t + \sigma_C^2 C_t^2\right) dt + 2\sigma_C C_t^2\, dW_t^C$, and since $a_{DC} C_t^2 D_t \ge 0$ the capital drift is bounded above by $(2r_C + \sigma_C^2) C_t^2$. The corresponding computation for D_t^2, however, produces the interaction term $+2b_{DC} C_t D_t^2$, whose naive control by Young's inequality introduces a

fourth-order term $C_t^2 D_t^2$ that cannot be dominated by $\mathbb{E}[C_t^2 + D_t^2]$ alone; a pure second-moment Grönwall argument therefore does not close. The estimate is nevertheless valid, and rather than reproving it we import it, with precise scope, from the stochastic Lotka–Volterra literature. The system (18) is exactly of the class treated by Mao et al. [20]: multiplicative (linear) environmental noise on a locally Lipschitz Lotka–Volterra drift. For this class their results establish (a) that solutions started in $\mathbb{R}^2_{>0}$ remain positive and do not explode in finite time almost surely, and (b) that all moments are controlled on compact time intervals, $\sup_{0\le t\le T} \mathbb{E}[C_t^p + D_t^p] < \infty$ for every $p \ge 1$ and $T > 0$; Nguyen and Yin [25] provide sharp refinements of such moment and long-time estimates for stochastic competitive and predator–prey Lotka–Volterra models. We use precisely statement (b) with $p = 2$, which gives the stated bound $M_T < \infty$, while the localisation $\tau_n \to \infty$ a.s. follows from statement (a) together with Fatou's lemma. We emphasize that this lemma is therefore *not* self-contained; its only role is to license the martingale property invoked in the proof of Theorem 4.4(iv). □

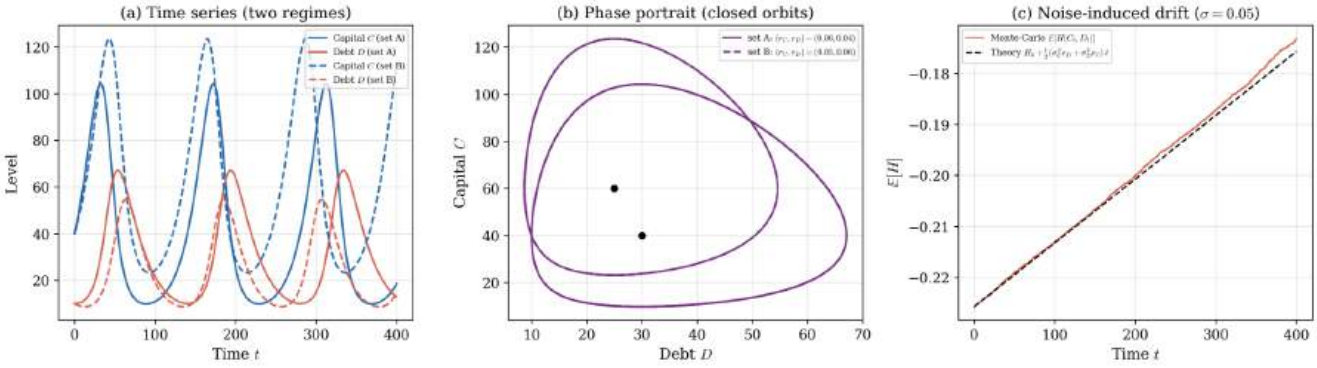


Figure 3. Numerical illustration of the debt–capital predator–prey system (16) and its stochastic perturbation (18), with $(r_C, r_D, a_{DC}, b_{DC}) = (0.06, 0.04, 0.002, 0.001)$ and initial condition $(D_0, C_0) = (10, 40)$. **(a)** Deterministic time series of debt $D(t)$ and capital $C(t)$ for two parameter regimes, illustrating the closed (neutrally stable) cycles guaranteed by Theorem 4.4(ii). **(b)** Phase portrait: every deterministic orbit is a closed curve encircling the interior equilibrium $E^* = (r_D/b_{DC},\, r_C/a_{DC})$ (Theorem 4.4(i)–(ii)). **(c)** Under Itô noise ($\sigma = 0.05$), the expected energy $\mathbb{E}[H(C_t, D_t)]$ drifts strictly outward; the Monte-Carlo estimate (solid) matches the theoretical rate $\frac{1}{2}(\sigma_C^2 r_D + \sigma_D^2 r_C)$ of Theorem 4.4(iv) (dashed), confirming the noise-induced fragility mechanism.

4.3 Three-Species Model: Financial Super-Predators

Motivation

The two-species model (16) captures debt–capital dynamics but abstracts away the role of highly leveraged speculative intermediaries—hedge funds, prime brokers, shadow-banking conduits—which simultaneously extract returns from both productive capital (via collateralized lending and securities financing) and outstanding corporate debt (via securitization and credit-default instruments). These agents constitute a *third trophic level* in the financial ecosystem, which we term *financial super-predators*.

Model formulation

Let $\mathcal{S}(t) > 0$ denote the aggregate activity level of financial super-predators (e.g., total assets under leveraged management, or outstanding repo-market positions). Introducing this third trophic level reorganizes the ecological roles of the first two variables. Whereas in the two-species model (16) debt D is the *predator* feeding on capital, once a super-predator is present both capital C and debt D act as *resources* from which $\mathcal{S}$ extracts returns, while C and D interact competitively. Accordingly C and D each carry autonomous growth and are consumed by $\mathcal{S}$, with $\mathcal{S}$ playing the role of apex predator. We emphasize that the three-species system below is therefore a *distinct* model rather than a direct reduction of (16): setting $\mathcal{S} \equiv 0$ does not recover (16), since the sign of the debt dynamics differs between the two formulations. The three-species system is:

$$\frac{dC}{dt} = r_C C - a_{DC}\, DC - e_{CS}\, C\mathcal{S}, \tag{20a}$$

$$\frac{dD}{dt} = r_D D - b_{DC}\, DC - c_{DS}\, D\mathcal{S}, \tag{20b}$$

$$\frac{d\mathcal{S}}{dt} = -r_{\mathcal{S}}\mathcal{S} + f_{DC}\, DC + g_{CS}\, C\mathcal{S}, \tag{20c}$$

where all parameters $r_C, r_D, r_{\mathcal{S}}, a_{DC}, b_{DC}, e_{CS}, c_{DS}, f_{DC}, g_{CS} > 0$. The term $e_{CS}C\mathcal{S}$ in (20a) represents the rate at which super-predators extract returns from capital (reducing net capital accumulation); $c_{DS}D\mathcal{S}$ in (20b) represents the rate at which super-predators extract returns from debt (reducing net debt expansion); $f_{DC}DC$ and $g_{CS}C\mathcal{S}$ in (20c) represent super-predator growth fueled by debt–capital interactions and direct capital exploitation, respectively. Table 2 collects the notation of this section and of Section 4.2.

Table 2. Notation for the financial models of Section 4. A dash indicates that the symbol does not appear in that model.

Symbol	**Two-species model** (16)	**Three-species model** (20)
r_C	autonomous net growth rate of capital	same
r_D	autonomous contraction rate of debt	autonomous expansion rate of debt
a_{DC}	debt-service drag of the D–C interaction on C	same
b_{DC}	new-lending accrual to D	repayment/deleveraging pressure on D
σ_C, σ_D	noise intensities in (18)	—
$r_{\mathcal{S}}$	—	autonomous decay rate of $\mathcal{S}$
e_{CS}	—	extraction from capital by $\mathcal{S}$
c_{DS}	—	extraction from debt by $\mathcal{S}$
f_{DC}	—	origination margin on D–C interactions accruing to $\mathcal{S}$
g_{CS}	—	direct exploitation of capital by $\mathcal{S}$

Economic microfoundation of the interaction signs

Each bilinear term in (20) embodies a mass-action hypothesis: encounters between two aggregates occur at a rate proportional to the product of their sizes—the same well-mixing idealization used throughout Section 2—and the coefficient measures the value transferred per unit of joint exposure. The economic content of each sign is then as follows. (i) $-a_{DC}DC$ in (20a): exactly as in the two-species model, debt-service obligations crowd out investment in proportion to the joint exposure of debt to capital. (ii) $-b_{DC}DC$ in (20b): in the two-species economy the same interaction *feeds* debt ($+b_{DC}CD$ in (16b)), because banks convert profitable capital into new loans that remain on the measured debt stock. With leveraged intermediaries present, that origination margin is rerouted: securitization and securities financing move newly originated claims off the debt stock D and onto intermediary balance sheets $\mathcal{S}$—captured by the term $+f_{DC}DC$ in (20c)—while amortization and deleveraging pressure on D remain. The net effect of the D–C interaction on D is therefore negative, and the sign reversal relative to (16) is not an ad hoc choice but the accounting counterpart of intermediation: the flow that previously accrued to D now accrues to $\mathcal{S}$. (iii) $-e_{CS}C\mathcal{S}$ and $-c_{DS}D\mathcal{S}$: the super-predator extracts returns from capital (collateralized-lending spreads, securities-financing fees and haircuts) and from debt (securitization spreads, credit-default premia), at rates proportional to its encounters with each resource. (iv) $+f_{DC}DC + g_{CS}C\mathcal{S}$ in (20c): super-predator growth aggregates the intermediation margin on debt–capital origination and the direct exploitation of capital; because part of the extracted value leaks to other sectors (fees, wages, taxes), the growth coefficients need not equal the extraction coefficients. We emphasize that this is a stylized, reduced-form representation: the mapping from $(C, D, \mathcal{S})$ to institutional balance sheets is conceptual, and the purpose of the model is to expose the qualitative consequences of a third trophic layer rather than to provide a calibrated institutional model.

Equilibrium analysis

Setting the right-hand sides of (20) to zero and dividing (20a) and (20b) by $C > 0$ and $D > 0$ respectively, an interior equilibrium $E^{**} = (C^{**}, D^{**}, \mathcal{S}^{**}) \in \mathbb{R}^3_{>0}$ must satisfy

$$r_C = a_{DC}D^{**} + e_{CS}\mathcal{S}^{**}, \qquad r_D = b_{DC}C^{**} + c_{DS}\mathcal{S}^{**}, \qquad r_{\mathcal{S}}\mathcal{S}^{**} = C^{**}\big(f_{DC}D^{**} + g_{CS}\mathcal{S}^{**}\big). \tag{21}$$

The first two conditions express D^{**} and C^{**} as decreasing affine functions of $\mathcal{S}^{**}$,

$$D(\mathcal{S}) = \frac{r_C - e_{CS}\mathcal{S}}{a_{DC}}, \qquad C(\mathcal{S}) = \frac{r_D - c_{DS}\mathcal{S}}{b_{DC}}, \tag{22}$$

positive precisely for $\mathcal{S} < r_C/e_{CS}$ and $\mathcal{S} < r_D/c_{DS}$, respectively. Substituting (22) into the third condition, interior equilibria correspond to roots $\mathcal{S}^{**} \in (0, \bar{\mathcal{S}})$, $\bar{\mathcal{S}} := \min\{r_C/e_{CS}, r_D/c_{DS}\}$, of the quadratic

$$\varphi(\mathcal{S}) := \big(r_D - c_{DS}\mathcal{S}\big)\big[f_{DC}r_C + (a_{DC}g_{CS} - e_{CS}f_{DC})\mathcal{S}\big] - a_{DC}b_{DC}r_{\mathcal{S}}\mathcal{S}. \tag{23}$$

Proposition 4.7 (Existence and uniqueness of the interior equilibrium)**.** *Assume $c_{DS}r_C > e_{CS}r_D$. Then system (20) has exactly one interior equilibrium $E^{**} \in \mathbb{R}^3_{>0}$: $\mathcal{S}^{**}$ is the unique root of φ in $(0, r_D/c_{DS})$, and C^{**}, D^{**} are given by (22).*

Proof. First, $\varphi(0) = r_D f_{DC} r_C > 0$. The assumption $c_{DS} r_C > e_{CS} r_D$ is equivalent to $r_D/c_{DS} < r_C/e_{CS}$, so $\bar{\mathcal{S}} = r_D/c_{DS}$ and $\varphi(\bar{\mathcal{S}}) = -a_{DC} b_{DC} r_{\mathcal{S}} \bar{\mathcal{S}} < 0$. Since φ is a polynomial of degree at most two that is positive at 0 and negative at $\bar{\mathcal{S}}$, it has an odd number of roots, counted with multiplicity, in $(0, \bar{\mathcal{S}})$—hence exactly one. Positivity of C^{**} and D^{**} follows from $\mathcal{S}^{**} < \bar{\mathcal{S}} \le r_C/e_{CS}$ and (22). □

If $c_{DS} r_C \le e_{CS} r_D$ an interior equilibrium may fail to exist; we do not pursue that case. For the parameter set of Figure 4, φ has the unique admissible root $\mathcal{S}^{**} \approx 7.532$, giving $E^{**} \approx (17.404, 22.468, 7.532)$.

Linearization and instability

Writing (20a)–(20b) in Kolmogorov form, $\dot{C} = C(r_C - a_{DC} D - e_{CS} \mathcal{S})$ and $\dot{D} = D(r_D - b_{DC} C - c_{DS} \mathcal{S})$, the per-capita growth rates of C and D vanish at E^{**} by (21); consequently the corresponding diagonal entries of the Jacobian vanish there. Together with $\partial_{\mathcal{S}} \dot{\mathcal{S}}\big|_{E^{**}} = -r_{\mathcal{S}} + g_{CS} C^{**} = -f_{DC} C^{**} D^{**}/\mathcal{S}^{**}$ (again by (21)), the Jacobian of (20) at E^{**} is

$$J(E^{**}) = \begin{pmatrix} 0 & -a_{DC} C^{**} & -e_{CS} C^{**} \\ -b_{DC} D^{**} & 0 & -c_{DS} D^{**} \\ f_{DC} D^{**} + g_{CS} \mathcal{S}^{**} & f_{DC} C^{**} & -\dfrac{f_{DC} C^{**} D^{**}}{\mathcal{S}^{**}} \end{pmatrix}. \tag{24}$$

Its characteristic polynomial is $p(\lambda) = \lambda^3 + p_2 \lambda^2 + p_1 \lambda + p_0$ with $p_2 = -\operatorname{tr} J(E^{**}) = f_{DC} C^{**} D^{**}/\mathcal{S}^{**} > 0$ and $p_0 = -\det J(E^{**})$.

Theorem 4.8 (Instability of interior coexistence and the debt-extinction exponent)**.** *Let all parameters of (20) be positive and assume $c_{DS} r_C > e_{CS} r_D$, so that the interior equilibrium E^{**} of Proposition 4.7 exists and is unique. Then:*

(i) *(No stable interior coexistence.)*

$$\det J(E^{**}) = \frac{C^{**} D^{**}}{\mathcal{S}^{**}} \Big(a_{DC} b_{DC} f_{DC} C^{**} D^{**} + b_{DC} e_{CS} f_{DC} C^{**} \mathcal{S}^{**} + a_{DC} c_{DS} f_{DC} D^{**} \mathcal{S}^{**} + a_{DC} c_{DS} g_{CS} (\mathcal{S}^{**})^2 \Big) > 0, \tag{25}$$

so $p_0 = -\det J(E^{**}) < 0$ and $p(\lambda)$ has a real positive root. Hence E^{**} is unstable for every *choice of positive parameters: no parameter regime renders E^{**} locally asymptotically stable, and no Hopf bifurcation of E^{**} occurs.*

(ii) *(Boundary dynamics.) The face $\{D = 0\}$ is invariant, and on it (20) reduces to the classical Lotka–Volterra pair $\dot{C} = C(r_C - e_{CS} \mathcal{S})$, $\dot{\mathcal{S}} = \mathcal{S}(-r_{\mathcal{S}} + g_{CS} C)$, all of whose orbits in the open face are closed curves around $(\bar{C}, \bar{\mathcal{S}}) = (r_{\mathcal{S}}/g_{CS}, r_C/e_{CS})$ (Proposition 2.2). Along every such closed orbit γ of period T_γ,*

$$\frac{1}{T_\gamma} \oint_\gamma C \, dt = \frac{r_{\mathcal{S}}}{g_{CS}}, \qquad \frac{1}{T_\gamma} \oint_\gamma \mathcal{S} \, dt = \frac{r_C}{e_{CS}}.$$

(iii) *(Uniform transversal exponent.) The transversal Floquet exponent of every boundary orbit γ in the D-direction equals*

$$\lambda_D = r_D - b_{DC} \frac{r_{\mathcal{S}}}{g_{CS}} - c_{DS} \frac{r_C}{e_{CS}}, \tag{26}$$

independently of γ. If $\lambda_D < 0$, every boundary cycle is transversally linearly stable and debt decays exponentially at rate $|\lambda_D|$ near the face; if $\lambda_D > 0$, every boundary cycle is transversally unstable and debt re-invades.

Proof. Part (i). Expanding $\det J(E^{**})$ from (24) along the first row gives (25), a sum of manifestly positive terms (the identity is also readily verified by direct computation). Thus $p(0) = p_0 = -\det J(E^{**}) < 0$ while $p(\lambda) \to +\infty$ as $\lambda \to +\infty$, so p has a real root $\lambda_+ > 0$ and E^{**} has a nontrivial unstable manifold. Equivalently: local asymptotic stability would require all eigenvalues to have negative real parts, which forces $\det J = \lambda_1 \lambda_2 \lambda_3 < 0$ (either three negative real eigenvalues, or one negative real eigenvalue λ_1 and a complex pair $\alpha \pm i\beta$ with $\alpha < 0$, giving $\det J = \lambda_1(\alpha^2 + \beta^2) < 0$); this contradicts (25). Since (25) holds for all positive parameters, no stability boundary—and in particular no Hopf bifurcation of E^{**}—exists.

Part (ii). On $\{D = 0\}$ we have $\dot{D} = 0$, so the face is invariant, and the restricted system is the stated Lotka–Volterra pair, to which Proposition 2.2 applies under the correspondence $(x, y, r, a, m, b) \mapsto (C, \mathcal{S}, r_C, e_{CS}, r_{\mathcal{S}}, g_{CS})$. For the averages, integrate $\frac{d}{dt} \ln \mathcal{S} = -r_{\mathcal{S}} + g_{CS} C$ over one period of γ: periodicity gives $0 = -r_{\mathcal{S}} T_\gamma + g_{CS} \oint_\gamma C \, dt$, i.e. the first identity; the second follows in the same way from $\frac{d}{dt} \ln C = r_C - e_{CS} \mathcal{S}$.

Part (iii). Linearizing the D-equation of (20) about a boundary solution $(C(t), 0, \mathcal{S}(t))$ on γ gives the scalar variational equation $\dot{D} = D\,[\, r_D - b_{DC} C(t) - c_{DS} \mathcal{S}(t) \,]$, so the transversal Floquet multiplier over one period is $\exp\big(\int_0^{T_\gamma} (r_D -$

$b_{DC}C - c_{DS}\mathcal{S})\,dt\big) = \exp(T_\gamma \lambda_D)$ by the averages of part (ii). The value (26) is independent of γ because the averages are. Transversal linear stability (resp. instability) of γ is equivalent to this multiplier being smaller (resp. larger) than one, i.e. to $\lambda_D < 0$ (resp. $\lambda_D > 0$). □

Remark 4.9 (Numerical verification)**.** *For the parameter set of Figure 4, $E^{**} \approx (17.404, 22.468, 7.532)$ and the eigenvalues of (24) are $\{+0.0324,\ -0.0175 \pm 0.0201\,i\}$: a saddle-focus, as guaranteed by part (i). The extinction exponent is $\lambda_D = 0.04 - 0.001 \cdot 20 - 0.003 \cdot 30 = -0.070 < 0$, predicting exponential extinction of debt near the boundary cycles; the empirical decay rate of $\ln D(t)$ in the simulation of Figure 4 over $t \in [200, 550]$ is ≈ -0.075, in agreement with (26).*

Remark 4.10 (Outlook: cyclical and complex dynamics in damped variants)**.** *Theorem 4.8(i) rules out Hopf bifurcations of the interior equilibrium for (20) itself. Damped variants—for instance, logistic self-limitation of capital, which reintroduces a negative diagonal entry in the Jacobian—can in principle support stable coexistence, Hopf bifurcations, and the period-doubling routes to complex dynamics documented for three-species Lotka–Volterra systems by Gardini et al. [8] and classified by Zeeman [31]. Whether a financial super-predator variant of this type exhibits such a route is an open question that we leave for future work; we emphasize that the present model and Figure 4 exhibit no such route (there $\lambda_D < 0$ and the long-run behaviour is a boundary cycle), and we accordingly make no chaos claim for (20).*

Economic implications of Theorem 4.8

1. *No stable coexistence.* The presence of a financial super-predator makes balanced interior coexistence of productive capital, debt, and intermediation structurally impossible: instability of E^{**} holds for *all* positive parameters, in sharp contrast to the two-species model, whose interior equilibrium is a neutral center for all positive parameters (Theorem 4.4). Fragility here is intrinsic to the trophic structure, not a matter of parameter values.
2. *A sharp debt-extinction criterion.* The closed-form exponent (26) decides the fate of the debt market near the boundary regime: ordinary credit survives only if its autonomous expansion rate r_D exceeds $b_{DC}r_{\mathcal{S}}/g_{CS} + c_{DS}r_C/e_{CS}$, the drag exerted through the boundary-cycle averages of capital and super-predator activity.
3. *Wealth concentration.* Equation (20c) shows that $\mathcal{S}$ grows at the expense of both C and D, concentrating financial returns in the shadow-banking sector [9]; in the regime $\lambda_D < 0$ of Figure 4 this culminates in the crowding-out of ordinary credit altogether.

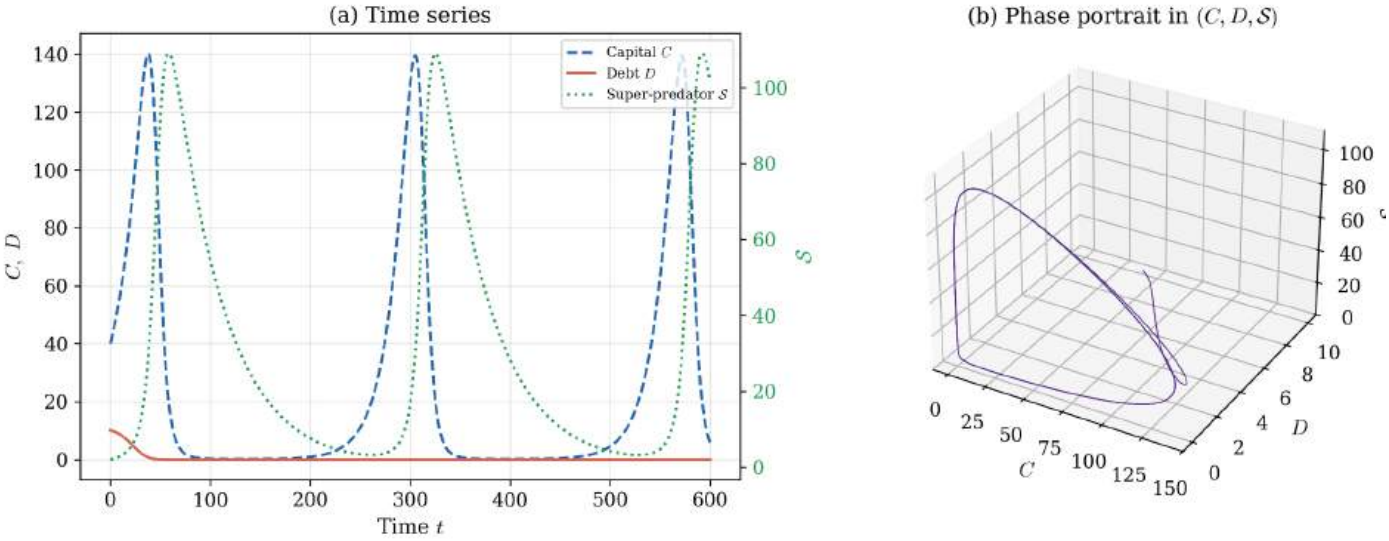


Figure 4. Numerical simulation of the three-species super-predator model (20) with $(r_C, r_D, r_{\mathcal{S}}, a_{DC}, b_{DC}, c_{DS}, e_{CS}, f_{DC}, g_{CS}) = (0.06, 0.04, 0.02, 0.002, 0.001, 0.003, 0.002, 5\times10^{-5}, 0.001)$ and $(C_0, D_0, \mathcal{S}_0) = (40, 10, 2)$, illustrating Theorem 4.8. **(a)** Time series: the interior equilibrium $E^{**} \approx (17.40, 22.47, 7.53)$ is a saddle-focus (Theorem 4.8(i); Remark 4.9), and since $\lambda_D = -0.070 < 0$ (Theorem 4.8(iii)) the debt coordinate D (red, solid, left axis) is driven to extinction at the predicted exponential rate, while capital C (blue, dashed, left axis) and the super-predator $\mathcal{S}$ (green, dotted, right axis) settle onto a neutral Lotka–Volterra cycle of the boundary system on the $D = 0$ face (Theorem 4.8(ii)). The figure should accordingly *not* be read as bounded three-trophic coexistence. **(b)** Corresponding non-planar trajectory in $(C, D, \mathcal{S})$-space, approaching the boundary cycle.

5 Numerical Experiments and Empirical Context

5.1 From Differential Equations to Finite-Size Stochastic Models

Continuous ODE models rest on two key idealizations: (i) perfectly mixing, homogeneous populations (mass-action kinetics) and (ii) a deterministic aggregation that suppresses finite-size fluctuations. Agent-based models (ABMs) relax these idealizations by simulating the discrete decisions of heterogeneous, boundedly rational individuals [3, 7]. The model studied in this section takes a step in that direction at the population level, and we deliberately do *not* call it an agent-based model: it does not track individual agents' states or heterogeneous decision rules. Rather, it is a finite-size *stochastic market model*, the diffusion-scale description of an underlying market of N traders switching between buying and selling at density-dependent rates: aggregate stocks of order N evolve under density-dependent drift, and the $O(1/\sqrt{N})$ noise is the central-limit fluctuation of such a system. The two levels of description are mathematically complementary: the ODE provides closed-form equilibria and Lyapunov results, while the finite-size model quantifies how far a large but finite market deviates from them; Theorem 5.1 makes the connection precise, with the deterministic ODE emerging in the joint limit of infinitely many agents and vanishing time step.

5.2 A Finite-Size Stochastic Market Model with Herding

We formulate a discrete-time stochastic generalization of the buyer–seller model (14) for a market of size N. Let $\Delta t > 0$ be the time step, and let B_t and S_t denote aggregate buying and selling stocks, both of order N. Two explicit scaling assumptions tie the model to the market size. First, mass-action interactions are *density dependent*,

$$a_{BS} = \frac{\alpha_{BS}}{N}, \qquad b_{BS} = \frac{\beta_{BS}}{N}, \tag{27}$$

with $\alpha_{BS}, \beta_{BS} > 0$ fixed as N varies: each unit of buying stock interacts with the *fraction*, not the number, of selling counterparties. Second, aggregate noise has central-limit scale, $\sigma = \sigma_0/\sqrt{N}$ and $\sigma_P = \sigma_P^0/\sqrt{N}$. The model reads

$$B_{t+\Delta t} = B_t + \Delta t\big(r_B(t)B_t - a_{BS}B_tS_t\big) + \sigma B_t\sqrt{\Delta t}\,\varepsilon_t^B, \tag{28a}$$

$$S_{t+\Delta t} = S_t + \Delta t\big(-m_S S_t + b_{BS}B_tS_t\big) + \sigma S_t\sqrt{\Delta t}\,\varepsilon_t^S, \tag{28b}$$

$$P_{t+\Delta t} = P_t\left[1 + \eta\,\Delta t\,\frac{B_t - S_t}{N} + \sigma_P\sqrt{\Delta t}\,\varepsilon_t^P\right], \tag{28c}$$

where $\varepsilon_t^B, \varepsilon_t^S, \varepsilon_t^P \overset{\text{i.i.d.}}{\sim} \mathcal{N}(0,1)$ are independent standard normal shocks and $\eta > 0$ governs price sensitivity to the normalized order imbalance. (With the step $\Delta t = 1$ used in the simulation of Figure 5, the factor Δt in (28c) is immaterial; it matters only for the continuum limit below.) Herding behavior is incorporated by making the buyer growth rate depend on lagged price momentum:

$$r_B(t) = r_B^0 + \kappa\,\frac{P_t - P_{t-1}}{P_{t-1}}, \qquad \kappa \geq 0, \tag{29}$$

where $r_B^0 > 0$ is the baseline growth rate and κ is the trend-following (chartist) coefficient, consistent with empirically documented herding in financial markets [19].

In terms of the *densities* $x_t^{(N)} = B_t/N$ and $y_t^{(N)} = S_t/N$, the scalings (27) turn (28) into

$$x_{t+\Delta t}^{(N)} = x_t^{(N)} + \Delta t\big(r_B(t)x_t^{(N)} - \alpha_{BS}x_t^{(N)}y_t^{(N)}\big) + \frac{\sigma_0}{\sqrt{N}}\,x_t^{(N)}\sqrt{\Delta t}\,\varepsilon_t^B, \tag{30a}$$

$$y_{t+\Delta t}^{(N)} = y_t^{(N)} + \Delta t\big(-m_S y_t^{(N)} + \beta_{BS}x_t^{(N)}y_t^{(N)}\big) + \frac{\sigma_0}{\sqrt{N}}\,y_t^{(N)}\sqrt{\Delta t}\,\varepsilon_t^S, \tag{30b}$$

$$P_{t+\Delta t}^{(N)} = P_t^{(N)}\left[1 + \eta\,\Delta t\,\big(x_t^{(N)} - y_t^{(N)}\big) + \frac{\sigma_P^0}{\sqrt{N}}\sqrt{\Delta t}\,\varepsilon_t^P\right], \tag{30c}$$

whose drift part is precisely the explicit Euler discretization, with step Δt, of the ODE system

$$\dot{x} = r_B^0 x - \alpha_{BS}xy, \qquad \dot{y} = -m_S y + \beta_{BS}xy, \qquad \dot{P} = \eta P\,(x - y). \tag{31}$$

The (x, y) subsystem is the buyer–seller Lotka–Volterra system (14) in density variables; the multiplicative price equation is the density-scaled counterpart of the price-impact rule (15), formulated in relative changes so that P remains positive.

Two distinct limits are therefore in play, and we keep them separate. As $N \to \infty$ at *fixed* Δt, the noise vanishes and the natural deterministic limit is the Euler map, *not* the continuous-time ODE; the ODE (31) is recovered only in the additional limit $\Delta t \to 0$. The following theorem, the third novel analytical contribution of this paper, makes both steps precise.

Theorem 5.1 (Mean-field and continuum limit of the stochastic market model)**.** *Assume $\kappa = 0$ (no herding), the density scaling (27), and the noise scaling $\sigma = \sigma_0/\sqrt{N}$, $\sigma_P = \sigma_P^0/\sqrt{N}$. Fix $T > 0$ and an initial condition $(x_0, y_0, P_0) \in \mathbb{R}^3_{>0}$ independent of N. Let $z_k^{(N)} = (x_{k\Delta t}^{(N)}, y_{k\Delta t}^{(N)}, P_{k\Delta t}^{(N)})$ denote the stochastic process (30), let $\bar z_k = (\bar x_k, \bar y_k, \bar P_k)$ denote the deterministic Euler iterates of (31) with step Δt from the same initial condition, and let $z(t) = (x(t), y(t), P(t))$ denote the solution of (31). Then there exist $\Delta t_0 > 0$ and constants $C_1(T), C_2(T) < \infty$ such that for all $\Delta t \in (0, \Delta t_0]$:*

(i) *(Law of large numbers at fixed Δt.)* $\max\limits_{0\le k\le \lfloor T/\Delta t\rfloor} \mathbb{E}\big[\,\big\|z_k^{(N)} - \bar z_k\big\|^2\,\big] \le \dfrac{C_1(T)}{N}$, *and consequently, for fixed Δt,* $\max_{k\le\lfloor T/\Delta t\rfloor}\big\|z_k^{(N)} - \bar z_k\big\| \to 0$ *in probability as $N \to \infty$.*

(ii) *(Continuum limit of the Euler map.)* $\max\limits_{0\le k\le \lfloor T/\Delta t\rfloor} \|\bar z_k - z(k\Delta t)\| \le C_2(T)\,\Delta t$.

(iii) *(Joint limit.) For every sequence $\Delta t_N \to 0$ with $N\Delta t_N \to \infty$,*

$$\max_{0\le k\le \lfloor T/\Delta t_N\rfloor} \big\|z_k^{(N)} - z(k\Delta t_N)\big\| \longrightarrow 0 \quad \text{in probability as } N \to \infty.$$

In this precise sense the deterministic Lotka–Volterra dynamics (31) are the joint large-N, small-Δt limit of the stochastic market model, while at fixed Δt the limit is the deterministic Euler map.

Proof. Throughout, $(x(t), y(t))$ lies on a closed Lotka–Volterra orbit (Proposition 2.2 applied to (31)) and $P(t) = P_0 \exp\big(\eta \int_0^t (x - y)\,ds\big)$ is bounded and bounded away from zero on $[0, T]$; fix a compact set $K \subset \mathbb{R}^3_{>0}$ containing a ρ-neighbourhood, $\rho > 0$, of $\{z(t) : t \in [0, T]\}$, and let L be a Lipschitz constant on K for the drift map $F(x, y, P) = (r_B^0 x - \alpha_{BS} xy,\ -m_S y + \beta_{BS} xy,\ \eta P(x - y))$.

Part (ii). This is the classical convergence estimate for the explicit Euler method applied to the locally Lipschitz, C^1 vector field F: while the exact solution remains in K, the local truncation error per step is $O(\Delta t^2)$, and the discrete Grönwall inequality propagates it to a global error $C_2(T)\Delta t$ over $\lfloor T/\Delta t\rfloor$ steps [11, Chapter II]. Choosing Δt_0 small enough also guarantees $\bar z_k \in K$ with $\operatorname{dist}(\bar z_k, \partial K) \ge \rho/2$ for all $k \le \lfloor T/\Delta t\rfloor$ and $\Delta t \le \Delta t_0$.

Part (i). Let $\delta_k = z_k^{(N)} - \bar z_k$ and let $\tau = \min\{k : z_k^{(N)} \notin K\}$. For $k < \tau$ the update gives $\delta_{k+1} = \delta_k + \Delta t\big[F(z_k^{(N)}) - F(\bar z_k)\big] + \zeta_k$, where ζ_k collects the noise terms and satisfies $\mathbb{E}[\zeta_k \mid \mathcal{F}_k] = 0$ and $\mathbb{E}[\|\zeta_k\|^2 \mid \mathcal{F}_k] \le c_K \Delta t/N$ with $c_K := \big(\sigma_0^2 + (\sigma_P^0)^2\big) \sup_K (x^2 + y^2 + P^2)$. Squaring, taking conditional expectations (the cross term with ζ_k vanishes), and using $\|\delta + \Delta t\,\Delta F\|^2 \le (1 + C\Delta t)\,\|\delta\|^2$ with $C = 2L + L^2$ for $\Delta t \le 1$, we obtain

$$\mathbb{E}\big[\big\|\delta_{(k+1)\wedge\tau}\big\|^2\big] \le (1 + C\Delta t)\,\mathbb{E}\big[\|\delta_{k\wedge\tau}\|^2\big] + \frac{c_K \Delta t}{N}.$$

The discrete Grönwall inequality over $k \le \lfloor T/\Delta t\rfloor$ yields $\max_k \mathbb{E}[\|\delta_{k\wedge\tau}\|^2] \le c_K T e^{CT}/N =: C_1(T)/N$, uniformly in $\Delta t \in (0, \Delta t_0]$. On the event $\{\max_k \|\delta_{k\wedge\tau}\| \le \rho/2\}$ the stopped process never exits K, so $\tau > \lfloor T/\Delta t\rfloor$ and the stopped and unstopped deviations coincide; by the union bound and Chebyshev's inequality,

$$\mathbb{P}\Big(\max_{0\le k\le\lfloor T/\Delta t\rfloor} \|\delta_{k\wedge\tau}\| > \epsilon\Big) \le \sum_{k=0}^{\lfloor T/\Delta t\rfloor} \frac{\mathbb{E}[\|\delta_{k\wedge\tau}\|^2]}{\epsilon^2} \le \frac{(T/\Delta t + 1)\,C_1(T)}{N\epsilon^2} \tag{32}$$

for every $\epsilon \in (0, \rho/2]$, which tends to 0 as $N \to \infty$ at fixed Δt. This proves both assertions of part (i).

Part (iii). By the triangle inequality and part (ii), $\max_k \big\|z_k^{(N)} - z(k\Delta t_N)\big\| \le \max_k \|\delta_k\| + C_2(T)\Delta t_N$. Given $\epsilon > 0$, the second term is eventually below $\epsilon/2$, and by (32) with $\epsilon/2$ the first exceeds $\epsilon/2$ with probability at most $O\big(1/(N\Delta t_N \epsilon^2)\big) \to 0$ since $N\Delta t_N \to \infty$. □

Remark 5.2. *The condition $N\Delta t_N \to \infty$ in part (iii) stems from the elementary union bound in (32); it could be weakened by controlling the martingale part of δ_k with Doob's maximal inequality, at the cost of heavier notation. We do not pursue this refinement here.*

Remark 5.3. *Theorem 5.1 establishes that the predator–prey ODE is the joint large-N, small-Δt limit of the stochastic market model. For $N < \infty$, stochastic fluctuations of order $O(1/\sqrt{N})$ generate the fat-tailed returns and volatility clustering documented in Section 5.4 below, without any exogenous news shocks; in the joint limit these finite-size effects vanish and the smooth deterministic oscillations of the ODE are recovered.*

Remark 5.4 (Scope: the herding case $\kappa > 0$)**.** *Theorem 5.1 is stated for $\kappa = 0$ and* does not apply *when $\kappa > 0$: the buyer growth rate $r_B(t)$ in (29) then depends on the lagged price ratio P_t/P_{t-1}, the process is no longer Markovian in*

(B_t, S_t, P_t), *and density-dependent convergence arguments in the spirit of Kurtz [16] do not apply directly. We therefore leave the mean-field limit of the* $\kappa > 0$ *system as an open problem; we expect it to require McKean–Vlasov techniques for non-Markovian, path-dependent interactions. The finite-*N *herding case is explored only as* exploratory numerics*: in the simulation of Figure 5 (*$N = 1000$*,* $\kappa = 0.4$*) the trend-following feedback produces a leptokurtic log-return distribution and pronounced volatility clustering, neither of which is present in the* $\kappa = 0$ *joint limit.*

Figure 5 presents the finite-N stochastic market dynamics (with herding, $\kappa > 0$) for the parameter set

$$(r_B^0, m_S, a_{BS}, b_{BS}, \sigma_0, \sigma_P^0, \eta, \kappa) = (0.05, 0.05, 3\times10^{-4}, 3\times10^{-4}, 0.04, 0.05, 0.1, 0.4),$$

with $N = 1000$ and $\Delta t = 1$ over $T = 500$ periods; via (27) these values correspond to $\alpha_{BS} = \beta_{BS} = 0.3$.

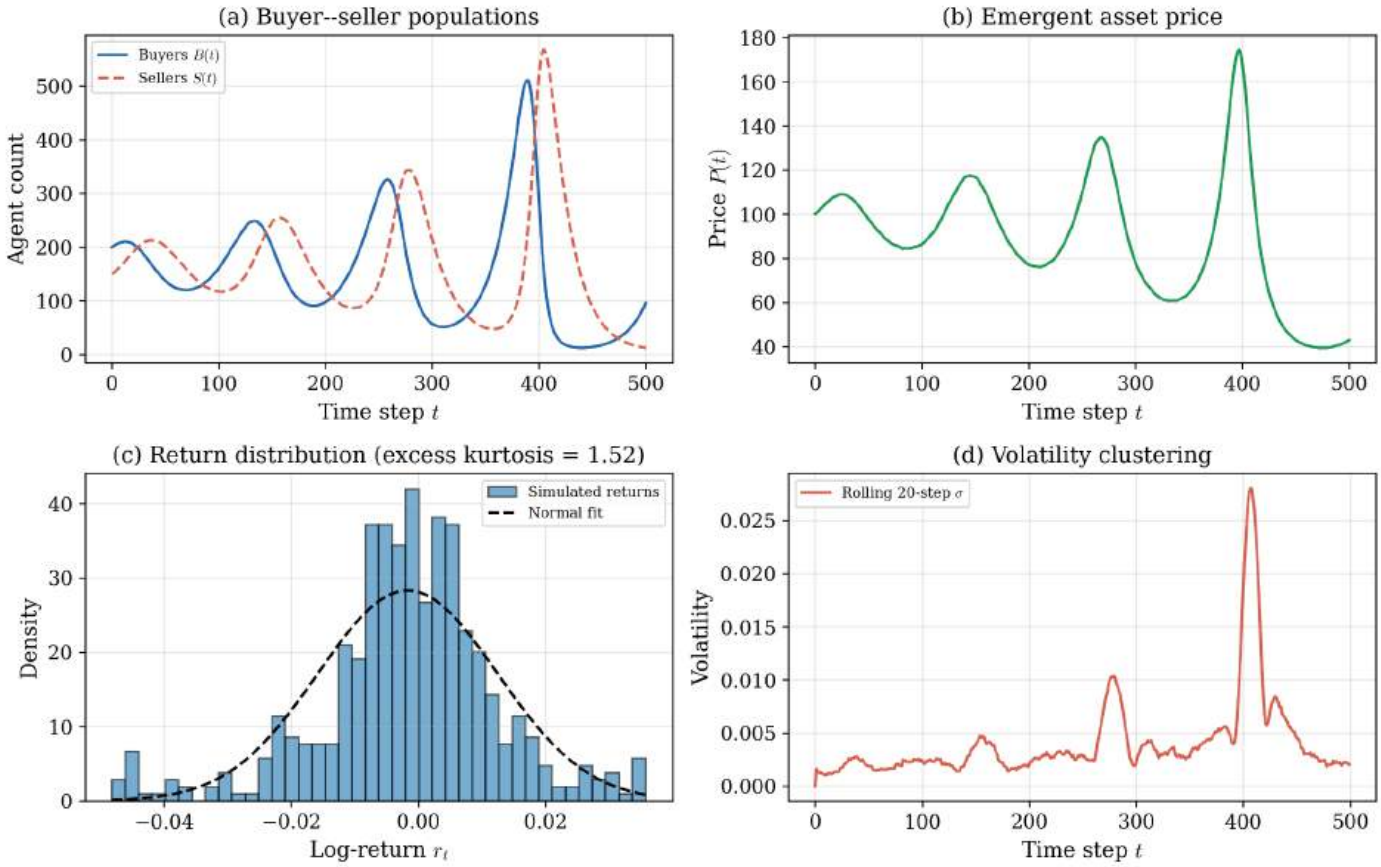


Figure 5. Stochastic simulation of the market model (28) over $T = 500$ periods with $N = 1000$, $\Delta t = 1$, and parameter values $(r_B^0, m_S, a_{BS}, b_{BS}, \sigma_0, \sigma_P^0, \eta, \kappa) = (0.05, 0.05, 3\times10^{-4}, 3\times10^{-4}, 0.04, 0.05, 0.1, 0.4)$ (seed 42). **(a)** Buyer (blue) and seller (red, dashed) aggregates exhibit bounded, anti-correlated oscillations around the deterministic predator–prey cycle. **(b)** Emergent asset price $P(t)$ oscillates with the order imbalance. **(c)** The log-return distribution is leptokurtic (excess kurtosis 1.52 for this seed), departing from the Gaussian fit. **(d)** The rolling volatility exhibits clustering. Because $\kappa = 0.4 > 0$, Theorem 5.1 does *not* apply to this simulation: panels (a)–(d) are exploratory numerics for the herding regime, whose mean-field limit remains open (Remark 5.4). For $\kappa = 0$, Theorem 5.1 guarantees that such finite-size effects vanish in the joint limit $N \to \infty$, $\Delta t \to 0$.

5.3 Numerical Implementation, Reproducibility, and Sensitivity

All simulations were carried out in Python 3.11 with NumPy, SciPy, and Matplotlib; the Jupyter notebook reproducing every figure is provided as supplementary material. Deterministic systems (Figures 1, 2, 3(a)-(b), and 4) were integrated with `scipy.integrate.solve_ivp` (explicit Runge–Kutta RK45; `max_step` $= 0.02$ for Figure 1, and `rtol` $= 10^{-10}$, `atol` $= 10^{-12}$ for the others). The stochastic debt–capital system (18) in Figure 3(c) was simulated by Euler–Maruyama with $\Delta t = 0.05$ and 4000 Monte-Carlo paths (NumPy `default_rng`, seed 0); the market model (28) in Figure 5 uses $\Delta t = 1$, $N = 1000$, and seed 42. All figures are rendered at 300 dpi.

Regarding sensitivity, the qualitative conclusions drawn from Figures 1–3 are not parameter-tuned–the center structure, the first integrals, and the drift rate $\frac{1}{2}(\sigma_C^2 r_D + \sigma_D^2 r_C)$ are theorems valid for *all* positive parameter values (Propositions 2.2 and 3.2, Theorem 4.4), so only quantitative features such as period and amplitude vary with the parameters. The long-run outcome in Figure 4 is likewise characterized exactly, for every parameter choice, by the sign of the closed-form exponent

(26) together with the unconditional instability of E^{**} (Theorem 4.8); the displayed extinction regime corresponds to $\lambda_D < 0$, and $\lambda_D > 0$ would instead produce re-invasion of debt. For the stochastic simulation of Figure 5, whose fine structure is seed-dependent, we re-ran the experiment for seeds 0–9: the excess kurtosis of log-returns ranged over [1.38, 2.03] (positive in every run) and volatility clustering was present in all runs, so the qualitative conclusions of panels (c)–(d) are robust to the realization of the noise.

5.4 Predecessor-Model Evidence

The *predecessor* models on which our framework builds have independent empirical support, summarized below. We stress that these studies validate the established models (Goodwin, Crookes–Blignaut, Montero, Keen), not the specific new claims of this paper; direct empirical tests of Theorems 4.4, 4.8, and 5.1 are left for future work.

1. *Goodwin cycles in OECD economies.* Harvie [12] estimated the Goodwin model (8) for ten OECD countries, documenting quantitative agreement between the model's predictions and the observed counter-cyclical relationship between the wage share and the employment rate, with structurally stable parameters across countries.

2. *Steel industry trophic cascades.* Crookes and Blignaut [5] calibrated system (13) to South African industry production indices for 1970–2010, reporting goodness-of-fit $R^2 > 0.85$ for the cyclical component.

3. *Equity return distributions.* Montero [22] demonstrated that the stochastically perturbed buyer–seller system (14) produces return distributions with excess kurtosis in the range $[3, 7]$, consistent with the empirically documented fat tails of daily returns on major equity indices.

4. *Pre-crisis US debt dynamics.* Keen [15] calibrated a Minskyan debt–capital model to US data for 1945–2007, showing that the ratio of private debt to GDP exhibits growing excursions in the decade preceding the 2008 financial crisis, qualitatively consistent with the noise-induced outward energy drift of Theorem 4.4(iv).

5.5 Comparative Summary of Model Properties

Table 3 provides a unified comparison of the five main model classes analyzed in this paper, listing the predator–prey species, the equilibrium type, and the key novel result associated with each.

Table 3. Comparative properties of the predator–prey models developed in this paper. Novel results established herein are indicated in boldface.

Model	Prey	Predator	Equilibrium type	Key result
Basic LV (1)	x	y	Nonlinear center	First integral; Props. 2.2–2.5
Goodwin (8)	Employment v	Wage share ω	Nonlinear center	LV isomorphism; Prop. 3.2
Debt–Capital (16)	Capital C	Debt D	Center / noise drift	**Minsky formulation; Thm. 4.4**
Super-predator (20)	C, D	$\mathcal{S}$	Unstable interior; boundary cycles	**Instability & extinction exponent; Thm. 4.8**
Stoch. market model (28)	Buyers B	Sellers S	Noisy LV cycles	**Mean-field & continuum limit; Thm. 5.1**

6 Policy Implications

The predator–prey framework developed in this paper suggests a set of qualitatively grounded policy readings. Each is obtained by identifying the structural parameter that, when perturbed, changes the amplitude of cyclical fluctuations, the equilibrium leverage, or—for the three-species system—the fate of the debt market, according to the results established in Theorems 4.4–5.1. An important caveat applies throughout this section: statements linking real-world policy instruments to model parameters are *interpretive mappings within the model*, not quantitative results established by the analysis; we therefore use conditional wording ("may be interpreted as", "could be represented as") deliberately.

Wage policy and automatic stabilizers. In the Goodwin model (8), the amplitude of business cycles is proportional to the distance of the orbit from the center E^* given in (11). Raising the unemployment insurance replacement rate may be interpreted, within the model, as reducing the Phillips-curve slope ρ (i.e., wage sensitivity to employment), which by

Proposition 3.2 compresses the orbit in the (ω, v)-plane and moderates cycle amplitude. A statutory minimum-wage floor could be represented as a lower bound on ω, preventing wage-share trajectories from entering the deflationary region $\omega \ll \omega^*$ [12].

Macroprudential regulation and noise-induced fragility. By Theorem 4.4(iv), the conserved energy of the stochastic debt–capital system drifts strictly outward at the rate $\frac{1}{2}(\sigma_C^2 r_D + \sigma_D^2 r_C) > 0$ under *any* noise; there is no deterministic stable regime to be "restored" by an r_D-versus-r_C inequality. Macroprudential policy nonetheless has two natural readings within the model. First, measures that suppress debt-side volatility—loan-to-value limits, countercyclical capital buffers, debt-service coverage requirements—could be represented as reducing σ_D, and hence the term $\sigma_D^2 r_C$ in the drift, slowing the outward energy migration in expectation. Second, by Theorem 4.4(iii) the equilibrium leverage ratio $D^*/C^* = b_{DC} r_C/(a_{DC} r_D)$ is increasing in r_C and decreasing in r_D and is lowered by increasing a_{DC} (which stricter debt-service requirements may be read as doing); shifting this ratio governs how the unavoidable noise-driven excursions are distributed between the debt and capital coordinates. Keen [15] proposes a *debt jubilee*—a one-time reduction in D—as a discrete intervention returning a high-leverage trajectory to a lower sublevel set of H, i.e., closer to E^*.

Regulating financial super-predators. Theorem 4.8 changes the nature of the policy question for the three-species system: because the interior equilibrium is unstable for *all* positive parameters, no adjustment of extraction or origination coefficients can stabilize interior coexistence. Within the model, policy instead operates on *which boundary regime prevails*, through the extinction exponent (26), whose comparative statics are $\partial\lambda_D/\partial c_{DS} = -r_C/e_{CS} < 0$, $\partial\lambda_D/\partial g_{CS} = +b_{DC} r_{\mathcal{S}}/g_{CS}^2 > 0$, and $\partial\lambda_D/\partial r_{\mathcal{S}} = -b_{DC}/g_{CS} < 0$. Within the interpretation of the model, restrictions on credit-default instruments and securitization spreads could be represented as reducing c_{DS}, which raises λ_D and favours the survival of ordinary credit relative to the intermediated boundary regime; Tobin-type transaction taxes could be represented as reducing the profitability of intermediation (lower f_{DC}, higher effective $r_{\mathcal{S}}$), mechanisms discussed qualitatively by Stiglitz [29] and Goldstein [9]. We stress that these are interpretive mappings; the model itself establishes only the dependence of λ_D and E^{**} on the structural parameters.

Market transparency and information policy. By Theorem 5.1, the stochastic market model converges to the deterministic dynamics in the joint limit $N \to \infty$, $\Delta t \to 0$. Policies that deepen markets—mandatory pre-trade transparency, central clearing, a consolidated tape—may be interpreted, within the model, as increasing the effective size N, which reduces the $O(1/\sqrt{N})$ fluctuations and improves the approximation of the stochastic system by the deterministic predator–prey dynamics, in which bubble and crash dynamics are absent. Similarly, circuit breakers or short-selling restrictions could be represented as reducing the trend-following coefficient κ in (29), limiting the positive-feedback amplification that generates fat-tailed returns in the finite-N system; we note that the $\kappa > 0$ regime lies outside the scope of Theorem 5.1 (Remark 5.4).

7 Conclusion and Future Research

This paper has developed a rigorous, unified mathematical framework for applying predator–prey dynamical systems to economic and financial phenomena. The main analytical results are as follows.

Starting from the classical Lotka–Volterra equations, we established positive invariance and global existence of solutions (Proposition 2.1), proved the existence of a conserved Hamiltonian via explicit computation (Proposition 2.2), and derived the period formula for small-amplitude oscillations (Corollary 2.3). For the Rosenzweig–MacArthur logistic extension, we identified the precise carrying-capacity threshold $K_c = 2x^* + 1/(ah)$ with $x^* = m/(b - mah)$, at which a Hopf bifurcation occurs and limit cycles emerge (Proposition 2.5).

In the economic domain, we proved that the Goodwin growth-cycle model is an exact algebraic isomorphism of the Lotka–Volterra system (Proposition 3.2), thereby transferring all conservation and periodicity results to the macroeconomic setting.

In the financial domain, we derived a two-species debt–capital predator–prey model from microeconomic first principles (Assumption 4.2), constructed an explicit first integral / Lyapunov function, and gave a rigorous Lyapunov-based formulation of Minsky's hypothesis: the deterministic system is a neutral center for all positive parameters, while under Itô noise the expected energy drifts strictly outward at the rate $\frac{1}{2}(\sigma_C^2 r_D + \sigma_D^2 r_C)$ (Theorem 4.4), so that no deterministic r_D-versus-r_C threshold governs stability. This complements Asada's [2] predator–prey treatment of Minsky's hypothesis. We then introduced and analyzed a three-species super-predator system: under an explicit parameter condition a unique interior equilibrium exists (Proposition 4.7), but it is unstable for *all* positive parameter values, so stable interior coexistence is impossible; on the $D = 0$ boundary face the dynamics reduce to a classical Lotka–Volterra pair, and the closed-form transversal exponent λ_D of (26) decides, uniformly across all boundary cycles, whether debt is driven to extinction (Theorem 4.8), in quantitative agreement with the simulations.

Finally, we formulated a finite-size stochastic market generalization of the buyer–seller model with herding, with explicit density-dependent scaling, and proved a two-step limit theorem (Theorem 5.1): at fixed time step the size-N

process converges in probability to the deterministic Euler map, and in the joint limit $N \to \infty$, $\Delta t \to 0$ it converges in probability, uniformly on compact time intervals, to the deterministic Lotka–Volterra ODE.

The results of this paper open several mathematically rich avenues for future investigation.

Behavioral and heterogeneous-agent extensions

Incorporating prospect theory [14] and salience-weighted attention into the buyer–seller market model (28) would yield a model in which the effective predation rate a_{BS} depends on the recent history of losses and gains. A rigorous mean-field analysis analogous to Theorem 5.1 in this non-Markovian setting would require new techniques from the theory of McKean–Vlasov equations.

Network-embedded predator–prey models

Real economies are networks: firms, banks, and households are connected through credit, supply-chain, and ownership relationships. Embedding the dynamics of (20) on a random graph [13] would reveal how network topology (degree distribution, clustering, assortativity) shapes the amplitude and propagation speed of financial instability, and would raise new questions about how network structure reshapes the extinction exponent λ_D of Theorem 4.8.

Stabilized variants, bifurcation, and chaos analysis.

Theorem 4.8 rules out Hopf bifurcations of the interior equilibrium for (20) itself (Remark 4.10). Damped variants—for example, logistic self-limitation of capital—restore the possibility of stable coexistence and Hopf bifurcations, and are the natural setting in which to investigate period-doubling routes to complex dynamics with dedicated numerical bifurcation software (e.g., AUTO-07P, MATCONT) and computer-assisted proof techniques.

Bayesian structural estimation.

Bayesian estimation of the Goodwin model (8) and the debt–capital model (16) via particle-filter methods applied to high-frequency national-accounts and credit data would sharpen the quantitative content of the framework, produce posterior distributions over the equilibrium leverage ratio D^*/C^* and the extinction exponent λ_D, and enable formal hypothesis testing against competing macro-finance models.

Ecological–economic coupling and sustainability.

Predator–prey models are structurally suited to coupling economic growth with biophysical limits [26]. Introducing a natural-capital "prey" variable—depleted by economic "predation" via resource extraction or carbon emissions—into the Goodwin framework would yield a mathematically tractable, empirically calibratable model for planetary-boundary sustainability analysis.

Partial differential equation extensions.

The reaction–diffusion system (6) raises natural questions about the existence of traveling-wave solutions connecting spatially homogeneous steady states, the Turing instability mechanism in the context of economic geography, and the well-posedness of the associated boundary-value problems in weighted Sobolev spaces.

In summary, the predator–prey paradigm developed in this paper provides a rigorous, parsimonious, and empirically tractable mathematical framework for analyzing the cyclical, fragile, and self-referential dynamics of modern financial capitalism. The integration of this framework with machine learning, high-frequency microstructure data, and network-theoretic tools represents a promising agenda for both mathematical research and policy analysis.

Conflicts of Interest

The authors declare no conflicts of interest.

Author Contributions

We describe contributions following the CRediT taxonomy. **Deepak Bastola:** Conceptualization, Methodology, Formal analysis, Writing – original draft. **Pitambar Acharya:** Conceptualization, Methodology, Formal analysis, Writing – original draft. *(Pitambar Acharya and Deepak Bastola contributed equally and are joint first authors.)* **Dipak Dulal:** Writing – review & editing. **Pawan Kumar BK:** Writing – review & editing. All authors read and approved the final manuscript.

Funding

This research received no external funding.

Code Availability Statement

The code used in this study is publicly available on GitHub at: https://github.com/deepakbastola/PredatorPrey.

Institutional Review Board Statement

Not applicable. This study did not involve human participants or animals.

Informed Consent Statement

Not applicable.

Generative AI Disclosure

Generative AI was used as a language support tool during the preparation of this manuscript. Its use was limited to improving clarity, refining wording, correcting grammatical errors, and enhancing overall readability. All AI-assisted suggestions were independently reviewed, revised where appropriate, and approved by the authors, who retain full responsibility for the accuracy, originality, and integrity of the final manuscript.

References

[1] L. M. Addison, B. S. Bhatt, and D. R. Owen. A prey–predator model for investing in stocks. *International Journal of Pure and Applied Mathematics*, 107(2):487–502, 2016.

[2] T. Asada. Modeling financial instability. *European Journal of Economics and Economic Policies: Intervention*, 9(2): 215–232, 2012.

[3] R. Axtell. Why agents? On the varied motivation for agent-based modeling in the social sciences. *Journal of Artificial Societies and Social Simulation*, 11(4), 2008. Article 9.

[4] C. Chiarella, G. Iori, and J. Perelló. The impact of heterogeneous trading rules on the limit order book and order flows. *Journal of Economic Dynamics and Control*, 33(3):525–537, 2009.

[5] D. Crookes and J. Blignaut. Predator–prey analysis using system dynamics: an application to the steel industry. *South African Journal of Economic and Management Sciences*, 19(5):733–748, 2016.

[6] M. Desai, B. Henry, A. Mosley, and M. Pemberton. A clarification of the Goodwin model of the growth cycle. *Journal of Economic Dynamics and Control*, 30(12):2661–2670, 2006.

[7] J. M. Epstein and R. Axtell. *Growing Artificial Societies: Social Science from the Bottom Up*. Brookings Institution Press, Washington, D.C., 1996.

[8] L. Gardini, R. Lupini, and M. G. Messia. Hopf bifurcation and transition to chaos in the Lotka–Volterra equation. *Journal of Mathematical Biology*, 27(3):259–272, 1989.

[9] J. Goldstein. A three-class predator–prey model with financial super-predators: The financial profit squeeze. Technical Report Working Paper No. 515, Political Economy Research Institute, University of Massachusetts Amherst, 2020.

[10] R. M. Goodwin. A growth cycle. In C. H. Feinstein, editor, *Socialism, Capitalism and Economic Growth*, pages 54–58. Cambridge University Press, Cambridge, 1967.

[11] P. Hartman. *Ordinary Differential Equations*. SIAM, Philadelphia, 2nd edition, 2002.

[12] D. Harvie. Testing Goodwin: growth cycles in ten OECD countries. *Cambridge Journal of Economics*, 24(3):349–376, 2000.

[13] M. O. Jackson and B. W. Rogers. Meeting strangers and friends of friends: how random are social networks? *American Economic Review*, 97(3):890–915, 2007.

[14] D. Kahneman and A. Tversky. Prospect theory: an analysis of decision under risk. *Econometrica*, 47(2):263–291, 1979.

[15] S. Keen. *Debunking Economics: The Naked Emperor Dethroned?* Zed Books, London, 2nd edition, 2011.

[16] T. G. Kurtz. Solutions of ordinary differential equations as limits of pure jump Markov processes. *Journal of Applied Probability*, 7(1):49–58, 1970.

[17] Y. A. Kuznetsov. *Elements of Applied Bifurcation Theory*. Springer, New York, 3rd edition, 2004.

[18] A. J. Lotka. Analytical note on certain rhythmic relations in organic systems. *Proceedings of the National Academy of Sciences*, 6(7):410–415, 1920.

[19] T. Lux and M. Marchesi. Scaling and criticality in a stochastic multi-agent model of a financial market. *Nature*, 397 (6719):498–500, 1999.

[20] X. Mao, G. Marion, and E. Renshaw. Environmental Brownian noise suppresses explosions in population dynamics. *Stochastic Processes and their Applications*, 97(1):95–110, 2002.

[21] H. P. Minsky. *Stabilizing an Unstable Economy*. Yale University Press, New Haven, 1986.

[22] M. Montero. Predator–prey model for stock market fluctuations, 2008. Preprint, arXiv:0810.4844.

[23] J. D. Murray. *Mathematical Biology I: An Introduction*. Springer, New York, 3rd edition, 2002.

[24] J. D. Murray. *Mathematical Biology II: Spatial Models and Biomedical Applications*. Springer, New York, 3rd edition, 2003.

[25] D. H. Nguyen and G. Yin. Coexistence and exclusion of stochastic competitive Lotka–Volterra models. *Journal of Differential Equations*, 262(3):1192–1225, 2017.

[26] E. Ostrom. A general framework for analyzing sustainability of social-ecological systems. *Science*, 325(5939):419–422, 2009.

[27] M. L. Rosenzweig. Paradox of enrichment: destabilization of exploitation ecosystems in ecological time. *Science*, 171 (3969):385–387, 1971.

[28] L. Shaikhet and A. Korobeinikov. Persistence and stochastic extinction in a Lotka–Volterra predator–prey stochastically perturbed model. *Mathematics*, 12(10):1588, 2024.

[29] J. E. Stiglitz. *Freefall: America, Free Markets, and the Sinking of the World Economy*. W. W. Norton & Company, New York, 2010.

[30] V. Volterra. Fluctuations in the abundance of a species considered mathematically. *Nature*, 118(2972):558–560, 1926.

[31] M. L. Zeeman. Hopf bifurcations in competitive three-dimensional Lotka–Volterra systems. *Dynamics and Stability of Systems*, 8(3):189–217, 1993.

Publisher's Note. Statements, opinions, and data contained in publications are solely those of the individual author(s) and contributor(s). The publisher and editors disclaim responsibility for injury to people or property resulting from ideas, methods, instructions, or products referred to in the content.

Journal of Applied Mathematics, Statistics, and Computational Sciences
JAMSCS

OA
OPEN ACCESS

Copyright © Authors, 2026

Research Article

Nevanlinna–Pick Interpolation in Selected Subalgebras of $H^\infty(\mathbb{D})$

Debendra P. Banjade and Jeremiah Dunivin

Coastal Carolina University

Received: 2026-06-01
Revised: 2026-07-25
Accepted: 2026-08-01
Published: 2026-10-21

Article:

Open access under the Creative Commons Attribution (CC BY 4.0) license.

Abstract

Given a collection K of positive integers, let $H^\infty_K(\mathbb{D})$ denote the set of all bounded analytic functions defined on the unit disk $\mathbb{D}$ in $\mathbb{C}$ whose k^{th} derivative vanishes at zero, for all $k \in K$. We establish a Nevanlinna-Pick interpolation result for the subalgebra $H^\infty_K(\mathbb{D})$. This work is a generalization of the interpolation theorem that Davidson, Paulsen, Raghupathi, and Singh proved for the algebra $H^\infty_{\{1\}}(\mathbb{D})$ in [9].

1 Introduction

The algebras we are interested in this paper are defined as follows:
Let $K \subset \mathbb{Z}_+$ and define

$$H^\infty_K(\mathbb{D}) = \{f \in H^\infty(\mathbb{D}) : f^{(k)}(0) = 0, \quad \text{for} \quad \text{all} \ \ k \in K\}.$$

We consider those sets K for which $H^\infty_K(\mathbb{D})$ is an algebra under pointwise multiplication of functions. Obviously, not every set K defines an algebra (for example, let $K = \{2\}$). Though there is not a complete characterization of the set K for which $H^\infty_K(\mathbb{D})$ is an algebra, Ryle and Trent [20] have given certain criteria that the set K must meet. We state some of these criteria as Lemmas 3.1 and 3.2 in Section 3.

Furthermore, we endow $H^\infty(\mathbb{D})$ with the usual supremum norm, which we define below.

Definition 1.1. Let f be a function defined on $\mathbb{D}$. The *supremum norm* $||f||_\infty$ of f is defined as the least upper bound for the set of all moduli of f. Formally, we write

$$||f||_\infty = \sup\{|f(z)| : z \in \mathbb{D}\}.$$

Nevanlinna and Pick proved an interpolation result for the algebra $H^\infty(\mathbb{D})$. Their theorem shows that an interpolant exists in this algebra precisely when the associated Pick matrix is positive semidefinite.

Nevanlinna–Pick Interpolation Theorem. *Given distinct points $z_1, z_2, ..., z_n$ in the unit disk $\mathbb{D}$ in the complex plane and complex numbers $w_1, w_2, ..., w_n$ in $\mathbb{D}$, there exists a function f in $H^\infty(\mathbb{D})$ with $f(z_i) = w_i$ for $i = 1, 2, \ldots, n$ and $\|f\|_\infty \leq 1$ if and only if the associated Pick matrix*

$$\left[\frac{1 - w_i\overline{w_j}}{1 - z_i\overline{z_j}}\right]_{i,j} \quad \text{is} \quad \text{positive} \quad \text{semidefinite.}$$

Davidson, Paulsen, Raghupathi, and Singh [9] proved an interpolation result for $H^\infty_{\{1\}}(\mathbb{D})$, the collection of all bounded, analytic functions f on $\mathbb{D}$, satisfying the constraint $f'(0) = 0$ (see Theorem 1.2 in [9]).

Interpolation Theorem on $H^\infty_{\{1\}}(\mathbb{D})$ (Davidson, Paulsen, Raghupathi, and Singh). *Let $z_1, z_2, ..., z_n$ be distinct points in $\mathbb{D}$, and let $w_1, w_2, ..., w_n$, be in $\mathbb{D}$. Then there exists an analytic function f in $H^\infty_{\{1\}}(\mathbb{D})$ with $\|f\|_\infty \leq 1$ such that $f(z_i) = w_i$ for $i = 1, 2, \ldots, n$ if and only if there exists $\lambda \in \mathbb{D}$ so that*

$$\left[\frac{z_i^2\overline{z_j^2} - \varphi_\lambda(w_i)\overline{\varphi_\lambda(w_j)}}{1 - z_i\overline{z_j}}\right]_{i,j} \quad \text{is} \quad \text{positive} \quad \text{semidefinite,}$$

where $\varphi_\lambda(z) = \frac{z-\lambda}{1-\overline{\lambda}z}$ denotes the elementary Möbius transformation.

Observing that all functions in $H^\infty_{\{1\}}(\mathbb{D})$ have first derivatives that vanish at zero, it is natural to define our desired set as follows.

Definition 1.2. Let K denote a nonempty collection of positive integers and define the set $H^\infty_K(\mathbb{D})$ as the set of all functions in $H^\infty(\mathbb{D})$ whose k^{th} derivative vanishes at zero, for all $k \in K$. Formally, define

$$H^\infty_K(\mathbb{D}) := \{f \in H^\infty(\mathbb{D}) : f^{(k)}(0) = 0, \text{ for all } k \in K\}.$$

We assume that $H^\infty_K(\mathbb{D})$ is an algebra. As we shall see in Section 2, this assumption is necessary.

Although [9] is the primary inspiration for this work, Carleson's corona theorem and Wolff's problem of ideals have also been established for $H^\infty_K(\mathbb{D})$, see [18] and [7], respectively. Thus, we found it plausible that a similar interpolation condition holds for the subalgebra $H^\infty_K(\mathbb{D})$. Indeed, we will prove the interpolation results for $H^\infty_K(\mathbb{D})$ in Theorem 4.1 and Corollary 4.2 in Section 4 of this paper.

In the next section, we will briefly consider examples of sets K that may or may not yield an algebra, demonstrating that we must make the assumption that $H^\infty_K(\mathbb{D})$ is an algebra. Section 3 is devoted to all results that will be used to assist us in proving Theorem 4.1 and Corollary 4.2.

2 The Subalgebra $H^\infty_K(\mathbb{D})$

We consider those sets K for which $H^\infty_K(\mathbb{D})$ is an algebra. As the next example shows, not all sets K yield an algebra.

Example 2.1. The set $H^\infty_{\{2\}}(\mathbb{D})$ is not an algebra, because it fails to be closed under pointwise multiplication. Consider the functions $f(z) = z$ and $g(z) = z$ on $\mathbb{D}$. Clearly, f and g are analytic and bounded, so $f, g \in H^\infty(\mathbb{D})$. Further, $f''(0) = g''(0) = 0$, so $f, g \in H^\infty_{\{2\}}(\mathbb{D})$. But for the product $f(z)g(z) = z^2$, we have $\big(fg\big)''(z) = 2$, which does not vanish at zero. Thus, $fg \notin H^\infty_{\{2\}}(\mathbb{D})$, so it is not closed under pointwise multiplication. Therefore, $H^\infty_{\{2\}}(\mathbb{D})$ is not an algebra.

However, the set $H^\infty_{\{1,3\}}(\mathbb{D})$ is an algebra.

Example 2.2. Let $f, g \in H^\infty_{\{1,3\}}(\mathbb{D})$. For the sum $f + g$, we have

$$(f+g)'(0) = f'(0) + g'(0) = 0 \quad \text{and} \quad (f+g)'''(0) = f'''(0) + g'''(0) = 0,$$

so $f + g \in H^\infty_{\{1,3\}}(\mathbb{D})$. For the first derivative of the product fg,

$$(fg)'(z) = f'(z)g(z) + f(z)g'(z),$$

which implies that

$$\begin{aligned}(fg)'(0) &= f'(0)g(0) + f(0)g'(0)\\ &= 0 \cdot g(0) + f(0) \cdot 0\\ &= 0.\end{aligned}$$

Similarly, the third derivative of fg yields

$$(fg)'''(z) = f'''(z)g(z) + 3f''(z)g'(z) + 3f'(z)g''(z) + f(z)g'''(z),$$

and thus

$$\begin{aligned}(fg)'''(0) &= f'''(0)g(0) + 3f''(0)g'(0) + 3f'(0)g''(0) + f(0)g'''(0)\\ &= 0 \cdot g(0) + 3f''(0) \cdot 0 + 3 \cdot 0 \cdot g''(0) + f(0) \cdot 0\\ &= 0.\end{aligned}$$

Therefore, $fg \in H^\infty_{\{1,3\}}(\mathbb{D})$. Since $H^\infty_{\{1,3\}}(\mathbb{D})$ is closed under both pointwise multiplication and addition, we conclude that it is an algebra.

The above examples show that not every K yields an algebra. A complete characterization of such sets K is an open problem worthy of investigation. Nevertheless, we will proceed to assume that a K is given such that $H^\infty_K(\mathbb{D})$ is an algebra.

3 Preliminaries

Ryle and Trent have conducted a thorough analysis on the subalgebra $H^\infty_K(\mathbb{D})$, revealing the rich structure and interesting properties it possesses (see Chapter 4 in [20]). Furthermore, they provide necessary criteria that K must satisfy

whenever $H^\infty_K(\mathbb{D})$ is an algebra. We catalog some of these attributes below (see Lemmas 4.2.1, 4.2.2, 4.2.4, and Corollary 4.2.1 in [20]).

Lemma 3.1. ***(Ryle and Trent)*** *Let $K \subset \mathbb{Z}_+$ such that $H^\infty_K(\mathbb{D})$ is an algebra. Then*

(i) $k_0 \notin K$ if and only if $\varphi(z) = z^{k_0} \in H^\infty_K(\mathbb{D})$.
(ii) If $j, k \notin K$, then $j + k \notin K$.
(iii) If $j \notin K$, then $nj \notin K$ for all $n \geq 2$.
(iv) Suppose $k_0 \in K$. If $1 < j < k_0$ satisfies $j \notin K$, then $k_0 - j \in K$.

Given an algebra $H^\infty_K(\mathbb{D})$, the following lemma demonstrates that some collection of positive integers absent from K exists. (see Corollary 1 in [19]).

Lemma 3.2. ***(Ryle and Trent)*** *If $H^\infty_K(\mathbb{D})$ is an algebra, then there exists $d \in \mathbb{Z}_+$, a finite set $\{n_i\}_{i=1}^p \subset \mathbb{Z}_+$ with $n_1 < \cdots < n_p$ and $\gcd(n_1, \ldots, n_p) = 1$, and a positive integer $N_0 > n_p$ so that*

$$\mathbb{Z}_+ \setminus K = \{n_1 d, n_2 d, \ldots, n_p d, N_0 d, (N_0 + j)d : j \in \mathbb{Z}_+\}.$$

These lemmas show that every function $f \in H^\infty_K(\mathbb{D})$ has the following power series representation

$$f(z) = \alpha_0 + \alpha_1 z^{n_1 d} + \alpha_2 z^{n_2 d} + \cdots + \alpha_p z^{n_p d} + \alpha_{p+1} z^{N_0 d} + \sum_{j=1}^{\infty} \alpha_{p+j+1} z^{(N_0+j)d},$$

where the coefficient $\alpha_i \in \mathbb{C}$. In order to improve our understanding of these results, we provide a couple of examples below.

Example 3.3. Given $H^\infty_K(\mathbb{D})$ we show the particular power series representation of functions in this algebra.

i. If $f \in H^\infty_{\{1\}}(\mathbb{D})$, then the power series representation of f is

$$f(z) = \alpha_0 + \alpha_2 z^2 + \alpha_3 z^3 + \alpha_4 z^4 + \sum_{i=5}^{\infty} \alpha_i z^i.$$

ii. If $f \in H^\infty_{\{1,3\}}(\mathbb{D})$, then the power series representation of f is

$$f(z) = \alpha_0 + \alpha_2 z^2 + \alpha_4 z^4 + \alpha_5 z^5 + \sum_{i=6}^{\infty} \alpha_i z^i.$$

Because we will be taking derivatives of function compositions, we will be using Bruno's Formula below (see [13] for more information).

Bruno's Formula. *Let f and g denote functions with a sufficient number of derivatives. Then the k^{th} derivative of the composition $g \circ f$ is*

$$\frac{d^k}{dz^k}\Big[g(f(z))\Big] = \sum \frac{k!}{b_1!\, b_2! \cdots b_k!} \cdot g^{(b)}(f(z)) \cdot \prod_{\ell=1}^{k} \Big(\frac{f^{(\ell)}(z)}{\ell!}\Big)^{b_\ell}$$

where the sum is over all k-tuples of nonnegative integers $(b_1, \ldots, b_k)$ satisfying the constraint

$$\sum_{\ell=1}^{k} \ell\, b_\ell = k,$$

and $b := b_1 + b_2 + \cdots + b_k$.

We use Bruno's formula in the following example, which serves as a motivation for Lemmas 3.5 and 3.6 below.

Example 3.4. When $k = 3$, Bruno's formula shows that we take the triples (b_1, b_2, b_3) satisfying the equation $b_1 + 2b_2 + 3b_3 = 3$. Clearly, the only solutions are $(3, 0, 0)$, $(1, 1, 0)$ and $(0, 0, 1)$. Given $(3, 0, 0)$, the first term has the form

$$\frac{3!}{3!0!0!} \cdot g^{(3+0+0)}(f(z)) \cdot \left(\frac{f^{(1)}(z)}{1!}\right)^3 \left(\frac{f^{(2)}(z)}{2!}\right)^0 \left(\frac{f^{(3)}(z)}{3!}\right)^0 = g^{(3)}(f(z))\big[f^{(1)}(z)\big]^3.$$

Further, the solution $(1,1,0)$ yields the term

$$\frac{3!}{1!1!0!}\cdot g^{(1+1+0)}(f(z))\cdot\left(\frac{f^{(1)}(z)}{1!}\right)^1\left(\frac{f^{(2)}(z)}{2!}\right)^1\left(\frac{f^{(3)}(z)}{3!}\right)^0 = 3g^{(2)}(f(z))f^{(1)}(z)f^{(2)}(z).$$

Finally, the solution $(0,0,1)$ provides the last term of the form

$$\frac{3!}{0!0!1!}\cdot g^{(0+0+1)}(f(z))\cdot\left(\frac{f^{(1)}(z)}{1!}\right)^0\left(\frac{f^{(2)}(z)}{2!}\right)^0\left(\frac{f^{(3)}(z)}{3!}\right)^1 = g^{(1)}(f(z))f^{(3)}(z).$$

Therefore,

$$(g\circ f)^{(3)}(z) = g^{(3)}(f(z))\big[f^{(1)}(z)\big]^3 + 3g^{(2)}(f(z))f^{(1)}(z)f^{(2)}(z) + g^{(1)}(f(z))f^{(3)}(z).$$

Note that each solution to the constraint generates a term in the above equation. Now, consider the algebra $H^\infty_{\{1,3\}}(\mathbb{D})$. If $f\in H^\infty_{\{1,3\}}(\mathbb{D})$, we see from the first three equations that a nonzero component b_j in (b_1,b_2,b_3) exists such that $j\in\{1,3\}$. We show that this is always true.

Lemma 3.5. *Suppose K is a set of positive integers such that $H^\infty_K(\mathbb{D})$ is an algebra. If $k\in K$, then for every k-tuple $(b_1,b_2,\dots,b_k)$ satisfying*

$$\sum_{\ell=1}^{k}\ell\, b_\ell = k,$$

there exists an $\ell_j\in\{\ell_1,\ell_2,\dots,\ell_t\}$ such that $\ell_j\in K$, where $b_{\ell_1},b_{\ell_2},\dots,b_{\ell_t}$ are the nonzero components of $(b_1,b_2,\dots,b_k)$.

Proof. Let $k\in K$. Assume instead that $\ell_j\notin K$, for all $\ell_j\in\{\ell_1,\ell_2,\dots,\ell_t\}$. By Lemma 3.1.(iii), the product $\ell_j\, b_{\ell_j}\notin K$. Further,

$$\sum_{j=1}^{t}\ell_j\, b_{\ell_j}\notin K,$$

by Lemma 3.1.(ii). Since $b_m=0$ for each $m\in\{1,2,\dots,k\}\setminus\{\ell_1,\ell_2,\dots,\ell_t\}$,

$$\sum_{\ell=1}^{k}\ell\, b_\ell = \sum_{j=1}^{t}\ell_j\, b_{\ell_j} = k\notin K,$$

which is a contradiction, as we know $k\in K$. □

We now show that $H^\infty_K(\mathbb{D})$ is a right ideal in $H^\infty(\mathbb{D})$.

Lemma 3.6. *Suppose that $H^\infty_K(\mathbb{D})$ is an algebra. If $g\in H^\infty(\mathbb{D})$ and $f\in H^\infty_K(\mathbb{D})$, then $g\circ f\in H^\infty_K(\mathbb{D})$.*

Proof. Let $g\in H^\infty(\mathbb{D})$ and $f\in H^\infty_K(\mathbb{D})$. Then $g\circ f\in H^\infty(\mathbb{D})$. If $k\in K$, Bruno's formula allows us to write

$$\big(g(f(z))\big)^{(k)} = \sum\frac{k!}{b_1!\,b_2!\cdots b_k!}\cdot g^{(b)}(f(z))\cdot\prod_{\ell=1}^{k}\Big(\frac{f^{(\ell)}(z)}{\ell!}\Big)^{b_\ell}$$

where the sum is over all k-tuples of nonnegative integers $(b_1,\dots,b_k)$ satisfying the constraint

$$\sum_{\ell=1}^{k}\ell\, b_\ell = k,$$

and $b:=b_1+b_2+\cdots+b_k$. For each solution $(b_1,b_2,\dots,b_k)$, there exist nonzero components $b_{\ell_1},b_{\ell_2},\dots,b_{\ell_t}$ in $(b_1,b_2,\dots,b_k)$, because $k>0$. By Lemma 3.5, there exists an $\ell_j\in\{\ell_1,\ell_2,\dots,\ell_t\}$ such that $\ell_j\in K$, and thus

$$\left(\frac{f^{(\ell_j)}(z)}{\ell_j!}\right)^{b_{\ell_j}} = 0 \quad\text{at}\quad z=0.$$

Therefore, every term in the sum vanishes at $z=0$, so $(g(f(0)))^{(k)}=0$. Hence, $g\circ f\in H^\infty_K(\mathbb{D})$. □

We now establish a trivial inequality.

Lemma 3.7. *Suppose $K = \{1, k_1, k_2, \ldots, k_p\}$ is a subset of $\mathbb{Z}_+$ where $k_p = \max K$. If m is the smallest positive integer not in K, then $k_p < m\left\lceil \frac{k_p}{m} \right\rceil$.*

Proof. Since

$$\left\lfloor \frac{k_p}{m} \right\rfloor \leq \frac{k_p}{m} < \left\lfloor \frac{k_p}{m} \right\rfloor + 1 = \left\lceil \frac{k_p}{m} \right\rceil$$

we conclude that

$$k_p < m\left\lceil \frac{k_p}{m} \right\rceil.$$

□

The following propositions will be used to prove Lemma 3.11 below. We first show that if $H^\infty_K(\mathbb{D})$ is an algebra, $1 \in K$.

Proposition 3.8. *If $K \subset \mathbb{Z}_+$ is nonempty such that $H^\infty_K(\mathbb{D})$ is an algebra, then $1 \in K$.*

Proof. Assume to the contrary that $1 \notin K$. Let k be the smallest positive integer in K. Then $k - 1 \notin K$ where $1 \leq k - 1$. If $k - 1 = 1$, then $k = 2 \in K$. By Lemma 3.1.(i), $z \in H^\infty_K(\mathbb{D})$ and $z^2 \notin H^\infty_K(\mathbb{D})$. However, $H^\infty_K(\mathbb{D})$ is an algebra, so $z \cdot z = z^2 \in H^\infty_K(\mathbb{D})$, a contradiction. Therefore, $1 < k - 1$. But since $k - 1 < k$ with $k - 1 \notin K$ and $k \in K$, Lemma 3.1.(iv) implies that $k - (k - 1) = 1 \in K$, another contradiction. Thus, we must have $1 \in K$. □

If K only has consecutive integers, then either K is finite, containing all positive integers less than some integer, or $K = \mathbb{Z}_+$.

Proposition 3.9. *Suppose $H^\infty_K(\mathbb{D})$ is an algebra. If K only contains consecutive integers, then $K = \{1, 2, \ldots, k\}$ for some integer k, or $K = \mathbb{Z}_+$.*

Proof. Suppose for each $k \in \mathbb{Z}_+$, $K \neq \{1, 2, \ldots, k\}$. By Proposition 3.8, $1 \in K$. But $K \neq \{1\}$. Since K only has consecutive integers, $2 \in K$. Similarly, if $k \in K$, then $k + 1 \in K$. Thus, $K = \mathbb{Z}_+$. □

Lastly, we show that if there is a smallest integer m not in K, then K contains all positive integers less than m.

Proposition 3.10. *Let $H^\infty_K(\mathbb{D})$ be an algebra with $K \neq \mathbb{Z}_+$. Let m be the smallest positive integer not in K. Then K contains every positive integer $j < m$.*

Proof. By Proposition 3.8, $K \neq \emptyset$. Since K and $\mathbb{Z}_+ \setminus K$ partition $\mathbb{Z}_+$ and $m = \min\left(\mathbb{Z}_+ \setminus K\right)$, every positive integer $j < m$ must be in K. □

We show that a smallest positive integer $m \notin K$ can be found, so that a function f can be written as a product of functions involving m.

Lemma 3.11. *Let $K \subset \mathbb{Z}_+$ be a proper nonempty set such that $H^\infty_K(\mathbb{D})$ is an algebra. Let $f \in H^\infty_K(\mathbb{D})$ with $f(0) = 0$. Then there exists a smallest positive integer $m \notin K$ and an analytic function h on $\mathbb{D}$ such that*

$$f(z) = z^m h(z).$$

Proof. It is enough to assume that f is not identically zero and nonconstant on $\mathbb{D}$. If K only contains consecutive integers, then because K is a proper subset of $\mathbb{Z}_+$, Proposition 3.9 tells us that $K = \{1, 2, 3 \ldots, k\}$, for some $k \in \mathbb{Z}_+$. Then the smallest positive integer not in K is $k + 1$. Now, if $f \in H^\infty_K(\mathbb{D})$ and $f(0) = 0$, it follows that f has the following representation:

$$\begin{aligned} f(z) &= \alpha_{k+1} z^{k+1} + \sum_{i=k+2}^{\infty} \alpha_i z^i \\ &= z^{k+1} h(z), \end{aligned}$$

where $h(z) = \alpha_{k+1} + \sum_{k+2}^{\infty} \alpha_i z^i$ is analytic, as desired.

If K contains a pair of nonconsecutive integers, let k_i and k_{i+1} denote the smallest such pair. Then $m = k_i + 1$ is the smallest positive integer not in K. By Proposition 3.10 every positive integer $j < k_i + 1$ is in K, so that $f^{(j)}(0) = 0$. Because $f(0) = 0$, we know that f has the following representation for all positive integers $\ell \notin K \cup \{m\}$:

$$\begin{aligned} f(z) &= \alpha_m z^m + \sum_{\ell} c_\ell z^\ell \\ &= z^m h(z), \end{aligned}$$

where $h(z) = \alpha_m + \sum_\ell c_\ell z^{\ell-m}$ is an analytic function, as desired. □

Let f be an analytic function on $\mathbb{D}$ such that $||f||_\infty \leq 1$. If there is a point $z_0 \in \mathbb{D}$ such that $f(z_0) \in \mathbb{D}$, then the image $f(\mathbb{D})$ is completely contained in $\mathbb{D}$. To prove this claim, recall that the Open Mapping Theorem says that the image of an open set under a nonconstant analytic mapping is open.

Lemma 3.12. *Let $f \in H^\infty(\mathbb{D})$ such that $||f||_\infty \leq 1$. If there is a point $z_0 \in \mathbb{D}$ such that $f(z_0) \in \mathbb{D}$, then $|f(z)| < 1$ for all $z \in \mathbb{D}$.*

Proof. If f is constant, then $f(z) = f(z_0)$ for all $z \in \mathbb{D}$, and the result follows. Otherwise, the Open Mapping Theorem and $||f||_\infty \leq 1$ imply that the image $f(\mathbb{D})$ is an open set contained in $\mathbb{D}$. Thus, $|f(z)| < 1$ for all $z \in \mathbb{D}$. □

4 The Interpolation Theorem On The Subalgebra $H^\infty_K(\mathbb{D})$

We are now ready to present our main theorem.

Theorem 4.1. *Let $K = \{1, k_1, k_2, \ldots, k_p\}$ with $1 < k_1 < k_2 < \ldots < k_p$ denote a set of positive integers such that $H^\infty_K(\mathbb{D})$ is an algebra. Let $z_1, z_2, \ldots, z_n$ be distinct points in $\mathbb{D}$ and $w_1, w_2, \ldots, w_n$ be points in $\mathbb{D}$.*
There exists an analytic function $f \in H^\infty_K(\mathbb{D})$ with $f(z_i) = w_i$ for $i = 1, 2, \ldots, n$ and $||f||_\infty \leq 1$ if and only if there exists a $\lambda \in \mathbb{D}$ such that

$$\left[\frac{z_i^{m\eta}\,\overline{z_j^{m\eta}} - \varphi_\lambda^\eta(w_i)\,\overline{\varphi_\lambda^\eta(w_j)}}{1 - z_i\overline{z_j}}\right] \quad \textit{is} \quad \textit{positive} \quad \textit{semidefinite},$$

where m is the smallest positive integer not in K, and $\eta = \left\lceil \frac{k_p}{m} \right\rceil$.

Proof. First, we suppose $z_i \neq 0$ for all $i = 1, 2, \ldots, n$. Assume that there exists $f \in H^\infty_K(\mathbb{D})$ such that $||f||_\infty \leq 1$ and $f(z_i) = w_i$. Set $\lambda = f(0)$, which is in $\mathbb{D}$ by Lemma 3.12. Define $g(z) = \varphi_\lambda(f(z))$. Since $\varphi_\lambda \in H^\infty(\mathbb{D})$ and $f \in H^\infty_K(\mathbb{D})$, it follows from Lemma 3.6 that $g \in H^\infty_K(\mathbb{D})$. Moreover, $g(z_i) = \varphi_\lambda(w_i)$ for $i = 1, 2 \ldots, n$, and $g(0) = \varphi_\lambda(\lambda) = 0$.

Consequently, we know from Lemma 3.11 that a smallest positive integer $m \notin K$ exists such that $g(z) = z^m \ell(z)$ where $||\ell||_\infty \leq 1$. Since $H^\infty_K(\mathbb{D})$ is an algebra, we have that

$$\underbrace{g(z)\,g(z)\,\cdots\,g(z)}_{\eta = \left\lceil \frac{k_p}{m} \right\rceil \text{ times}} = g^\eta(z) = \varphi_\lambda^\eta(f(z)) = z^{m\eta} h(z) \in H^\infty_K(\mathbb{D}),$$

where $h(z) = \ell^\eta(z)$ and $||h||_\infty \leq 1$. Applying the Nevanlinna-Pick Theorem on $h \in H^\infty(\mathbb{D})$ and the points $z_1, z_2, \ldots, z_n$, the matrix

$$\left[\frac{1 - h(z_i)\overline{h(z_j)}}{1 - z_i\overline{z_j}}\right] \quad \text{is} \quad \text{positive} \quad \text{semidefinite.}$$

Moreover, the matrix

$$\left[\frac{z_i^{m\eta}\overline{z_j^{m\eta}} - g^\eta(z_i)\,\overline{g^\eta(z_j)}}{1 - z_i\overline{z_j}}\right]$$

equals

$$\begin{bmatrix} z_1^{m\eta} & 0 & \ldots & 0 \\ 0 & z_2^{m\eta} & \ldots & 0 \\ \vdots & \vdots & \ddots & \vdots \\ 0 & 0 & \ldots & z_n^{m\eta} \end{bmatrix} \left[\frac{1 - h(z_i)\overline{h(z_j)}}{1 - z_i\overline{z_j}}\right] \begin{bmatrix} \overline{z_1^{m\eta}} & 0 & \ldots & 0 \\ 0 & \overline{z_2^{m\eta}} & \ldots & 0 \\ \vdots & \vdots & \ddots & \vdots \\ 0 & 0 & \ldots & \overline{z_n^{m\eta}} \end{bmatrix}.$$

Consequently,

$$\left[\frac{z_i^{m\eta}\overline{z_j^{m\eta}} - g^\eta(z_i)\,\overline{g^\eta(z_j)}}{1 - z_i\overline{z_j}}\right] = \left[\frac{z_i^{m\eta}\overline{z_j^{m\eta}} - \varphi_\lambda^\eta(w_i)\,\overline{\varphi_\lambda^\eta(w_j)}}{1 - z_i\overline{z_j}}\right] \quad \text{is} \quad \text{positive} \quad \text{semidefinite.}$$

Now suppose $z_1 = 0$. Then $\lambda = f(0) = f(z_1) = w_1$, and thus the first row and column of the matrix above are zero; and the same reasoning applies to the remaining entries of the matrix.

Conversely, it suffices to assume that $z_i \neq 0$ for all $i = 1, 2, \ldots, n$. Suppose there exists a $\lambda \in \mathbb{D}$ such that

$$\left[\frac{z_i^{m\eta}\overline{z_j^{m\eta}} - \varphi_\lambda^\eta(w_i)\,\overline{\varphi_\lambda^\eta(w_j)}}{1 - z_i\overline{z_j}}\right] \quad \text{is} \quad \text{positive} \quad \text{semidefinite.}$$

Since the above matrix equals

$$\begin{bmatrix} z_1^{m\eta} & 0 & \dots & 0 \\ 0 & z_2^{m\eta} & \dots & 0 \\ \vdots & \vdots & \ddots & \vdots \\ 0 & 0 & \dots & z_n^{m\eta} \end{bmatrix} \left[\frac{1 - z_i^{-m\eta} \varphi_\lambda^\eta(w_i)\, \overline{z_j^{-m\eta}\, \varphi_\lambda^\eta(w_j)}}{1 - z_i \overline{z_j}} \right] \begin{bmatrix} \overline{z_1^{m\eta}} & 0 & \dots & 0 \\ 0 & \overline{z_2^{m\eta}} & \dots & 0 \\ \vdots & \vdots & \ddots & \vdots \\ 0 & 0 & \dots & \overline{z_n^{m\eta}} \end{bmatrix},$$

we get that

$$\left[\frac{1 - z_i^{-m\eta} \varphi_\lambda^\eta(w_i)\, \overline{z_j^{-m\eta}\, \varphi_\lambda^\eta(w_j)}}{1 - z_i \overline{z_j}} \right] \quad \text{is} \quad \text{positive} \quad \text{semidefinite.}$$

By the Nevanlinna-Pick Theorem, there exists an $h \in H^\infty(\mathbb{D})$ with $||h||_\infty \leq 1$, so $h(z_i) = z_i^{-m\eta} \varphi_\lambda^\eta(w_i)$. Define $f(z) = \psi(z^{m\eta} h(z))$ where ψ is the inverse Möbius transformation of φ_λ^η. Clearly, $f \in H^\infty(\mathbb{D})$, $||f||_\infty \leq 1$, and $f(z_i) = \psi(z_i^{m\eta}\, h(z_i)) = \psi(z_i^{m\eta}\, z_i^{-m\eta}\, \varphi_\lambda^\eta(w_i)) = w_i$, for all $i = 1, 2, \dots, n$.

Moreover, $z^{m\eta} h(z) \in H^\infty(\mathbb{D})$. Now, for each $k \in K$, we have that

$$\big(z^{m\eta} h(z)\big)^{(k)} = \sum_{i=0}^{k} \binom{k}{i} \big(z^{m\eta}\big)^{(i)} \big(h(z)\big)^{(k-i)}.$$

And, for each $i = 0, 1, \dots, k$,

$$\big(z^{m\eta}\big)^{(i)} = \frac{k!}{(k-i)!} \cdot z^{m\eta - i}$$

By Lemma 3.7, $m\eta - i > 0$, so $\big(z^{m\eta} h(z)\big)^{(k)} = 0$ at $z = 0$. Thus, $z^{m\eta} h(z) \in H_K^\infty(\mathbb{D})$. Since $\psi \in H^\infty(\mathbb{D})$, we conclude from Lemma 3.6 that $f(z) = \psi(z^{m\eta} h(z)) \in H_K^\infty(\mathbb{D})$. □

Remark. If $K = \{1\}$, then $m = 2$ and $\eta = 1$ give us the result of [9] on $H_{\{1\}}^\infty(\mathbb{D})$.

Corollary 4.2. *Let K be an infinite proper subset of $\mathbb{Z}_+$ such that $H_K^\infty(\mathbb{D})$ is an algebra and*

$$\mathbb{Z}_+ \setminus K = \{n_1 d, n_2 d, \dots, n_p d, N_0 d, (N_0 + j)d : j \in \mathbb{Z}_+\}$$

for some positive integer d, some finite set $\{n_i\}_{i=1}^p \subset \mathbb{Z}_+$ where $n_1 < n_2 < \cdots < n_p$ and a positive integer $N_0 > n_p$. Moreover, let $K_1 \subset \mathbb{Z}_+$ such that

$$\mathbb{Z}_+ \setminus K_1 = \{n_1, n_2, \dots, n_p, N_0, N_0 + j \ : \ j \in \mathbb{Z}_+\}.$$

Let $z_1, z_2, \dots, z_n$ be distinct points in $\mathbb{D}$ and $w_1, w_2, \dots, w_n$ be points in $\mathbb{D}$. Then there exists an $f \in H_K^\infty(\mathbb{D})$ with $f(z_i) = w_i$ for $i = 1, 2, \dots, n$ and $||f||_\infty \leq 1$ if and only if there exists a $\lambda \in \mathbb{D}$ such that

$$\left[\frac{z_i^{n_1 d\, \eta} \overline{z_j^{n_1 d\, \eta}} - \varphi_\lambda^\eta(w_i) \overline{\varphi_\lambda^\eta(w_j)}}{1 - z_i^d\, \overline{z_j^d}} \right] \quad \textit{is} \quad \textit{positive} \quad \textit{semidefinite}$$

where n_1 is the smallest positive integer not in K_1 and $\eta = \left\lceil \frac{N_0 - 1}{n_1} \right\rceil$.

Proof. Let $f \in H_K^\infty(\mathbb{D})$ such that $f(z_i) = w_i$ and $||f||_\infty \leq 1$. By our assumption on $\mathbb{Z}_+ \setminus K$, we see that f has the following representation

$$f(z) = \alpha_0 + \alpha_1\, z^{n_1 d} + \alpha_2\, z^{n_2 d} + \cdots + \alpha_p\, z^{n_p d} + \alpha_{p+1}\, z^{N_0 d} + \sum_{j=1}^{\infty} \alpha_{p+j+1}\, z^{(N_0 + j)d},$$

where $\alpha_i \in \mathbb{C}$. Setting $V = z^d$, we have a function F defined by

$$F(V) = \alpha_0 + \alpha_1\, V^{n_1} + \alpha_2\, V^{n_2} + \cdots + \alpha_p\, V^{n_p} + \alpha_{p+1}\, V^{N_0} + \sum_{j=1}^{\infty} \alpha_{p+j+1}\, V^{N_0 + j}.$$

Consequently, F is contained in the algebra $H_{K_1}^\infty(\mathbb{D})$. Also, $||F||_\infty \leq 1$ since $||f||_\infty \leq 1$, and $F(V_i) = F(z_i^d) = f(z_i) = w_i$.

By Theorem 4.1, there exists a $\lambda \in \mathbb{D}$ such that

$$\left[\frac{V_i^{n_1\eta}\,\overline{V_j^{n_1\eta}} - \varphi_\lambda^\eta(V_i)\overline{\varphi_\lambda^\eta(V_j)}}{1 - V_i\,\overline{V_j}}\right] \quad \text{is} \quad \text{positive} \quad \text{semidefinite}$$

where n_1 is the smallest positive integer not in K_1 and $\eta = \left\lceil \frac{N_0-1}{n_1} \right\rceil$. Since $V_i = z_i^d$ and $\overline{V_j} = \overline{z_j^d}$, we conclude that

$$\left[\frac{z_i^{n_1 d\,\eta}\overline{z_j^{n_1 d\,\eta}} - \varphi_\lambda^\eta(w_i)\overline{\varphi_\lambda^\eta(w_j))}}{1 - z_i^d\,\overline{z_j^d}}\right] \quad \text{is} \quad \text{positive} \quad \text{semidefinite.}$$

Conversely, suppose there is a $\lambda \in \mathbb{D}$ such that the above matrix is positive semidefinite. Set $V_i = z_i^d$ and $\overline{V_j} = \overline{z_j^d}$, so that

$$\left[\frac{V_i^{n_1\eta}\,\overline{V_j^{n_1\eta}} - \varphi_\lambda^\eta(w_i)\overline{\varphi_\lambda^\eta(w_j)}}{1 - V_i\,\overline{V_j}}\right] \quad \text{is} \quad \text{positive} \quad \text{semidefinite.}$$

By Theorem 4.1, there exists an $F \in H^\infty_{K_1}(\mathbb{D})$ such that $F(V_i) = w_i$ and $||F||_\infty \leq 1$. Further, we have

$$F(V) = \alpha_0 + \alpha_1\,V^{n_1} + \alpha_2\,V^{n_2} + \cdots + \alpha_p\,V^{n_p} + \alpha_{p+1}\,V^{N_0} + \sum_{j=1}^{\infty}\alpha_{p+j+1}\,V^{N_0+j}.$$

Defining $f(z) = F(z^d)$, we see that

$$f(z) = \alpha_0 + \alpha_1\,z^{n_1 d} + \alpha_2\,z^{n_2 d} + \cdots + \alpha_p\,z^{n_p d} + \alpha_{p+1}\,z^{N_0 d} + \sum_{j=1}^{\infty}\alpha_{p+j+1}\,z^{(N_0+j)d}.$$

Clearly, $f \in H^\infty_K(\mathbb{D})$, $||f||_\infty \leq 1$ and $f(z_i) = F(z_i^d) = w_i$, for all $i = 1, 2, \ldots, n$. We conclude that f is our desired interpolation function. □

5 Conclusion and Open Problems

In this paper, we have extended the interpolation result for $H^\infty_{\{1\}}(\mathbb{D})$ to all algebras $H^\infty_K(\mathbb{D})$ where K is a nonempty subset of $\mathbb{Z}_+$. However, questions have naturally arisen during this investigation. For the classical Nevanlinna-Pick interpolation result, the interpolation function is unique if and only if the associated Pick matrix is singular. This fact inspires the following question.

Question 5.1. Are there necessary and sufficient conditions to guarantee that the the interpolation function in $H^\infty_K(\mathbb{D})$ is unique?

Lemma 3.6 shows that $H^\infty_K(\mathbb{D})$ is a right ideal in $H^\infty(\mathbb{D})$ for any set K yielding an algebra. However, Example 3.4 suggests that it is not always a left ideal, which leads us to our next question.

Question 5.2. Suppose $g \in H^\infty_K(\mathbb{D})$ and $f \in H^\infty(\mathbb{D})$. Under what conditions is the composition $g \circ f \in H^\infty_K(\mathbb{D})$?

Acknowledgements: The authors would like to thank the referee whose encouragement and valuable insights were paramount in assuring that this paper could achieve its highest quality and potential. Also, the authors would like to thank A. Incognito and Tavan T. Trent for important feedback on the first version of this manuscript.

References

[1] M. B. Abrahamse, *The Pick interpolation theorem for finitely connected domains*, Michigan Math. J. **26** (1979), 195-203

[2] J. Agler and J.E. McCarthy, *Complete Nevanlinna-Pick kernels*, J. Funct. Anal. **175** (2000), 111-124

[3] J. Agler and J.E. McCarthy, *Pick interpolation and Hilbert function spaces*, Graduate Studies in Mathematics, **44**, American Mathematical Society, Providence, RI, (2002)

[4] W. Arveson, *Interpolation problems in nest algebras*, J. Funct. Anal., **20** (1975), 208-233

[5] J. Ball, V. Bolotnikov, and S. ter Horst *A constrained Nevanlinna-Pick interpolation problem for matrix-valued functions* , Indiana Univ. Math. J **1** (2010), 15-51

[6] J. Ball and T. T. Trent *Unitary colligations, reproducing kernel Hilbert Spaces, and Nevanlinna–Pick Interpolation in several variables*, J. Funct. Anal., **157** (1998), 1-61

[7] D. P. Banjade, C. D. Holloway, and T. T. Trent *A generalized Wolff's ideal theorem on some certain subalgebras of* $H^\infty(\mathbb{D})$, Integr. Equat. Oper. Th. **83** (2015), 483-496

[8] L. Carleson, *Interpolation by bounded analytic functions and the corona problem*, Annals of Math. **76** (1962), 547-559

[9] K. R. Davidson, V. I. Paulsen, M. Raghupathi, and D. Singh, *A constrained Nevanlinna-Pick interpolation problem*, Indiana Univ. Math. J. **58** (2009), 709-732

[10] K. R. Davidson and D.R. Pitts, *Nevanlinna-Pick interpolation for non-commutative analytic Toeplitz algebras*, Integr Equat. Oper. Th. **31** (1998), 321-337

[11] J. B. Garnett, *Bounded analytic functions*, Academic Press, New York (1981)

[12] S. Fedorov and V. Vinnikov, *On the Nevanlinna-Pick interpolation in multiply connected domains,*, J. Math. Sci., New York **105** 2001, no. 4, pp. 2109-2126 J. Math. Sci. (New York) 105 (2001), no. 4, 2109–2126.

[13] W. P. Johnson, *The curious history of Faà di Bruno's formula*, *Am. Math. Monthly*, **109**, 2002, pp. 217-227.

[14] R. Nevanlinna, *"Uber Beschränkungen Funktionen die in gegebenen Punkten vorgeschriebene Werte annehmen,*, *Ann. Acad. Sci. Fenn. Ser. A I Math.*, **13:1**, 1919

[15] N. K. Nikolski, *Treatise on the Shift Operator*, Springer-Verlag, New York (1985)

[16] G. Pick, *Über die Beschränkungen analytischer Funktionen, welche durch vorgegebene Funktionswerte bewirkt werden*, Math. Ann.,77 (1916), 7-23

[17] M. Rosenblum, *A corona theorem for countably many functions*, Integral Equa. Oper. Theory **3** (1980), no. 1, 125-137

[18] J. Ryle and T. Trent, *A corona theorem for certain subalgebras of* $H^\infty(\mathbb{D})$, Houston J. Math. **37** (2011), no. 4, 1143-1156

[19] J. Ryle and T. Trent, *A corona theorem for certain subalgebras of* $H^\infty(\mathbb{D})$ *II*, Houston J. Math **38** (2012), no. 4, 1277-1295

[20] J. Ryle, *A corona theorem for certain subalgebras of* $H^\infty(\mathbb{D})$, Dissertation, The University of Alabama, (2009).

[21] D. Sarason, *Generalized interpolation in* $H^\infty(\mathbb{D})$, Trans. Amer. Math. Soc. **127** (1967), 179- 203

[22] T. Trent, *Function theory problems and operator theory*, Proceedings of the Topology and Geometry Research Center, TGRC-KOSEF, Vol. 8, Dec. 1997

[23] T. Wolff, *A refinement of the corona theorem*, in Linear and Complex Analysis Problem Book, by V. P. Havin, S. V. Hruscev, and N. K. Nikolski (eds.), Springer-Verlag, Berlin (1984)